DOI: 10.1534/genetics.109.107102

A Combinatorial Interplay Among the 1-Aminocyclopropane-1-Carboxylate Isoforms Regulates Ethylene Biosynthesis in *Arabidopsis thaliana*

Atsunari Tsuchisaka,* Guixia Yu,* Hailing Jin,† Jose M. Alonso,‡,[1] Joseph R. Ecker,‡ Xiaoming Zhang,† Shang Gao† and Athanasios Theologis*,[2]

**Plant Gene Expression Center, Albany, California 94710,* †*Department of Plant Pathology, University of California, Riverside, California 92521 and* ‡*Salk Institute for Biological Studies, La Jolla, California 92037*

Manuscript received July 8, 2009
Accepted for publication August 13, 2009

ABSTRACT

Ethylene (C_2H_4) is a unique plant-signaling molecule that regulates numerous developmental processes. The key enzyme in the two-step biosynthetic pathway of ethylene is 1-aminocyclopropane-1-carboxylate synthase (ACS), which catalyzes the conversion of *S*-adenosylmethionine (AdoMet) to ACC, the precursor of ethylene. To understand the function of this important enzyme, we analyzed the entire family of nine ACS isoforms (ACS1, ACS2, ACS4-9, and ACS11) encoded in the Arabidopsis genome. Our analysis reveals that members of this protein family share an essential function, because individual *ACS* genes are not essential for Arabidopsis viability, whereas elimination of the entire gene family results in embryonic lethality. Phenotypic characterization of single and multiple mutants unmasks unique but overlapping functions of the various *ACS* members in plant developmental events, including multiple growth characteristics, flowering time, response to gravity, disease resistance, and ethylene production. Ethylene acts as a repressor of flowering by regulating the transcription of the *FLOWERING LOCUS C*. Each single and high order mutant has a characteristic molecular phenotype with unique and overlapping gene expression patterns. The expression of several genes involved in light perception and signaling is altered in the high order mutants. These results, together with the *in planta* ACS interaction map, suggest that ethylene-mediated processes are orchestrated by a combinatorial interplay among ACS isoforms that determines the relative ratio of homo- and heterodimers (active or inactive) in a spatial and temporal manner. These subunit isoforms comprise a combinatorial code that is a central regulator of ethylene production during plant development. The lethality of the null ACS mutant contrasts with the viability of null mutations in key components of the ethylene signaling apparatus, strongly supporting the view that ACC, the precursor of ethylene, is a primary regulator of plant growth and development.

THE gas ethylene (C_2H_4) has long been known to be a signaling molecule that regulates a variety of developmental processes and stress responses in plants (Abeles *et al.* 1992). These include seed germination, leaf and flower senescence, fruit ripening, cell elongation, nodulation, and pathogen responses. Ethylene production is enhanced by a variety of external factors, including wounding, viral infection, elicitors, hormone treatment, chilling injury, drought, Cd^{2+} and Li^{+} ions, O_3, SO_2, and other pollutants (Yang and Hoffman 1984; Abeles *et al.* 1992; Bleecker and Kende 2000; Thomma *et al.* 2001). Enhancement of ethylene production serves as a signaling mechanism with profound physiological consequences (Guo and Ecker 2004).

Ethylene is synthesized from methionine by its conversion to *S*-adenosylmethionine (AdoMet), which is converted by the enzyme 1-aminocyclopropane-1-carboxylate synthase (ACS, EC 4.4.1.14) into methylthioadenosine (MTA) and 1-aminocyclopropane-1-carboxylic acid (ACC), the precursor of ethylene (Bleecker and Kende 2000). ACC is oxidized to C_2H_4, CO_2, and HCN by ACC oxidase (ACO) (Dong *et al.* 1992). Alternatively, ACC can be diverted from conversion to ethylene by forming the conjugate N-malonyl-ACC (Yang and Hoffman 1984). The activity of ACS is regulated at the transcriptional level (Bleecker and Kende 2000; Guo and Ecker 2004) and posttranscriptional level (Argueso *et al.* 2007).

ACS is a cytosolic enzyme with a short half-life and requires pyridoxal phosphate (PLP) as a cofactor (Yang and Hoffman 1984; Yip *et al.* 1990). The enzyme functions as a homodimer whose active site is formed from the interaction of residues from the monomeric subunits, similar to AspAT (Tarun and Theologis 1998). In particular, the Y^{92} residue, which helps anchor

Supporting information is available online at http://www.genetics.org/cgi/content/full/genetics.109.107102/DC1.

Microarray sequence data have been submitted to the NCBI gene expression data repository under the accession no. GSE14496.

All mutants and transgenic lines have been deposited to the Arabidopsis Biological Resource Center (ABRC).

[1]*Present address:* Department of Genetics, North Carolina State University, Raleigh, NC 27695.

[2]*Corresponding author:* Plant Gene Expression Center, 800 Buchanan St., Albany, CA 94710. E-mail: theo@nature.berkeley.edu

the PLP cofactor to the ACS apoenzyme, interacts with active-site residue K^{278}, which forms a covalent Schiff base with the PLP cofactor from the adjacent subunit. The three-dimensional structure of ACS has confirmed this model (Capitani *et al.* 1999), and together with available biochemical data explains the catalytic roles of the conserved and nonconserved active site residues (Tarun and Theologis 1998).

ACS is encoded by a multigene family in every plant species examined (Bleecker and Kende 2000). The Arabidopsis genome contains 12 genes annotated as *ACS* (*ACS1–12*), dispersed among the five chromosomes (Arabidopsis Genome Initiative 2000). However, *ACS3* is a pseudogene whereas *ACS10* and *12* encode aminotransferases (Yamagami *et al.* 2003). The remaining nine genes (*ACS1*, *ACS2*, *ACS4–9* and *ACS11*) are authentic ACSs and constitute the Arabidopsis *ACS* gene family (Yamagami *et al.* 2003). Among the nine ACS polypeptides, eight of them (ACS2, ACS4–9, and ACS11) form functional homodimers and one (ACS1) forms a nonfunctional homodimer (Tsuchisaka and Theologis 2004a). The highly variable carboxylic end of the proteins serves as a regulatory domain responsible for post-translational regulation of the enzyme whereas the nonvariable amino terminus harbors the catalytic domain. The ACS proteins comprise three phylogenetic branches, depending on their C terminus heterogeneity (Wang *et al.* 2004; Argueso *et al.* 2007; Hansen *et al.* 2008).

The biological significance of multigene families in general and of the *ACS* gene family in particular is unknown. Biochemical characterization of the ACSs reveals that all active isoforms are biochemically distinct (Yamagami *et al.* 2003). This has been viewed to reflect that each isoform may have a distinct biological function defined by its biochemical properties, which in turn define its tissue-specific expression (Yamagami *et al.* 2003). For example, if a group of cells or tissues has low concentrations of the ACS substrate, AdoMet, then these cells express a high affinity (low K_m) ACS isozyme. Such a concept underscores the physiological fine-tuning of the cell and demands that the enzymatic properties of each isozyme be distinct. In addition, the subunits of all isozymes have the capacity to form active and inactive heterodimers in *Escherichia coli*. The ACS polypeptides can potentially form 45 homo- and heterodimers of which 25 are functional (Tsuchisaka and Theologis 2004a). Functional heterodimerization may further enhance the isozyme diversity of the family and provides physiological versatility by being able to operate in a broad gradient of AdoMet concentration in various cells/tissues during plant growth and development. The formation of heterodimers *in planta* is possible since the expression of the *ACS* gene family members is overlapping during plant development (Tsuchisaka and Theologis 2004b). However, it is not known whether ACS heterodimers are formed *in planta*.

To understand the function and regulatory roles of each *ACS* gene in ethylene production during plant development, we analyzed the family of nine ACS isoforms encoded by the Arabidopsis genome. We used a combination of approaches, including T-DNA insertions/*amiRNA* technology, genome expression profiling, and *in planta* interactome mapping to analyze the essential and nonessential roles of the Arabidopsis *ACS* genes. We found that disruption of any single *ACS* gene causes no overt phenotype but had unique effects on gene expression profiles, indicating that the ACSs perform distinct nonessential roles. But they must have at least one essential function in common since elimination of all *ACS* genes resulted in embryo lethality. Phenotypic characterization of single, double, and high order mutants revealed specific and overlapping functions among the various *ACS* gene family members on plant developmental events such as differential growth, flowering time, gravitostimulation, and disease resistance. These results, coupled with the findings of an *in planta* ACS "interactome" map suggest that ethylene-mediated processes are regulated by a combinatorial interplay among the nine ACS subunits, which can form 45 different dimeric isoforms. This interplay provides a combinatorial code that determines the relative ratio of homo- and heterodimers (active or inactive) in a spatio-temporal manner and is the central regulator of ethylene production during plant development. The lethality of the ACS null mutant, in contrast to the viability of null mutations in key components of the ethylene signaling apparatus, strongly support the idea that ACC, the precursor of ethylene, is a *primary* regulator of plant growth and development.

MATERIALS AND METHODS

Materials, strains, and transformation vectors: Restriction enzymes were obtained from New England BioLabs. All chemicals used for this study were of analytical grade and purchased from Aldrich and Sigma. Oligonucleotides were purchased from Operon Technologies (Alameda, CA). See File S1 in the supporting information for details regarding transformation and transgenic line selection protocols.

Plant material and growth conditions: *Arabidopsis thaliana* ecotype Columbia (Col) was used throughout this study. Growth conditions and characterization of mutant phenotypes are described in File S1.

Identification and characterization of T-DNA insertion alleles: We used a PCR-based approach to identify T-DNA insertion mutations in *ACS* gene family members. See File S1 for technical details and primer information and Figure S8 for the integration pattern of T-DNA.

Construction of high order mutants: We used the strategy outlined in File S1.

Inactivation of the *ACS8* and *ACS11* genes with an *amiR*: An artificial microRNA (*amiR*) containing transgene that specifically inhibit both *ACS8* and *ACS11* gene expression was constructed by overlapping PCR using the *pRS300* plasmid as template containing the MIR319a (Schwab *et al.* 2006). See File S1 for technical details and primer information.

Complementation of the *octuple* (*amiR*) line: The *amiR* target sequences of the *ACS8* and ACS*11* ORFs were mutated by site-directed mutagenesis giving rise to *ACS8m* and *ACS11m* ORFs that encode functional proteins. The *pQE80-ACS8* and *pQE801-ACS11* plasmids (Tsuchisaka and Theologis 2004a) were used as templates. See File S1 for technical details and primer information.

Mapping the insertion sites of the *amiR*, *amiR* complementation and BiFC transgenes: We used thermal asymmetric interlaced (TAIL) PCR for mapping the integration sites of the *amiR*, *amiR* complementation and BiFC transgenic lines following the procedure described in File S1.

Complementation of the *acs6-1* and *acs9-1* mutants: Both mutants were complemented by expressing the *ACS6* and *ACS9* ORFs from their own promoters (2.5 kb). The 3′-UTRs of each gene (1 kb) were also included in the constructs to ensure appropriate tissue-specific expression. See File S1 for technical details and primer information.

Ethylene production: Ethylene production was determined in 5- or 10-day-old light-grown seedlings and 30- or 40-day-old light-grown plants (only the aerial parts were used) as described in File S1.

Histochemical GUS Assay: The *ACSpromoter-GUS* constructs reported by Tsuchisaka and Theologis (2004b) were used to determine the *ACS* gene expression in the region of the shoot apical meristem (SAM) of young light-grown Arabidopsis seedlings. See File S1 for technical details.

RT–PCR analysis for *ACS* and flowering gene expression: Total RNA was isolated using RNeasy (QIAGEN, Valencia, CA) and polyA$^+$ RNA was purified from total RNA using Oligotex (QIAGEN). See File S1 for technical details and primer information.

Bimolecular fluorescence complementation (BiFC) *in planta:* The homo- and heterodimeric interactions among the various subunits of the *ACS* gene family members were determined *in planta* by BiFC (Hu *et al.* 2002). See File S1 for technical details regarding construct design and imaging of yellow fluorescence *in planta*.

Pathogen infection assay: Arabidopsis plants were grown at 24° under a 12 hr light/12 hr dark cycle for 4 weeks before the pathogen inoculation. See File S1 for pathogen strains used and other experimental details.

Global gene expression analysis: Total RNA was prepared using RNAqueous RNA isolation kit with Plant RNA isolation aid (Ambion, Austin, TX). After LiCl precipitation, RNA was purified using RNeasy columns (QIAGEN, Valencia, CA) and reprecipitated with LiCl. RNA pellets were washed with 70% EtOH (three times), and resuspended in DEPC-treated water. Affymetrix ATH1 array was used. Ten micrograms of total RNA was used for biotin-labeled cRNA probe synthesis. cRNA probe synthesis were performed according to the manufacturer's protocols (Affymetrix, Santa Clara, CA) Scanned arrays were analyzed with Affymetrix MAS 5.0 software and then normalized with gcRMA obtained from bioconductor (http://bioconductor.org). See File S1 for details regarding data analysis.

RESULTS

Characterization of *ACS* T-DNA insertion mutants: We used a PCR-based screening approach to identify T-DNA insertion mutations in *ACS* gene family members (see Experimental Procedures in File S1). Inactivation of the *ACS* genes by the T-DNA insertions was confirmed by RT–PCR analysis of RNA isolated from CHX-treated seedlings (to increase the very low basal level of *ACS* mRNA expression) using the "black" set of primers shown in Figure S1A. All T-DNA insertions inhibit the expression of wild-type (wt) full-length *ACS* mRNAs [Figure S1Ba; compare lane 3 (T/T) with lanes 1 (wt) and 2 (t/t)]. A small amount of *ACS2* transcript is detected in the *acs2-2* mutant, which may be due to a low level splicing event (Figure S1Ba; lane 3). Similar analysis using primers upstream ("red" set) and downstream of the insertions ("green" set of primers shown in Figure S1A) was also carried out and the results are shown in Figure S1Bb (red set) and Figure S1Bc (green set), respectively. *ACS* transcripts are detected in all mutants upstream of the insertion except *acs5-2* [Figure S1Bb; compare lane 3 (T/T) with lanes 1 (wt) and 2 (t/t)]. Accumulation of a larger truncated transcript in *acs5-1* is attributed to incomplete splicing (Figure S1Bb; lane 3). *ACS* transcripts are also detected in all mutants downstream of the insertion except *acs4-1* and *acs7-2* [Figure S1Bc; compare lane 3 (T/T) with lanes 1 (wt) and 2 (t/t)]. The transcripts detected with the "red set" or "green set" of primers may derive from full-length T-DNA insertion products that could have failed to be amplified for technical reasons using the "black set" of primers. However, the transcripts detected downstream of the insertions may also be generated by a promoter activity inside the T-DNA insertion. The potential proteins derived from these various transcripts are almost certainly enzymatically inactive. In addition all the transcripts detected downstream of the insertions cannot be translated because of the presence of early translational stop signals. The activity of the ACS4-1 protein truncated at Q^{331} (includes the key catalytic residue K^{273}) must be nil because deletion analysis reveals that the C terminus of *Le-ACS2* beyond the conserved R^{512} is necessary for enzyme activity (A. S. Tarun and A. Theologis, unpublished results). All lines were backcrossed twice.

Phenotypic characterization: We observed six major phenotypic alterations in the mutants in: (1) plant growth, (2) flowering time (bolting), (3) response to shoot gravitostimulation, (4) resistance to pathogens, (5) developmental defects, and (6) ethylene production. We examined single, double, *pentuple hexuple*, *heptuple*, and *octuple* mutants.

Single and double mutants: *Seedling growth:* The *acs1-1* and *acs9-1* mutations enhance the hypocotyl length in etiolated seedlings, while *acs4-1* has an inhibitory effect (Figure 1A). The effect of *acs2-1*, *acs5-2*, and *acs6-1* on hypocotyl growth is nil. However, light-grown seedlings of these six single mutants have greatly enhanced hypocotyl length (Figure 1B). The same mutations also enhance cotyledon size, with *acs1-1* having the most pronounced effect (Figure 1C). Etiolated seedlings of all single and double mutants examined have normal hook formation, and their response to gravitostimulation is normal (data not shown).

Growth of adult plants: All single mutants except *acs2-2* have the same height as wt plants during the early stages

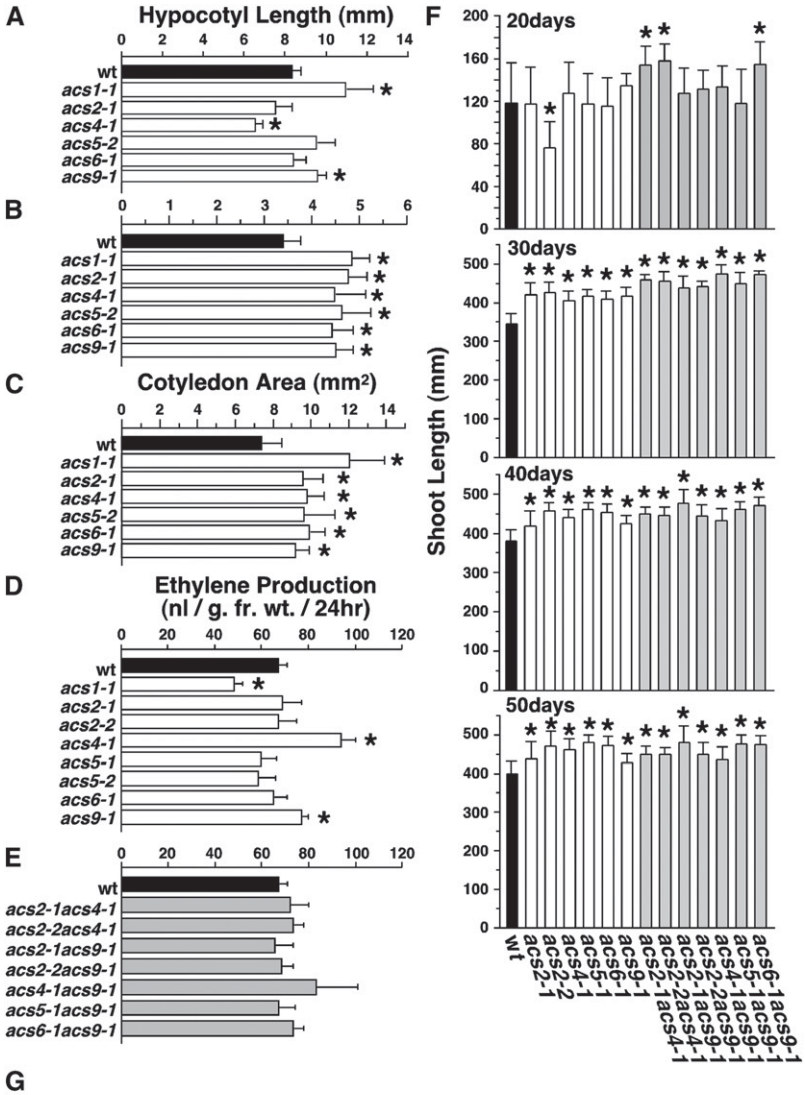

FIGURE 1.—Effect of the *acs* single and double mutants on various phenotypic parameters. Comparison of the hypocotyl length among wt and *acs* single mutants in 3-day-old etiolated is shown in A and in 10-day-old light-grown seedlings is shown in B. Comparison of the cotyledon area among wt and *acs* single mutants in 10-day-old light-grown seedlings is shown in C ($N = 10$ in A, B and C). (D) Comparison of the ethylene production among wt and *acs* single (D) and double (E) mutants in 5-day-old light-grown seedlings ($N = 3$ in D and E). Effect of single and double mutants on the shoot length of soil-grown plants during different developmental stages is shown in F ($N = 10$). The phenotypes of 40-day-old light-grown plants of wt and single mutants are shown in G. Bars represent the standard deviation (SD). The asterisk (*) above the bars indicates statistically significant difference between the mutant and the wt ($P < 0.01$). The absence of an asterisk indicates statistically insignificant difference between the mutant and the wt ($P > 0.05$).

of growth (20 day old). The *acs2-2* plants are much shorter than the wt plants, but another allele of *ACS2*, *acs2-1*, has no effect on plant height (Figure 1F/ 20 day old). However, after 30 days of growth all single mutants exhibit an obvious and statistically significant increase in height (Figure 1F). A visual phenotypic comparison of 40-day-old wt plants with those of single mutants is shown in Figure 1G.

The most prominent effect of inactivating multiple *ACS* genes is enhancement of plant height. Some of the double mutants examined, such as *acs2-1acs4-1* and *acs2-2acs4-1*, are taller than the single mutants during the early stages of plant growth (Figure 1F; compare the height of single with that of the double mutants after 20 days of growth), and all double mutants are taller than the single mutants after 30 days of growth (Figure 1F). However, as growth progresses there is no significant difference in shoot length between single and double mutants (Figure 1F; 50 days of growth). Overall,

the single mutants examined have phenotypic characteristics similar to wt plants. For example, their rosette leaf number, silique length, and seed number/silique are normal (Figure S2, A, C, and D). However, the diameter of the inflorescence stem of *acs1-1* is thinner than that of the wt (Figure S2B).

Ethylene production: Ethylene production is unaffected by inactivation of the ACS2, ACS5, and ACS6 isozymes (Figure 1D). However, inactivation of ACS1 (inactive isozyme) inhibits ethylene production by ~30% (Figure 1D). An enhancement in ethylene evolution is observed in the *acs4-1* (40%) and *acs9-1* (15%) mutants (Figure 1D). While single *acs* mutations have broad effects on ethylene production, ranging from inhibition to stimulation, this effect is not apparent in double *acs* mutants (Figure 1E).

Flowering time: The *acs1-1*, *acs6-1*, *acs7-1*, and *acs9-1* single mutants start to form bolts earlier than wt (Figure 2A); *acs2-1*, *acs4-1*, and *acs5-2* start to bolt at the same time as wt (Figure 2A). A strong antagonistic interaction between the two early flowering mutants, *acs6-1* and *acs7-1*, was noticed (Figure 2B). While both single mutants flower earlier than wt, the *acs6-1acs7-1* double mutant flowers later than wt (Figure 2, B and C). The double mutant has a higher rosette leaf number than the single mutants, consistent with its late flowering phenotype. Ethylene production is slightly inhibited by loss of *ACS7*, and is unaffected by loss of *ACS6* (Figure 2D). However, the inactivation of both genes enhances the loss of ethylene production detected in the *acs7-1* mutant (Figure 2D). These results reveal that total ethylene production by a seedling is not a good predictor for the flowering behavior of the mutants. While loss of ethylene production in the double mutant results in late flowering, slight (*acs7-1*) or no loss (*acs6-1*) of ethylene production in the single mutants results in early flowering. It appears that the amount of ethylene produced at the site(s) responsible for flowering initiation (leaf primordia in shoot apical meristem region; SAM) is likely the key determinant of flowering time.

The inhibitory effect of the *acs6-1acs7-1* double mutant on flowering time prompted us to investigate the expression of key regulators of flowering in young seedlings. The most dramatic effect of the double mutant is on the gene expression of the *FLOWERING REPRESSOR C* (*FLC*; Figure 2E). The *FLC* expression is enhanced in the double mutant compared to the wt control and the two single, *acs6-1* and *acs7-1* mutants in both 3- and 7-day-old seedlings (Figure 2E). The expression of *FLC* is inhibited in the *acs7-1* but is expressed in similar levels to the wt control in the *acs6-1* mutant (Figure 2E). Concomitantly with the increase in *FLC* gene expression, a decrease in the expression of the positive flowering regulator *FLOWERING LOCUS T* (*FT*) is detected in the double mutant compared to the wt and the two single mutants (Figure 2E). However, the *FT* expression is enhanced in the two early flowering single mutants compared to the wt in 7-day-old seedlings, which is consistent with their early flowering phenotype (Figure 2E). *FT* expression is undetectable in 3-day-old seedlings (Figure 2E). We noticed less dramatic changes in the expression of *SUPPRESSOR OF OVEREXPRESSION OF CONSTANS 1* (*SOC1*), a positive flowering regulator, in all three mutants, compared to the wt control in 7-day-old seedlings (Figure 2E). However, an enhancement in *SOC1* expression is detected in *acs7-1* in 3-day-old seedlings (Figure 2E). Finally, the expression of *CONSTANS* (*CO*) does not show any dramatic changes in any mutant in both 3- and 7-day-old seedlings, although its expression is slightly enhanced in the double mutant (Figure 2E).

Complementation of acs6-1 and acs9-1 mutants: To determine whether differences in flowering time of some single mutants is indeed due to the T-DNA insertions rather than to mutations in other chromosomal loci, we complemented the *acs6-1* and *acs9-1* mutations by transforming them with the corresponding full-length *cDNAs* expressed from their own promoters. A wide range of flowering time was observed among the transformants. Lines with flowering time similar to wt were among the transformants, indicating complementation and suggesting that the early flowering phenotype is linked to the T-DNA insertion in the corresponding gene. Surprisingly, some lines flowered later than wt plants. While the majority of the *acs9-1* transformants have a late flowering phenotype, only one *acs6-1* transformant (line no. 29) flowers later (compare the results shown in Figure S3A with those shown in Figure S3B). We were curious to know why complementation of two loss-of-function mutations, *acs6-1* and *acs9-1* (early flowering) with their corresponding *cDNAs*, gives rise to plants with a gain-of-function phenotype (late flowering). We investigated further some lines of both mutants that flower like wt, and some lines that flower early, like the mutants (early flowering), and some lines that flower late [Figure 2, F (*acs6-1*) and I (*acs9-1*)]. The expression profiles of the various *ACS* gene family members are altered and are different among the three types of transformants. Their *ACS* expression profiles are also different when compared to those of the wt and to the untransformed mutant lines (see Figure 2, G and J1, which show a quantitation of the RT–PCR data). For example, the RNA expression pattern of the line that flowers like wt is different from that of the wt control and both mutants (see Figure 2, G and J1). The same is true for the early- and late-flowering lines and the original mutants (Figure 2, G and J1). We noticed that the late flowering mutant *acs6-1* (line no. 29) overexpresses the *ACS6* transcript (Figure 2G). The absence of *ACS1* and *ACS9* transcripts in the data of Figure 2 (G and J1) is due to their low abundance in total RNA. However, we were able to detect overexpression of the *ACS9* transcript in the late flowering line no.18 of *acs9-1* using polyA$^+$ RNA for the RT–PCR analysis (Figure 2J2). The overexpression

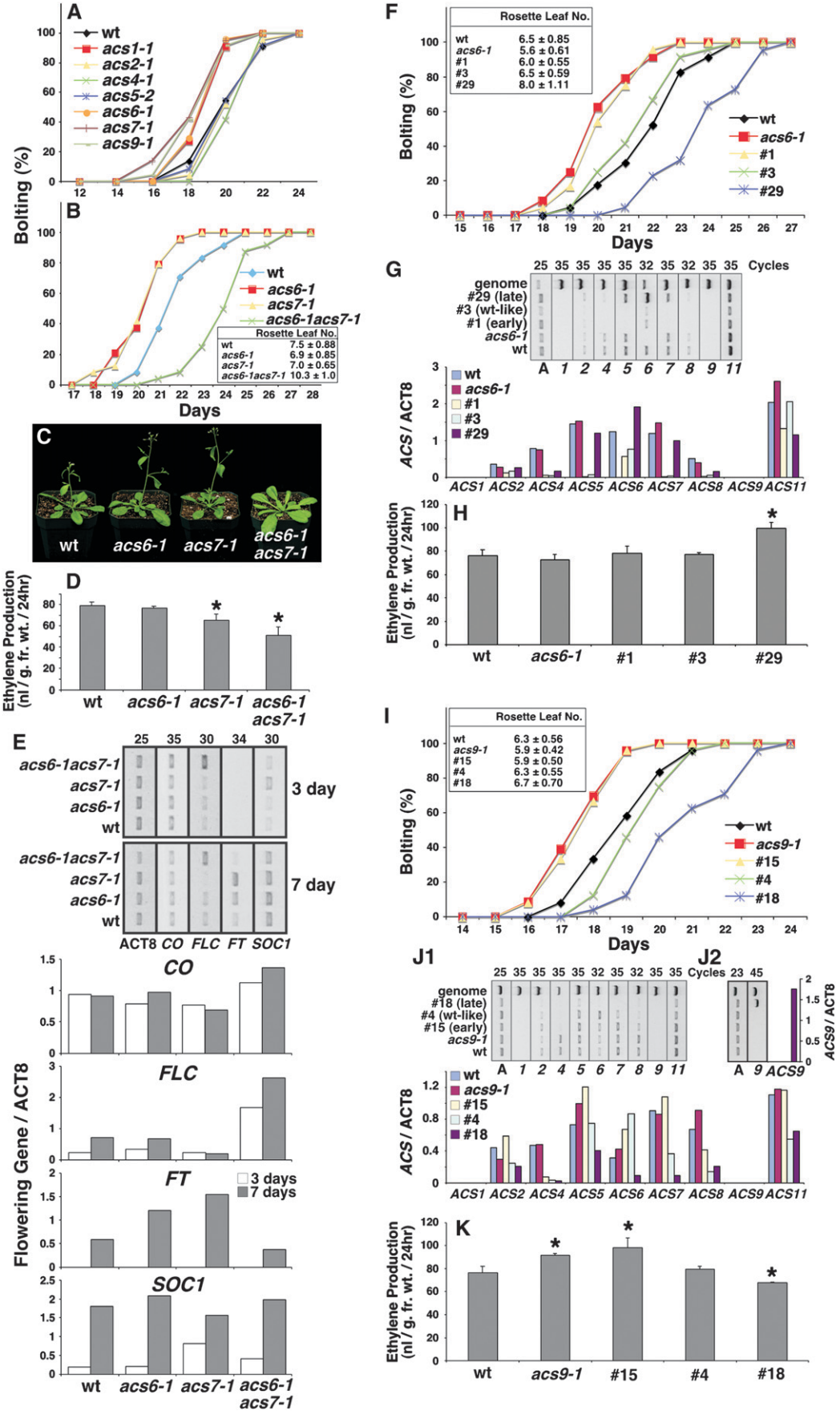
A
wt
acs1-1
acs2-1
acs4-1
acs5-2
acs6-1
acs7-1
acs9-1
Bolting (%)
B
wt
acs6-1
acs7-1
acs6-1acs7-1
Rosette Leaf No.
wt 7.5 ± 0.88
acs6-1 6.9 ± 0.85
acs7-1 7.0 ± 0.65
acs6-1acs7-1 10.3 ± 1.0
Days
C
wt
acs6-1
acs7-1
acs6-1 acs7-1
D
Ethylene Production (nl / g. fr. wt. / 24hr)
wt
acs6-1
acs7-1
acs6-1 acs7-1
E
acs6-1acs7-1
acs7-1
acs6-1
wt
3 day
7 day
ACT8 CO FLC FT SOC1
Flowering Gene / ACT8
CO
FLC
FT
SOC1
3 days
7 days
F
Rosette Leaf No.
wt 6.5 ± 0.85
acs6-1 5.6 ± 0.61
#1 6.0 ± 0.55
#3 6.5 ± 0.59
#29 8.0 ± 1.11
Bolting (%)
Days
G
Cycles
genome
#29 (late)
#3 (wt-like)
#1 (early)
acs6-1
wt
ACS / ACT8
ACS1 ACS2 ACS4 ACS5 ACS6 ACS7 ACS8 ACS9 ACS11
H
Ethylene Production (nl / g. fr. wt. / 24hr)
wt
acs6-1
#1
#3
#29
I
Rosette Leaf No.
wt 6.3 ± 0.56
acs9-1 5.9 ± 0.42
#15 5.9 ± 0.50
#4 6.3 ± 0.55
#18 6.7 ± 0.70
Bolting (%)
Days
J1
J2
genome
#18 (late)
#4 (wt-like)
#15 (early)
acs9-1
wt
ACS / ACT8
ACS9 / ACT8
K
Ethylene Production (nl / g. fr. wt. / 24hr)
wt
acs9-1
#15
#4
#18

of *ACS6* and *ACS9* transcripts in the late flowering mutants *acs6-1* (line no. 29) and *acs9-1* (line no. 18) may be due to high copy number of transgenes or to higher promoter activity due to a chromosomal position effect.

The different *ACS* gene expression patterns observed in the three types of transformant lines are reflected in the different amounts of ethylene produced in their 5-day-old light-grown seedlings. The early-flowering transformant of *acs6-1* (line no. 1) produces the same amount of ethylene as the *acs6-1* mutant and the wt control. The wt-like line no. 3 also produces the same amount of ethylene as the wt control, but the late-flowering line no. 29 is an ethylene overproducer (Figure 2H). Transformation of *acs6-1* created two new mutants; one that produces the same amount of ethylene as *acs6-1* but that flowers as the wt, and another that overproduces ethylene and flowers later than wt. The results of the *acs9-1* lines are different. The early-flowering line no. 15 produces more ethylene than the wt and the original *acs9-1* mutant, while the wt-like transformant line produces the same amount of ethylene as wt. Interestingly, production of ethylene in the late-flowering line of *acs9-1* is inhibited 10% (Figure 2K). These observations suggest that total ethylene production of an intact seedling is not a good predictor of flowering time. While the two late flowering lines of *acs6-1* and *acs9-1* mutants produce different amounts of ethylene compared to the wt control, they both have the same flowering time phenotype (compare the results of Figure 2H with those of K). Furthermore, we were surprised to observe that the transformant lines are also defective in their response to gravitostimulation and growth characteristics. The response to gravity was reduced in the late-flowering line of *acs6-1*, and all three lines of *acs9-1* have a reduced response to gravitostimulation (see Figure S4, A–C). On the other hand the hypocotyl growth of etiolated seedlings is enhanced in all three lines of both *acs6-1* and *acs9-1* transformants (Figure S4, A–C).

These results reveal a communication network among the ACS proteins. We imagine that introduction of an exogenous *ACS* gene disturbs the balance of ACS isoforms. Since ethylene is known to stimulate its own synthesis, the possibility exists that the exogenous *ACS* gene causes local changes in ethylene production (*e.g.*, leaf primordial in the SAM region) that alter the expression of various *ACS* gene family members. Also the striking phenotypes described earlier with the inactivation of ACS1 alone (*acs1-1*), which forms an inactive homodimer, are attributed to the loss of ACS1 heterodimers with other ACS isoforms.

Construction of high order mutants: We generated double, *triple*, *quadruple*, and *pentuple* mutants with the various insertion lines shown in Figure S1A. We did not characterize the double, *triple*, and *quadruple* mutants phenotypically in a great detail because of the large number of them and the absence of dramatic phenotypes. The most prominent effect of inactivating multiple *ACS* genes is the enhancement of plant height.

***pentuple* mutants:** *Plant growth:* All four *pentuple* mutants characterized are taller than the wt during the entire period of plant growth and development (Figure 3, A and C). Hypocotyl length of 10-day-old light-grown seedlings is longer in all four *pentuple* mutants compared to wt (Figure 3B). We subsequently compared the growth characteristics between the *pentuple2* with two ethylene perception mutants, *ein2-5* (Alonso *et al.* 1999) and *etr1-1* (Chang *et al.* 1993), respectively. The hypocotyl length of the *pentuple2*, *ein2-5*, and *etr1-1* etiolated (3 day old) and light-grown (10 day old) seedlings is longer than that of wt (Figure 3D). The *pentuple2* and *ein2-5* mutants are taller than wt throughout the plant life cycle; *etr1-1* plants become taller than the wt after 2 months of growth (Figure 3E). The *pentuple2* mutant, however, has a wt-like hook, in contrast to the hookless phenotype of *ein2-5* and *etr1-1* plants (Figure 3F). Since hypocotyl lengths are longer than the wt, the cortical cell length of 10-day-old light-grown *pentuple2*, *ein2-5*, and *etr1-1* mutant seedlings is

Figure 2.—Flowering time in the *acs* mutants. Effect of the *acs* single mutants (A) and *acs6-1acs7-1* double mutant (B) on flowering time ($N = 20$ in A and B). The inserted table in B shows the number of rosette leaves at the time of flowering initiation ($N = 20$). The phenotypes of 30-day-old light-grown plants of wt, *acs6-1*, *acs7-1*, and *acs6-1acs7-1* are shown in C and their ethylene production in 5-day-old light-grown seedlings is shown in D ($N = 3$). Expression of key flowering regulators in wt, *acs6-1*, *acs7-1*, and *acs6-1acs7-1* in 3- and 7-day-old light-grown seedlings is shown in E. The *ACT8* gene was used as a nondifferential expressed gene. Quantitation of the RT–PCR expression data is shown at the bottom of the panel. Complementation of the *acs6-1* mutant (F–H). The flowering time of the wt, *acs6-1*, and complementation line nos. 1, 3, and 29 is shown in F. The inserted table in F shows the number of rosette leaves at the time of flowering initiation (F; $N = 20$). The expression of the various *ACS* gene family members in wt, *acs6-1*, and complementation line nos. 1, 3, and 29 in 5-day-old light-grown seedlings is shown in G. The expression of each *ACS* gene was assessed by RT–PCR with total RNA and the "black set of primers" shown in Figure S1A.The *ACT8* gene was used as a nondifferential expressed gene. The number of PCR cycles is shown on the top of the panel. The graph shows quantitation of the *ACS* gene expression. The data were normalized relatively to the *ACT8* expression level (see materials and methods). Comparison of the ethylene production among wt, *acs6-1*, and complementation line nos. 1, 3, and 29 in 5-day-old light-grown seedlings is shown in H ($N = 3$). Complementation of the *acs9-1* mutant (I–K). The panels I–K present the data of similar experiments as panels F–H above except for the *acs9-1* mutant and its complementation line nos. 15, 4, and 18. The expression of the various *ACS* gene family members in panel J1 was also assessed using total RNA but the expression of the low abundance *ACS9* mRNA was also determined using polyA$^+$ RNA as shown in J2. Bars represent the standard deviation (SD). The asterisk (*) has been defined in the legend of Figure 1.

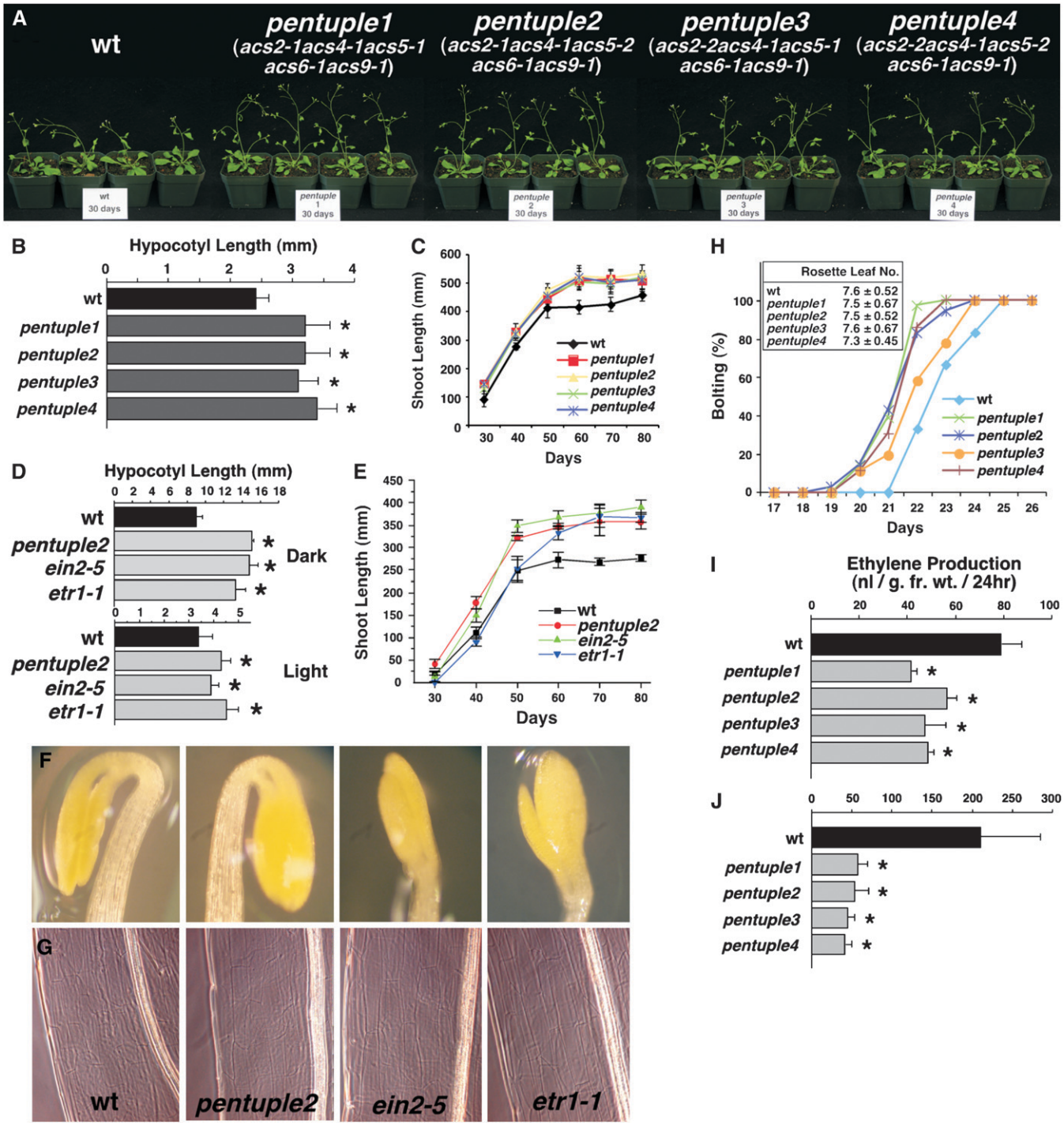

FIGURE 3.—Characterization of the *pentuple* mutants. The phenotypes of wt and various *pentuple* mutants of 30-day-old light-grown plants are shown in A. The *pentuple* mutants are *pentuple1*, *acs2-1acs4-1acs5-1acs6-1acs9-1*; *pentuple2*, *acs2-1acs4-1acs5-2acs6-1acs9-1*; *pentuple3*, *acs2-2acs4-1acs5-1acs6-1acs9-1*; and *pentuple4*, *acs2-2acs4-1acs5-2acs6-1acs9-1*. Comparison of the hypocotyl length in 10-day-old light-grown seedlings among wt and various *pentuple* mutants is shown in B. Similar comparison of the shoot length of light-grown plants during various stages of development is shown in C. $N = 10$ in both panels (B) and (C). Comparison of the hypocotyl length among wt, *pentuple2*, *ein2-5*, and *etr1-1* in 3-day-old etiolated seedlings and 10-day-old light-grown seedlings is shown in D ($N = 10$). Comparison of the shoot length of light-grown plants among wt, *pentuple2*, *ein2-5*, and *etr1-1* during various stages of development (E; $N = 10$). Hook formation in wt, *pentuple2*, *ein2-5*, and *etr1-1* in 3-day-old etiolated seedlings is shown in F. Hypocotyl cell size of wt, *pentuple2*, *ein2-5*, and *etr1-1* in 7-day-old light-grown seedlings is shown in G. The effect of the *pentuple* mutants on flowering time is shown in H ($N = 20$). The ethylene production in 5-day-old light-grown seedlings is shown in E ($N = 4$) and in 1-month-old light-grown *pentuple* plants is shown in F ($N = 6$). The asterisk (*) has been defined in the legend of Figure 1.

longer than in wt plants (Figure 3G), suggesting that their longer hypocotyl size is due to longitudinal cell expansion rather than an increase in cell number.

Flowering time: All the *pentuple* mutants start to flower earlier than do wt plants (Figure 3H). Rosette leaf number is the same in all four mutants and is similar to the rosette leaf number of wt plants, even though the mutants start to bolt earlier than wt (see inserted table in Figure 3H).

Ethylene production: Ethylene production is inhibited ~40% in young 5-day-old light-grown seedlings of the *pentuple1*, *3*, and *4* mutants; the inhibition is slightly smaller (30%) in the *pentuple2* mutant (Figure 3I). The inhibition of ethylene production is greater (almost 80%) in 1-month-old intact plants in all four *pentuple* mutants (Figure 3J). These results are consistent with the view that loss of ethylene biosynthetic capacity results in early flowering. Additional phenotypic parameters were studied and quantified during the course of the characterization of the *pentuple2* mutant. The findings are summarized in Table S1 and show that 80% loss in ACS biosynthetic capacity in the *pentuple2* mutant causes mild phenotypic abnormalities.

***hexuple*, *heptuple*, and *octuple* mutants:** Our ultimate goal was to construct a null ACS mutant in Arabidopsis. When the project initiated 9 years ago, we were able to identify insertions of five genes (*ACS2*, *ACS4*, *ACS5*, *ACS6*, and *ACS9*) leading to the construction and characterization of the *pentuple* mutants. However, 3 years ago the identification of insertion mutations in *ACS1* and *ACS7* enabled the construction of a *hexuple* mutant; *acs2-1acs4-1acs5-2acs6-1acs7-1acs9-1* and a *heptuple* mutant; *acs1-1acs2-1acs4-1acs5-2acs6-1acs7-1acs9-1*. Mutations in the two remaining genes, *ACS8* and *ACS11*, are not available, so we used artificial micro RNA (*amiR*) technology to inhibit their activity. An *amiR* sequence was designed to specifically inhibit both genes according to the rules described by Schwab *et al.* (2006). This *amiR* was introduced by transformation into the *hexuple* mutant, giving rise to the *octuple* mutant; *acs2-1acs4-1acs5-2acs6-1acs7-1acs9-1amiRacs8acs11*. The *hexuple* background was used for the construction of the *octuple* mutant to expedite the process since the *ACS1* gene, which is not inactivated in the *octuple* mutant, encodes an inactive homodimer, and its heterodimers ACS1/ACS8 and ACS1/ACS11 are also enzymatically inactive (Tsuchisaka and Theologis 2004a).

Growth of mature plants: The growth phenotypes of high order mutant plants during various stages of plant development are shown in Figure 4, A and B. The height of the *pentuple2*, *hexuple*, and *heptuple* mutants is greater than that of the wt after 40 days of growth, but the height of the *octuple* mutant is similar to that of the wt control (Figure 4A). However, the height of the *octuple* becomes greater than that of wt plants and very similar to that of the other high order mutants after 50 days of growth (Figure 4B). Eventually the *octuple* plants are the tallest among all the high order mutants (Figure 4C). Growth of the *octuple* mutant is delayed during the initial stages of plant development. The *octuple* plants are less bushy due to the reduced branching (Figure 4B). One of the most prominent characteristic of the *octuple* plants is their delayed senescence. While the wt, *pentuple2*, *hexuple*, and *heptuple* mutant plants start to senesce after 60 days of growth the *octuple* mutant plants are quite green and healthy.

Growth of seedlings: The hypocotyl length of etiolated seedlings is greatly enhanced in all four high order mutants compared to the wt control. There is a progressive increase in hypocotyl length among the *pentuple2*, *hexuple*, and *heptuple* mutants, but a reduction in the *octuple* mutant (Figure 4E). Two prominent phenotypic changes were observed in the *hexuple*, *heptuple*, and *octuple* mutants that are not seen in the *pentuple2* mutant. First, there is progressive loss of hook formation among these three mutants; the *octuple* mutant is hookless (Figure 4E). Second, their response to gravitostimulation is also greatly reduced compared to the wt control and *pentuple2* mutant (Figure 4G).

The enhancement of hypocotyl length in light-grown seedlings observed in the *pentuple2* mutant is inhibited in *hexuple*, *heptuple*, and *octuple* mutants (Figure 4F). Their hypocotyl lengths are similar to the wt control (Figure 4F). Two prominent phenotypic characteristics of light-grown *octuple* seedlings are as follows:

(1) reduced size of cotyledons compared to the wt control and to the other three high order mutants (Figure 4F).
(2) the size and shape of its leaves: the leaf blade is smaller and has a downward curling tip (Figure 4D), reminiscent of the *ifl1/rev* mutation of the *INTERFASCICULAR FIBRLESS/REVOLUTA* gene (Talbert *et al.* 1995).

The overall plant architecture of the *octuple* mutant plant is similar to the *ifl1/rev* with its cauline paraclades highly elongated (Talbert *et al.* 1995). This mutation is defective in auxin transport/signaling, resulting in abnormal fiber and vascular differentiation (Zhong and Ye 2001). All other high order mutants have normal leaves (data not shown).

Flowering time: The early flowering phenotype of the *pentuple2* mutant is greatly enhanced in the *hexuple* and *heptuple* mutants (Figure 5A). This phenotype is absent from the *octuple* mutant, but it still flowers somewhat earlier than do wt plants (Figure 5A). The number of rosette leaves is reduced in all mutants, but most dramatically in the *hexuple* and *heptuple* mutants (see inserted table in Figure 5A), a phenotypic characteristic that is in agreement with the observed early flowering phenotype.

The strong effect of the high order mutations on flowering time prompted us to investigate the expression of key regulators of flowering in young seedlings.

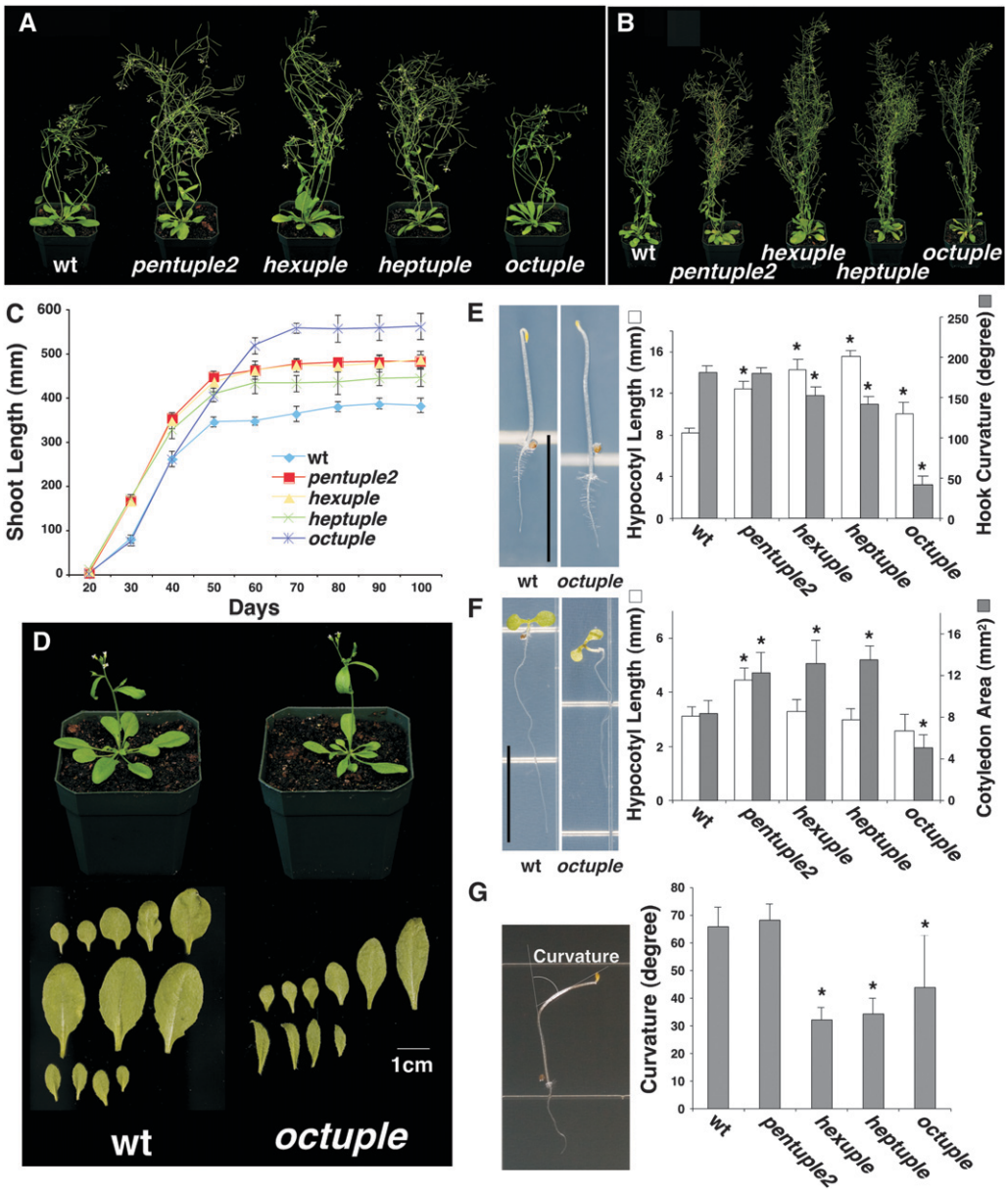

FIGURE 4.—Growth characteristics and phenotypic comparison among the high order mutant plants. The phenotypes of 40- (A) and 50-day-old mutant plants (B) are shown. The shoot length of the wt, *pentuple2*, *hexuple*, *heptuple*, and *octuple* light-grown mutant plants during various stages of development is shown in C ($N = 10$). The phenotypes of 30-day-old wt and *octuple* plants grown on soil are shown at the top, and their leaf number and shape are shown at the bottom of panel D. Bar = 1 cm. The photo in E compares the phenotypes of 3-day-old etiolated seedlings between wt and *octuple* mutant. Bar = 1 cm. The graph compares the hypocotyl length and hook curvature among wt, *pentuple2*, *hexuple*, *heptuple*, and *octuple* mutants ($N = 20$). The photo in F compares the phenotypes of 5-day-old light-grown seedlings between wt and *octuple* mutant. Bar = 1 cm. The graph compares the hypocotyl length and cotyledon area among wt, *pentuple2*, *hexuple*, *heptuple*, and *octuple* mutants ($N = 20$). The gravitotropic response of the various high order mutants in 3-day-old etiolated seedlings after 24 hr of gravitostimulation is shown in G ($N = 20$). Bars represent the standard deviation (SD). The asterisk (*) has been defined in the legend of Figure 1.

The most dramatic effect of the high order mutations is their inhibitory effect on expression of the flowering repressor *FLC* in 3- and 9-day-old seedlings (Figure 5B). Concomitantly with the decrease in *FLC* gene expression, an increase in *FT* gene expression is detected in the *hexuple*, *heptuple*, and *octuple* mutants in 3-day-old seedlings (Figure 5B). The *FT* expression is greatly enhanced in 9-day-old seedlings and is higher than in wt plants in all mutants (Figure 5B). The *SOC1* activator is expressed at low levels in 3-day-old seedlings and its expression is greatly enhanced in older seedlings. All mutants express *SOC1* at a level similar to that in the wt control in both 3- and 9-day-old seedlings (Figure 5B). *CO* gene expression does not show any dramatic changes in any mutant in both 3- and 9-day-old seedlings (Figure 5B). The early flowering phenotype of the high order mutants raises the question of whether all *ACS* gene family members are expressed in the leaf primordial where FLC exerts its negative role on FT (WIGGE *et al.* 2005; SEARLE *et al.* 2006). Figure 5C shows longitudinal sections of 5-day-old light-grown seedlings of *ACSpromoter-GUS* lines, showing that all *ACS* genes except *ACS9* are expressed in the shoot apical meristems (SAM) and in the neighboring tissues such as leaf primordial, stipules and the vasculature at that stage of development.

Ethylene production: Ethylene production is greatly inhibited in all high order mutants, with the *octuple* mutant having the lowest ethylene evolution in both 10-

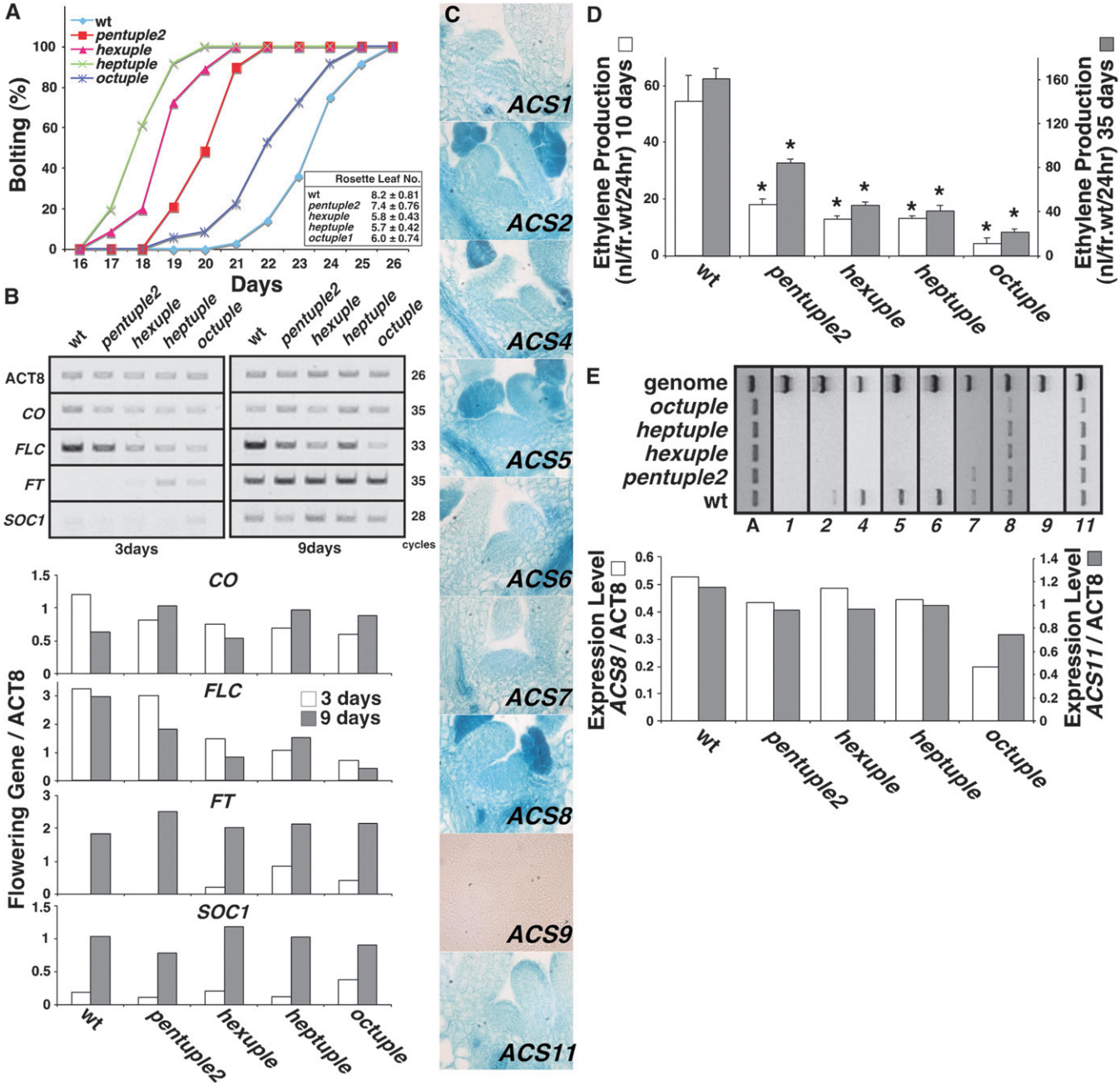

FIGURE 5.—Flowering time of the high order mutants (A–C). The flowering time of the high order mutants is shown in A ($N = 20$). The inserted table in A shows the number of the rosette leaves at the time of flowering ($N = 20$). The expression of key flowering regulators in wt, *pentuple*, *hexuple*, *heptuple*, and *octuple* in 3- and 9-day-old light-grown seedlings is shown in B. The *ACT8* gene was used as a nondifferential expressed gene. Quantitation of the RT–PCR expression data is shown at the bottom of the panel (see Experimental Procedures in File S1). The expression of the *ACS* gene family members in the region of the shoot apical meristems is shown in C. The panel shows longitudinal sections of 5-day-old light-grown *ACSpromoter-GUS* transgenic seedlings. Tissue sectioning was performed after 12 hr of GUS staining. Section thickness, 8 μm. *ACS* gene expression and ethylene production in the high order mutants (D and E). The ethylene production in 10- and 35-day-old light-grown wt, *pentuple2*, *hexuple*, *heptuple*, and *octuple* mutants is shown in D ($N = 4$). Bars represent the standard deviation (SD). The *ACS* gene expression in the *pentuple2*, *hexuple*, *heptuple*, and *octuple* mutants is shown in E. Five-day-old light-grown seedlings were collected and the expression of each *ACS* gene was accessed by RT–PCR using total RNA (see MATERIALS AND METHODS). The graph below shows quantitation of the *ACS8* (gray bar) and *ACS11* (white bar) gene expression data. The data were normalized relatively to the *ACT8* expression level (see MATERIALS AND METHODS).

day-old seedlings and 35-day-old plants (Figure 5D). Ethylene production is inhibited by 92 and 86% in the *octuple* seedlings and mature plants, respectively (Figure 5D). Both *hexuple* and *heptuple* mutants produce approximately the same amount of ethylene in both tissues, which corresponds to ~25% of the ethylene produced

by wt plants (Figure 5D). RT–PCR analysis with RNA from 5-day-old seedlings indicates that the low but detectable amount of ethylene produced by the *octuple* mutant is due to the incomplete inhibition of *ACS8* and *ACS11* gene expression by the *amiR* (Figure 5E). Inactivation of multiple *ACS* genes does not cause an enhancement of gene expression of the noninactivated genes (Figure 5E). For example, *ACS7*, *8*, and *11* gene expression in the *pentuple2* mutant is the same as in the wt control (Figure 5E). The same is true for the *hexuple* and *heptuple* mutants, where the expression of *ACS8* and *11* is not altered compared to the *pentuple2* mutant (Figure 5E). *ACS1* mRNA is of very low abundance and cannot be detected in isolated total or polyA$^+$ RNA.

Embryo lethality in the octuple/amiR lines: Attempts to isolate additional homozygous *octuple* mutant lines that produce less ethylene were unsuccesful. We screened 62 independent *amiR* transformants (out of 192 total) that were determined to have the *amiR* construct at a single locus and were unable to isolate another homozygous *octuple* line that produced less ethylene and expressed lower amounts of the *ACS8* and *11* mRNAs than the *octuple* line described above. These results suggested to us that such an *octuple* mutant line may not exist because it is not viable. Indeed, that was the case because the siliques of T1 plants from 24 independent *amiR* lines show signs of embryo lethality (Figure 6A). We see three types of siliques: some are like the ones of line no. 3; others are like those of line no. 20; others are like those of no. 24 (Figure 6A). Closer examination of the siliques of the viable *octuple* line show that they are shorter than those of the control, contain half of the seeds present in siliques of wt plants, and show signs of embryo lethality because of empty seed spaces (Figure 6B). It is interesting that heterozygous *octuple* plants have normal silique length but half the number of seeds than do wt plants and also show signs of embryo lethality (Figure 6B). The other high order mutants have normal size siliques and the same amount of seeds/silique as the wt control (Figure 6C). Furthermore, the embryonic lethality associated with the octuple mutant lines was recently confirmed by the isolation of a second *octuple* line that exists only as a heterozygous plant. No homozygous plants can be recovered from its progeny. Segregation analysis shows that seeds from this heterozygous line segregate in a ratio of 1 *hexuple* to 1 heterozygous for the *amiR* insertion. This ratio suggests male or female gametophytic defect in this second *octuple* line. A phenotypic comparison between these two *octuple* lines is presented in Figure S5. The results show that both lines have quite similar phenotypes but the silique phenotype is attenuated in the heterozygous line. All the experiments reported here have been carried out with the homozygous *octuple* line.

Specificity of the amiR: Is the embryonic lethality and the various seedling phenotypes observed in the *octuple* mutant lines due to the inhibition of *ACS8* and *11* gene expression by the *amiR* or is due to inhibition of other genes necessary for these various phenotypes? We carried out three experiments to address this question.

(1) We rescued the *octuple* light-grown and etiolated seedling phenotypes by germinating mutant seeds on plates containing various amounts of the ethylene precursor, ACC (Figure S5). The phenotypes of both types of *octuple* mutant seedlings reverted back to the wt phenotype (Figure S5). The *octuple* mutant leaves were wt-like after ACC treatment (Figure S5, A and B). However, the *octuple* is hypersensitive to ACC compared to the wt: the roots of the *octuple* are shorter and have a proliferation of root hairs, unlike the wt (Figure S5, A and B). The growth of *octuple* etiolated seedlings is inhibited to the same degree as in wt with exogenous ACC and their hookless phenotype is reverted to wt-like (Figure S5, C and D). They also show a hypersensitivity to ACC because of root hair proliferation unlike the wt (Figure S5, C and D). For both types of seedlings, the basis of this observed ACC hypersensitivity is unknown.

(2) We rescued the *octuple* phenotype by backcrossing the mutant to wt and selecting segregants that are homozygous for the *amiR* insertion but have lost the T-DNA insertion from various *ACS* genes. We isolated and analyzed five such segregant lines (Figure 6G). A visual comparison among the *octuple* mutant and the backcrossed lines in 20-day light-grown plants shows that the *octuple* phenotype has been reverted back to the wt- or *hexuple*-like phenotype. The small size and abnormal morphology of the rosette leaves, a prominent characteristic of the *octuple* mutant is reverted back to almost the wt- or *hexuple*-like rosette leaves in all lines (Figure 6D). Furthermore the small silique size and low seed number of the *octuple* mutant reverted to the wt-like phenotype (Figure 6, E and F). These data clearly show that the *ACS8* and *ACS11* genes are not essential for Arabidopsis viability and that the embryonic lethality of the *octuple* lines is not due to the nonspecific effect of the *amiR*. While the *octuple* silique phenotype is revered back to wt-like by activating endogenous *ACS* genes the phenotype of *octuple* siliques from ethylene-treated plants fail to revert back to wt-like (Figure S7, A, B, and C). This suggests that the embryonic lethality associated with the *octuple* phenotype maybe due to the low availabilty of endogenous ACC.

(3) We complemented the *octuple* mutant with a transgene that expresses *ACS8* and *ACS11* cDNAs with altered *amiR* target sequences but that encode enzymatically active isozymes. Three lines (nos. 8, 10, and 14) homozygous for the introduced transgene were isolated and compared to the *hexuple* mutant. A visual comparison among the mutant

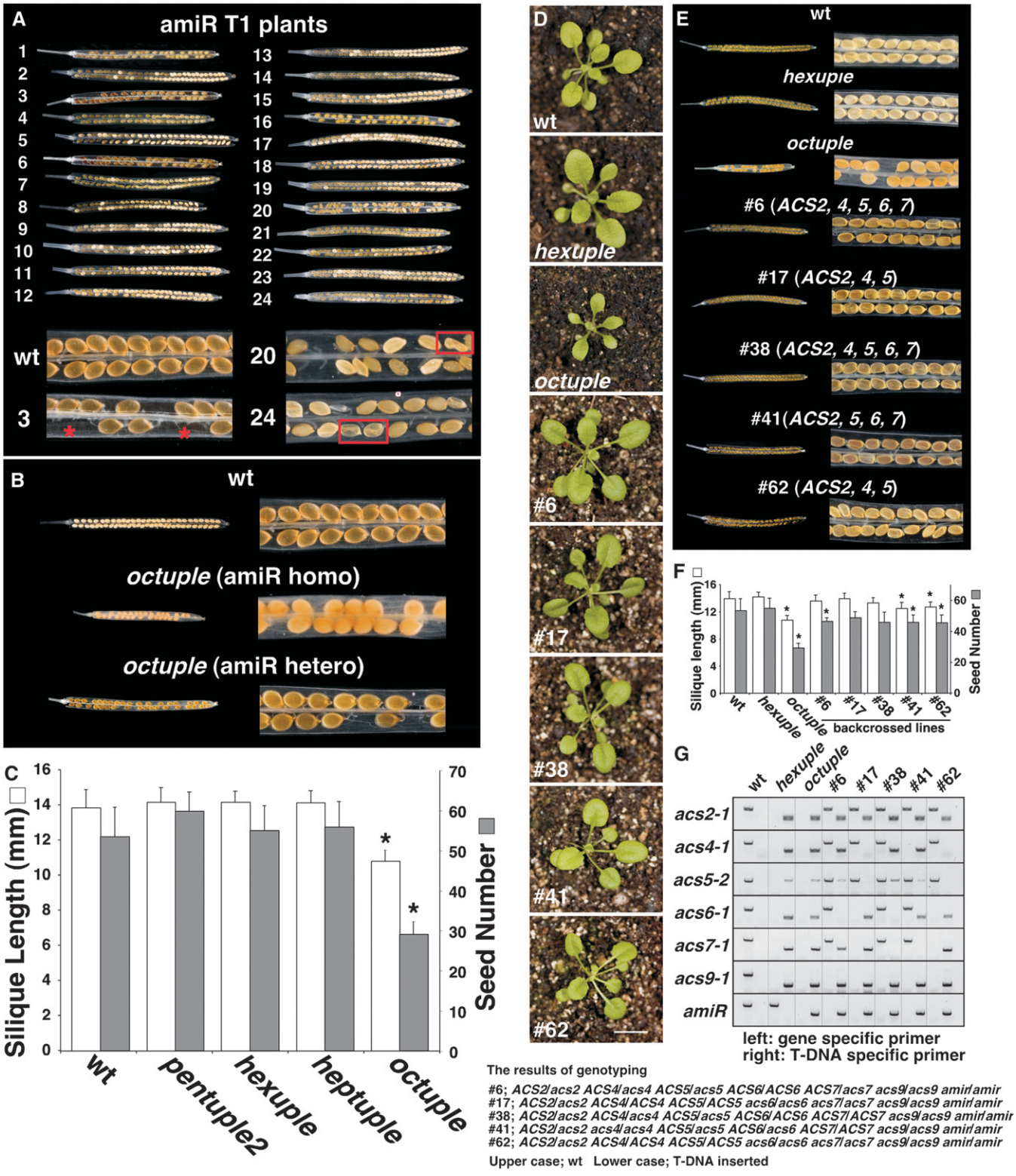

FIGURE 6.—Embryo lethality of the *octuple/amiR* lines (A–C). The siliques from 24 T1 independent *amiR* plants are shown in A, indicating embryo lethality. The three magnified siliques at the bottom show prezygotic lethality marked with an asterisk and embryonic lethality marked with a box. The silique morphology and seed content of the heterozygous and homozygous *octuple* (*amiR*) plants are shown in B. The silique length and seed content in the high order mutants are shown in C ($N = 10$). Bars represent the standard deviation (SD). The asterisk (*) has been defined in the legend of Figure 1. Rescue of the *octuple* mutant phenotype by backcrossing to wt (D–G). The photos in D compare the phenotypes of 20-day-old light-grown plants among wt, *hexuple*, *octuple*, and five backcrossed lines. Bar = 1 cm. The silique morphology of the backcrossed lines expressing different *ACS* genes is shown in E. Quantitative comparison of the silique length and seed content of the backcrossed lines among the wt, *hexuple*, and *octuple* mutants is shown in F ($N = 10$). The genotyping of the backcrossed lines is shown in G. The genotypes of the backcrossed lines are shown at the bottom. Bars represent the standard deviation (SD). The asterisk (*) has been defined in the legend of Figure 1.

and complemented lines in both etiolated and light-grown seedlings shows that the *octuple* phenotype has been reverted to the *hexuple*-like phenotype (Figure 7, A and B) The hookless phenotype of the etiolated *octuple* mutant seedlings is reverted to the *hexuple*-like hook in all three complemented lines (Figure 7A). The hypocotyl length of all three lines is longer than that of the *octuple* mutant, very similar to the *hexuple* mutant (Figure 7A; etiolated). The small cotyledon size, a prominent characteristic of the *octuple* mutant, is reverted back to almost the *hexuple*-like cotyledon size in all three complementation lines (Figure 7B; light grown). Ethylene production dramatically increased in all three lines and it is higher than that of the *hexuple* mutant (Figure 7C). The higher ethylene production of the complementation lines is due to the overexpression of the *ACS8* and *ACS11* transcripts by *35S* promoter (Figure 7D). We noticed that the three complementation lines overexpress one of the two *ACS* genes introduced into them, but not both: lines no. 8 and no. 14 overexpress only *ACS8*; line no. 10 overexpresses *ACS11* (Figure 7D). We think that this may be due to a recombination event during transformation resulting in the deletion of one of the genes in the *35S* double gene construct used for this experiment (see MATERIALS AND METHODS). Further examination of mature plants shows that while the small size of the rosette leaves has been corrected in the complemented lines, their *revoluta*-like morphology remains *octuple*-like (Figure 7E). The complementation lines also flower earlier than the *octuple* but not as early as the *hexuple* mutant (Figure 7F), indicating a partial phenotypic reversal. The same was observed with the reversal of the *octuple* silique phenotype. While silique length was partially corrected, the seed number per silique remained *octuple*-like in the complementation lines (Figure 7, G and H). We think that the partial reversal of some *octuple* phenotypes may be due to expression of only one of the two genes, but perhaps both *ACS8* and *ACS11* are required for correcting certain phenotypes. Alternatively, the *35S* promoter used for this experiment may not be active in some cells and tissues responsible for the phenotypic defects.

Response to pathogens: A vast amount of literature suggests that ethylene is involved in various pathogen responses (BROEKAERT *et al.* 2006). Here, we characterized the responses of the high order mutants to necrotrophic pathogens *Botrytis cinerea* and *Alternaria brassicicola*. The *pentuple2* mutant showed slightly enhanced susceptibility to *B. cinerea*, whereas *hexuple*, *heptuple*, and *octuple* mutants displayed much stronger disease symptoms compared with wt and *pentuple2* mutants (Figure 8). The disease symptoms progressed and led to complete decay of the *octuple* mutant at 7 days postinoculation (dpi) (Figure 8). However, we observed no significant difference between the mutants and wt after *A. brassicicola* infection (data not shown).

The ACS interactome map: The nine ACS proteins form active and inactive heterodimers in *E. coli* (TSUCHISAKA and THEOLOGIS 2004a), but it is not known whether ACS heterodimers form *in planta*. Furthermore, our results point to the operation of a combinatorial control mechanism among the nine ACS isoforms, so we determined the homo- and heterodimeric interaction among the various ACS subunits *in planta* using BiFC (HU *et al.* 2002). All possible active and inactive homo- and heterodimers of the *ACS* gene family members can be detected in auxin-treated Arabidopsis etiolated seedlings (Figure 9A). Auxin treatment was necessary for detecting the various homo- and heterodimeric interactions because the hormone enhances transcription of all the *ACS* gene family members except *ACS1* (YAMAGAMI *et al.* 2003). The root tip was used for the assay because our previous studies with *ACSpromoter-GUS* fusions have shown that most of the genes (but not *ACS1* and *ACS9*) are expressed in various root cell types after auxin treatment (TSUCHISAKA and THEOLOGIS 2004b). The heterodimeric interaction between bJun and bFos in the root tip of Arabidopsis served as a positive control (see left bottom of Figure 9A).

The data presented in Figure 9A provide the foundation for a meaningful estimation of the effect of inactivating various *ACS* genes on the composition and diversity of the *ACS* family in various cells and tissues. A diagrammatic presentation of the number of active and inactive isozymes in the various mutants is shown in Figure 9B. The data show the effect of deleting single or multiple genes on the relative ratio between active and inactive isozymes, and provide a framework for understanding the complexity of ethylene biosynthesis. This complexity is greatly magnified if one considers the heterogeneity of the C terminus among the ACS polypeptides, which is responsible for their stability (ARGUESO *et al.* 2007). The ACS proteins can be classified into three types on the basis of their C terminus: type 1 have the longest C terminus with a single putative calcium-dependent protein kinase (CDPK) phosphorylation site and three mitogen-activated protein kinase (MAPK) phosphorylation sites; type 2 have a medium size C terminus containing a single CDPK site; type 3 have a short C terminus with no predicted protein kinase phosphorylation sites. A diagrammatic presentation of the heterogeneity among the active and inactive isoform based on their C terminus is presented in Figure 9C. The relative ratio of all the different ACS isoforms shown in Figure 9C is greatly altered in the mutants presented in this analysis (Figure 9D). The homo- and heterodimerization capacity of ACS family coupled with its heterogeneity at the

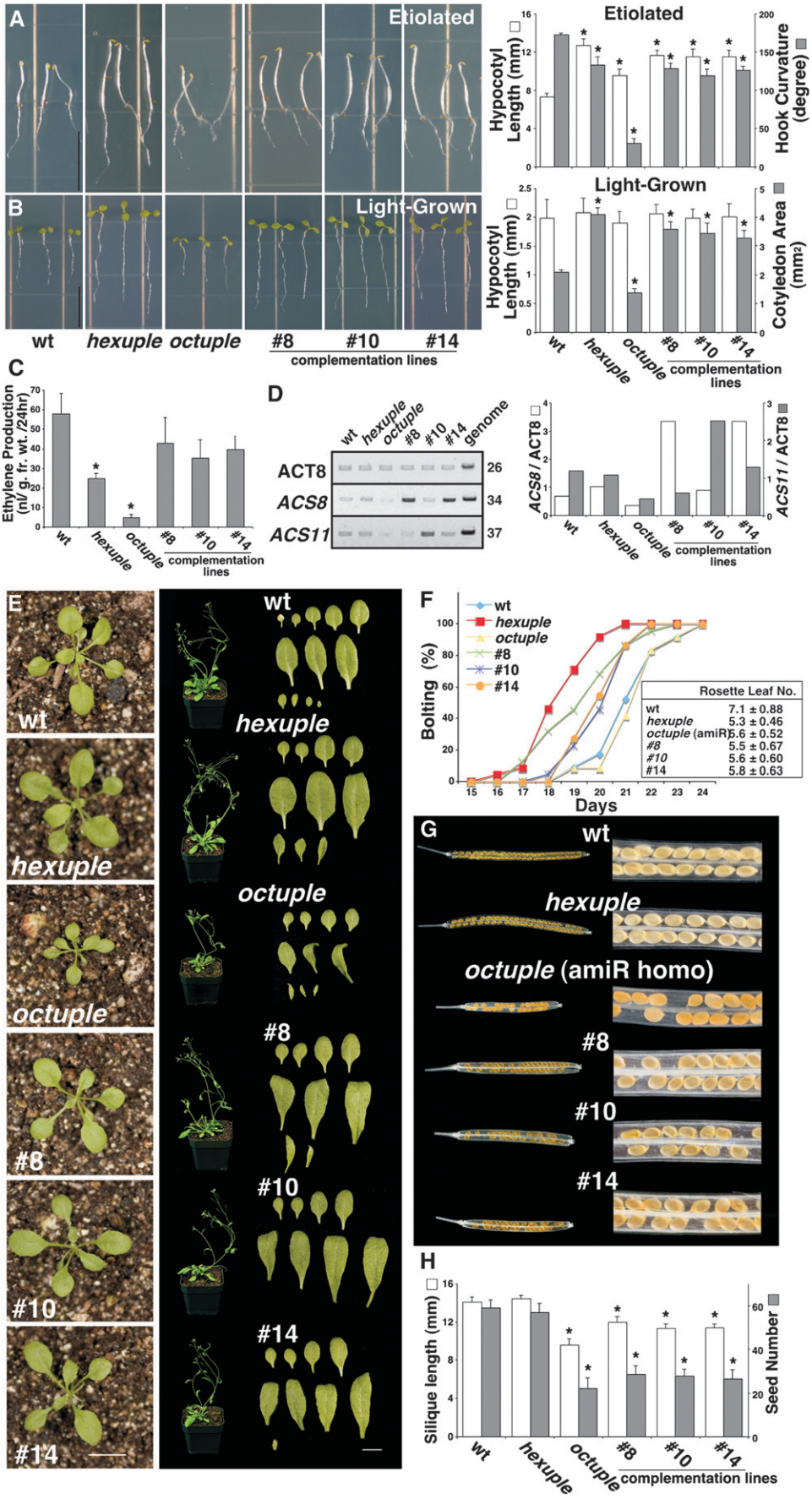

FIGURE 7.—Complementation of the *octuple* mutant. The photos in A compare the phenotypes of 3-day-old etiolated seedlings among wt, *hexuple*, *octuple*, and three complementation line nos. 8, 10, and 14. Bar = 1 cm. The graph on the right of A compares the hypocotyl length and hook curvature among wt, *hexuple*, *octuple*, and line nos. 8, 10, and 14 ($N = 10$). The photos in B compare the phenotypes of 5-day-old light-grown seedlings between wt, *hexuple*, *octuple*, and line nos. 8, 10, and 14. Bar = 1 cm. The graph on the right of B compares the hypocotyl length and cotyledon area among wt, *octuple*, and line nos. 8, 10, and 14. ($N = 10$). The comparison of the ethylene production among wt, *hexuple*, *octuple*, and line nos. 8, 10, and 14 in 5-day-old light-grown seedlings is shown in C ($N = 3$). The expression of the *ACS8* and *11* in wt, *hexuple*, *octuple*, and line nos. 8, 10, and 14 in 5-day-old light-grown seedlings is shown in D. The *ACT8* gene was used as a nondifferential expressed gene. The graph on the right of D shows the quantitation of the RT–PCR data. The photos in E compare the phenotypes of 20- (first column) and 40-day (second column)-old light-grown plants among wt, *hexuple*, *octuple*, and three transformation lines. Their rosette leaves are also compared (third column). The flowering time of wt, *hexuple*, *octuple*, and line nos. 8, 10, and 14 is shown in F. The silique morphology of wt, *hexuple*, *octuple*, and line nos. 8, 10, and 14 is shown in G. Quantitative comparison of the silique length and seed content of wt, *hexuple*, *octuple*, and line nos. 8, 10, and 14 is shown in H ($N = 10$). Bars represent the standard deviation (SD). The asterisk (*) has been defined in the legend of Figure 1.

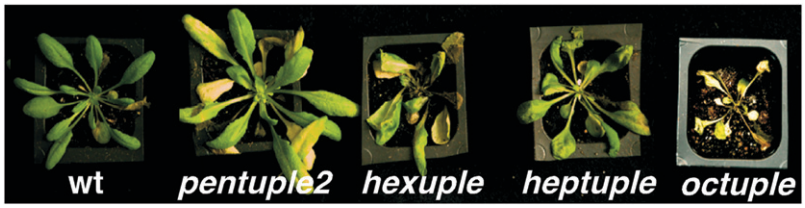

FIGURE 8.—Response of the high order mutants to pathogen infection. The *pentuple2*, *hexuple*, *heptuple*, and *octuple* mutants show increased disease symptoms to *Botrytis cinerea*. Plants were inoculated by spraying spore suspension of the *B. cinerea* (strain BO5-10) at a concentration of 2×10^5 spores/ml. The pictures were taken at 7 dpi. The experiments were repeated twice and similar results were observed.

C terminus provides a framework for understanding the complexity of ethylene biosynthesis as well as for interpreting the phenotypic defects of the various mutants.

Global gene expression analysis: To determine how the single and high order mutations affect the molecular phenotype of young Arabidopsis seedlings, we profiled their global gene expression. The results of the analysis are presented in Figure S9, Figure S10, Figure S11, Table S2, Table S3, Table S4, Table S5, Table S6, Table S7, Table S8, Table S9, and Table S10.

DISCUSSION

Lessons from the single mutants: *Each ACS performs a specific and unique function:* All the null mutants of any single *ACS* gene are viable. Mutations inactivating specific ACS isozymes affect three developmental pro-

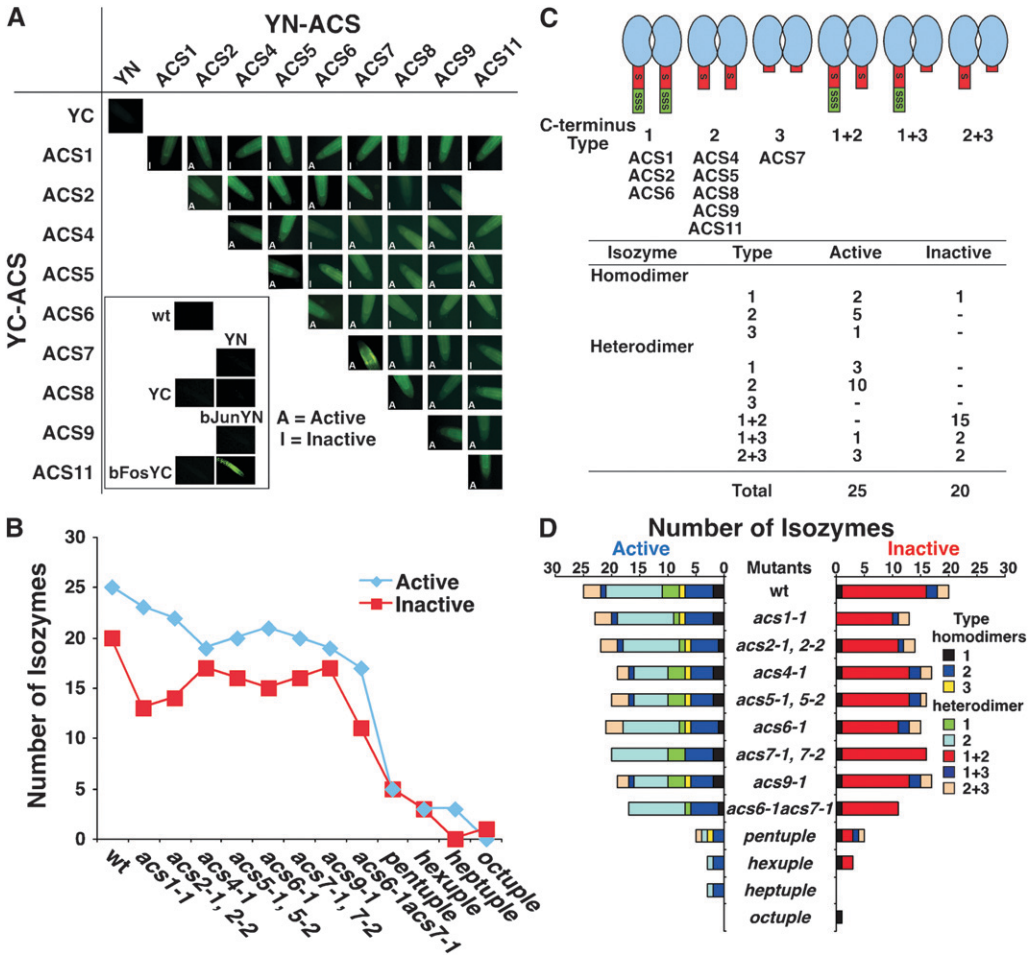

FIGURE 9.—The ACS interactome map. The homo- and heterodimeric interactions among the various ACS subunits, determined *in planta* by bimolecular fluorescence complementation (BiFC), are shown in A. The images show YFP expression in the root tips of 3-day-old etiolated seedlings. The heterodimeric interaction between Fos and Jun detected by BiFC in the root tip of 3-day-old etiolated seedlings is also shown at the bottom as a positive control. The number of active and inactive homo- and heterodimers in the various mutants is shown in B. The heterogeneity among the various active and inactive homo- and heterodimers based on the type of C terminus is shown in C. The number of active and inactive isozymes in the various mutants based on their type of C terminus is shown in D.

cesses: hypocotyl growth, flower time, and cotyledon size. Four single mutants, *acs1-1*, *acs6-1*, *acs7-1*, and *acs9-1*, flower earlier than does wt, suggesting that *ACS1*, *ACS6*, *ACS7*, and *ACS9* are negative regulators of the flowering process that are involved in proper regulation of flowering time. Remarkably, some interactions between ACSs appear to be antagonistic, because the early flowering phenotype of *acs6-1* and *acs7-1* is suppressed in the double mutant, which has a late flowering phenotype.

Some of the mutations affect the hypocotyl growth of etiolated seedlings positively or negatively. For example, *acs1-1* and *acs9-1* enhance hypocotyl length whereas *acs4-1* inhibits it, suggesting that *ACS1* and *ACS9* are negative regulators, whereas *ACS4* is a positive regulator of growth in the dark. A unique phenotypic alteration associated with the *acs1-1* mutation is inhibition of inflorescence stem diameter. All single mutants enhance hypocotyl length and the size of cotyledons in light-grown seedlings, with the *acs1-1* having the strongest effect. The enhancement in plant height in light-grown plants is evident throughout the life cycle. These data suggest that the ethylene produced by ACS1, ACS2, ACS4, ACS5, ACS6, and ACS9 isozymes acts as a negative regulator of plant growth in the light.

These developmental abnormalities do not correlate well with the total amount of ethylene produced in young seedlings. Loss of ACS4 and ACS9 function results in moderate ethylene overproduction, but loss of ACS1, which is the inactive isozyme, results in inhibition of ethylene evolution. The rest of the single mutants produce the same amount of ethylene as the wt. These results reveal an interaction among the ACS isoforms that regulate the overall output/activity of the ACS family. Again some of the interactions between ACSs are antagonistic, because ethylene overproduction caused by *acs4-1* and *acs9-1* is suppressed in the double mutant. Total ethylene production by a seedling appears not to be a good indicator/predictor for evaluating developmental phenotypic responses mediated by the hormone. We believe that the localized cellular sites of ethylene production, rather than the absolute amount of ethylene produced by an intact seedling or plant, determine the developmental response and outcome. Even though it is volatile and therefore highly diffusible, ethylene can induce different local responses depending on its site(s) of production and/or perception (Stepanova *et al.* 2008; Thomann *et al.* 2009). This agrees with the findings that the *ACS* genes have distinct patterns of expression during Arabidopsis development (Tsuchisaka and Theologis 2004b). Local hormone biosynthesis and deactivation have emerged as key regulatory factor in various developmental processes (Zhao 2008; Chandler 2009).

A second, independent evaluation of the relationship among the *ACS* genes is the global gene expression profiles of their mutants. Distinct differences between all single *acs* mutants and wt are apparent, suggesting that each ACS has a specific function. The differences in gene expression profiles between two alleles of the same gene may reflect dominant negative interactions of the truncated polypeptides with the rest of the family members resulting in alterations of ethylene production in specific cellular sites. When individual members of a gene family are disrupted and have no obvious phenotypic consequences, functional redundancy is offered as a possible explanation. Our data establish that every family member executes a unique function in each cell by regulating the cellular ethylene production via its interactions with the rest of the ACS family members.

Lessons from the high order mutants: *The ACS family members each perform a common essential function:* The phenotypes of the high order *acs* mutants led us to some simple conclusions and revealed a wealth of phenotypic complexity. To emphasize the most salient result, the inactivation of all nine genes caused embryonic lethality, indicating that the ethylene biosynthetic pathway is required for Arabidopsis viability. Our inability to recover a truly null *octuple* mutant that produces no ethylene was not due to a nonspecific effect of the *amiR* used to inactivate the *ACS8* and *ACS11* genes. The *octuple* mutant provides an excellent resource for constructing lines of plants expressing individual *ACS* genes. This strategy has the potential to assign specific biological function(s) to each ACS member.

Phenotypic resistance to the loss of ethylene: the pentuple paradox: We were quite surprised that inactivation of the ACS biosynthetic capacity by 80% in the *pentuple* mutant resulted in mild phenotypic changes. While flowering time and growth of etiolated and light-grown seedlings/plants were more pronounced in the *pentuple* mutants compared to the single mutants, the majority of its phenotypic characteristics/responses were similar to those of wt plants (Table S1). Its global gene expression profile was also quite similar to wt (see File S1, Results and Discussion). This may be due to the low sensitivity of the microarray analysis to detect changes in gene expression in specific cells and tissues responsible for the phenotypic changes. A *pentuple* mutant cell that expresses all four remaining noninactivated genes, *ACS1*, *ACS7*, *ACS8*, and *ACS11*, potentially has five active (ACS7/ACS7, ACS8/ACS8, ACS11/ACS11, ACS8/ACS11, and ACS7/ACS11) and five inactive homo- and heterodimeric isoforms (ACS1/ACS1, ACS1/ACS7, ACS1/ACS8, ACS1/ACS11, and ACS7/ACS11), and the *in planta* interactome map supports such a proposition. The difference in ethylene production between young seedlings and mature plants may reflect differences in the ratio of active and inactive isoforms. This may be due to differences in expression of the various genes and/or to preferential protein stabilization that compensates for the loss of ethylene bio-

synthetic capacity. The *hexuple* and *heptuple* mutants exhibited more marked phenotypic changes associated with reduced ethylene production. Inactivation of the ACS biosynthetic capacity by 88%, resulting in approximately 70–75% inhibition in total ethylene, revealed phenotypic changes associated with differential growth and response to pathogens. Response of these mutants to gravitostimulation is greatly diminished, and their hook structure is less prominent than in the *pentuple* mutant. Both mutations also enhanced phenotypes previously detected in the *pentuple* mutant such as enhanced plant growth, cotyledon size, and early flowering, and pathogen susceptibility. However, while their hypocotyl length of etiolated seedlings is further enhanced in both mutants compared to the *pentuple* mutant, their light-grown hypocotyl length is like that of wt, in sharp contrast to the *pentuple* mutant, which has longer hypocotyls than does wt. This may reflect a lower rate of cell growth at this low level of ethylene production because the mature *hexuple* and *heptuple* plants are taller than the *pentuple* plants.

The octuple Arabidopsis plant: The *octuple* mutant produces ~10% of the wt level ethylene because is not a truly null for ACS8 and ACS11. It is a handsome plant, the tallest among the high order mutants, lives longer than all the other mutants, senesces 3 weeks later than the wt, and produces fertile seeds, albeit at 50% yield compared to the wt and the other high order mutants. However, it is highly vulnerable because of its compromised defense to pathogens and probably to herbivores because of its defects in the glucosinolate biosynthetic pathway (see File S1, Results and Discussion). The delayed senescence of the *octuple* mutant reminds us that inhibition of plant senescence requires very low ethylene production. This is in agreement with the observation that inhibition of tomato fruit ripening by antisense RNA requires almost complete inhibition of ethylene production (Oeller *et al.* 1991). Many of the phenotypic characteristics of the *octuple* mutant reflect enhancement or reversal of those seen in the *hexuple* and *heptuple* mutations, but additional phenotypes were also observed. For example, an *octuple* etiolated seedling is indeed hookless and its hypocotyl length is longer than that of wt but shorter than that of the other high order mutants. Its response to gravity is diminished and is quite variable compared to the *hexuple* and *heptuple* mutants. A light-grown *octuple* seedling has the same hypocotyl length as the wt, but the size of its cotyledons is greatly inhibited. It appears that the rate of growth is greatly diminished in the *octuple* seedling and young plant, but its overall size as a mature plant is the tallest among all the other high order mutants. Furthermore, its susceptibility to pathogen is greatly enhanced, and it flowers later than the other two high order mutants. In addition we see changes in leaf size (smaller) and morphology, siliques size, and seed content/silique compared to the *hexuple* and *heptuple*, which have wt-like leaves and siliques. If all possible combinations and permutations of the nine *ACS* family members were constructed and analyzed ($N = 2^9 - 1 = 511$), the phenotypic complexity can be massive. The order of unmasking various phenotypic changes depends on the extent of the inactivation of the ACS biosynthetic capacity. Growth and flowering time are the most sensitive parameters to alterations in ethylene biosynthetic capacity. The two differential growth parameters, hook formation, response to gravity, resistance to pathogens, and inhibition of senescence are resilient to changes in ethylene biosynthetic capacity. It should be pointed out, however, that this order may be quite different if different combinations and permutations of gene mutations were analyzed. We constructed 91 mutants (~18% of all possible) and analyzed 26 mutants (~5% of total). It should be noted that the *ACS6* and *ACS9* overexpression lines shown in Figure 2 are defective to their response to gravity and etiolated hypocotyl growth (Figure S4), indicating that local disturbances in the ACS family have major phenotypic consequences. This observation reveals the operation of a communication network among the ACS members that controls local ethylene production.

Ethylene functions as a transcriptional rheostat: It is of a great interest that Arabidopsis genes respond differentially to different ethylene concentrations (De Paepe *et al.* 2004). The global gene expression profiles of the single and high order mutants shown in File S1 (Results and Discussion) resemble an ethylene dose response curve of the transcriptional output of all Arabidopsis cells at a given developmental stage. The *pentuple* mutant behaves like its ACS activity is balanced, as if the positive and negative influences on its ACS activity are equal. Results of our analysis of the mutants reinforce the concept that ethylene acts as a rheostat to regulate transcription of key genes involved in numerous developmental and physiological processes. We believe this is a consequence of a combinatorial interplay among the various ACS isoforms that regulate ethylene production in a temporal and spatial manner.

Highlights of the genome expression profiling analysis: A discussion on the most highly induced and repressed genes in the high order mutants listed in Table S10, A and B is presented in File S1 (Results and Discussion). Among them are genes involved in glucosinolate metabolism and light perception/signaling.

Ethylene and plant growth: Ethylene is the simplest of the six small molecule hormones plants use to integrate a myriad of extrinsic (*e.g.*, light) and intrinsic signals to regulate cell expansion and ensure optimal growth and development (Davies 2004; Nemhauser *et al.* 2006; Michael *et al.* 2008). Comparative global gene expression analysis has shown that each hormone regulates unique and nonoverlapping transcriptional networks (Nemhauser *et al.* 2006), suggesting that cell expansion driven by each specific hormone is qualitatively distinct.

Recently, the DELLA repressor proteins whose activity is regulated by gibberelic acid (GA) have emerged as key integrators of plant growth by light and high order hormonal signals including ethylene (Fu and Harberd 2003; Achard *et al.* 2006; Schwechheimer 2008; Schwechheimer and Willige 2009). The enlarged cotyledon size of the *acs* mutants can be attributed to the loss of DELLA function. The same phenotypic abnormality has been seen in the *spt10* mutant of the *SPATULA* (*SPT*) gene which is a repressor of the GA biosynthetic gene GA3 oxidase (Penfield *et al.* 2006). Since ethylene is known to positively regulate DELLA repressing function by inhibiting GA biosynthesis and enhancing DELLA function (Achard *et al.* 2003, 2007; Schwechheimer 2008) the prospect arises that the enlarged cotyledon phenotype of the *acs* mutants may be due to the loss of DELLA function. Alternatively, loss of DELLA function may be due to the inhibition of ethylene-regulated auxin production (Swarup *et al.* 2007; Stepanova *et al.* 2008; Tao *et al.* 2008). Auxin is known to enhance DELLA repressing function (Fu and Harberd 2003).

Ethylene generally inhibits growth of plants (Vandenbussche *et al.* 2005; Dugardeyn and Van Der Straeten 2008), but in a few cases it stimulates cell expansion (Smalle *et al.* 1997). Results of our analysis of *acs* mutants clearly demonstrate that ethylene is a repressor of cell growth in dark- or light-grown plants, because progressive inhibition of the ethylene biosynthetic capacity causes a progressive enhancement of plant size. The stimulatory effect of the loss of ethylene biosynthetic capacity on plant growth is in sharp contrast to the loss of auxin, GA, and BR biosynthetic capacity, which causes dwarfism (Sun *et al.* 1992; Li *et al.* 1996; Zhao 2008). Some of the phenotypes of the high order *acs* mutants, such as long hypocotyl and internodal length, early flowering, and decreased seed yield seen in the *octuple* mutant are reminiscent of those observed in shade avoidance syndrome (SAS) (Smith and Whitelam 1997; Jiao *et al.* 2007; Tao *et al.* 2008). More broadly, the repressing activity of ethylene on plant growth is reminiscent of the similar activity of light on plant expansion (Chen *et al.* 2004; Jiao *et al.* 2007). The long hypocotyls of light-grown *acs* mutants is reminiscent of the reduced capacity of the light-mediated inhibition of hypocotyl elongation in the *hy* mutants of Arabidopsis (Chory *et al.* 1989). Our microarray data also indicate the operation of an extensive communication network between light signaling and ethylene biosynthesis, since expression of many light-related genes is altered by the loss of ethylene production (Vandenbussche *et al.* 2005; Michael *et al.* 2008; Alabadí and Blázquez 2009). The possibility exists that the *acs* mutants are also defective in clock-regulated growth because the expression of key clock components, such as *LHY* and *FKF*, has been altered in the mutants (Thain *et al.* 2004; Michael *et al.* 2008). Since ethylene interacts with all the known hormone biosynthetic and signaling pathways it is reasonable to suggest that all these pathways have been uncoupled and the growth of the various mutants is an expression of the growth capacity present in Arabidopsis cells under various levels of ethylene production.

Ethylene and differential growth: *Hook formation:* Recognition of ethylene's involvement in localized differential growth in response to light (phototropism), gravity (gravitropism), and formation of an apical hook to ensure early seedling establishment is as old as the discovery of the hormone (Neljubow 1901). It is generally accepted that localized differential growth is due to auxin gradients that are established by local auxin biosynthesis and directional intercellular auxin transport (Tanaka *et al.* 2006; Vanneste and Friml 2009). The development of an apical hook involves a complex interplay of at least three hormone-responsive pathways: ethylene, auxin, GA and light (Achard *et al.* 2003; Li *et al.* 2004). It is yet not clear whether asymmetric auxin biosynthesis is due to asymmetric expression of ACS isoforms or asymmetric expression of the auxin biosynthetic enzymes (Stepanova *et al.* 2008). Alternatively, the ethylene-regulated *HOOKLESS* (*HLS1*) gene may be responsible for auxin asymmetry by regulating auxin signaling via ARF2 (Li *et al.* 2004). Our data indicate that the loss of hook formation is quite resistant to the loss of ethylene biosynthetic capacity. It was not until the partial loss of the *ACS8* and *ACS11* genes in the *octuple* mutant that a hookless phenotype resulted.

Gravity sensing: It is widely accepted that asymmetric auxin distribution is responsible for the differential cell elongation on opposite sides of cells that leads to gravitotropic curvature upon gravitostimulation (Terao-Morita and Tasaka 2004). Loss-of-function mutations in the auxin-regulated transcriptional activator *NPH4/ARF7* disrupts the gravitotropic response in Arabidopsis (Harper *et al.* 2000). Ethylene is involved in gravity sensing by suppressing the NPH4/ARF7 loss-of-function phenotype and this may explain to diminished response of the *acs* mutants to gravitostimulation. However, it is quite intriguing that while the high order *acs* mutants have lost their ability to respond to gravity, they are not agravitropic. This suggests that a component of the gravity sensing apparatus responsible for gravitostimulation maybe defective in the mutants (Terao-Morita and Tasaka 2004). It also suggests that the ethylene produced by the *octuple* mutant is sufficient for maintaining an auxin biosynthesis/signaling apparatus for proper gravity sensing. Our gene expression profiling data raise the possibility that blue-light mediated processes, such as tropisms, may be defective in the high order *acs* mutants. Expression of two homologs of *NON PHOTOTROPIC HYPOCOTYL 3* (*NPH3*), a BTB/POZ-containing protein involved in phototropism signaling, is induced in the *hexuple* and *heptuple* mutants

(Table S10; Cheng *et al.* 2007; Pedmale and Liscum 2007).

Ethylene and flowering time: Ethylene is known to be involved in the flowering process (Abeles *et al.* 1992; Boss *et al.* 2004; Achard *et al.* 2006). One of the highlights of our analysis is that ethylene represses flowering in Arabidopsis. Inactivation of specific *ACS* gene products enhances flowering time, and this enhancement is further potentiated by the progressive loss of ACS biosynthetic capacity in the high order mutants. We attribute the diminished early flowering phenotype of the *octuple* mutant to major alterations in the flowering machinery caused by the severe inhibition in ethylene production.

Several lines of evidence indicate that ethylene controls flowering time through a rheostat in which the level of ethylene production in the leaf primordial/SAM is proportional to the lateness to flower. For example, complementation of transgenic *acs6-1* and *acs9-1* mutants by their corresponding *ORFs* results in a broad range of flowering times, presumably due to variation in *ACS6* or *ACS9* expression caused by variation in transgene copy number and/or chromosomal position effects. Our data indicate that ethylene exerts its effect on flowering by regulating the expression of the *FLOWERING LOCUS C* (*FLC*) (Michaels and Amasino 2001). *FLC* also acts as a rheostat to repress flowering (Michaels and Amasino 1999) through repression of the floral pathway integrators *FLOWERING LOCUS T* (*FT*) and *SUPPRESSOR OF OVEREXPRESSION OF CONSTANS* (*SOC1*) (Blázquez and Weigel 2000; Samach *et al.* 2000; Wigge *et al.* 2005). The early flowering phenotype of the high order *acs* mutants is associated with a progressive loss of *FLC* mRNA in light-grown seedlings and a concomitant increase of the positive flowering activator *FT* mRNA. The opposite is observed in the late flowering double mutant *acs6-1acs7-1*. The increase in *SOC1* mRNA is moderate. The early flowering phenotype appears not to be due to a disruption in the photoperiodic-regulated flowering process because the mRNA of *CONSTANS* (*CO*), a master regulator of this process, is slightly repressed in the *acs* mutants. In addition two key components of the photoperiodic-regulated flowering machinery, *LHY*, a component of the clock and *FKF*, a novel blue light photoreceptor that controls CO transcript pattern (Bäurle and Dean 2006; Imaizumi and Kay 2006), are repressed in the *acs* mutants. We do not know whether ethylene regulates *FLC* transcription directly or indirectly. All known hormonal networks interfere with the flowering process (Boss *et al.* 2004), and since ethylene communicates with all of them (Nemhauser *et al.* 2006; Alabadí and Blázquez 2009) the possibility exists that the effect of ethylene on early flowering is indirect. Alternatively, ethylene may regulate *FLC* expression by regulating the chromatin state, which has emerged as an important mechanism in the control of *FLC* expression (Bäurle and Dean 2006; Domagalska *et al.* 2007; Pien *et al.* 2008).

It has been recently shown that ethylene delays flowering by modulating DELLA activity. Ethylene-enhanced DELLA accumulation in turn delays flowering via repression of the floral meristem-identity genes *LEAFY* (*LFY*) and *SOC1* (Achard *et al.* 2007). These findings are based on the observation that constitutively active ethylene signaling in the *ctr1* mutant reduces GA levels, and the late flowering phenotype of the *ctr1* mutant is partially rescued by loss-of-function mutations in DELLA genes (Achard *et al.* 2007). A possible explanation for this difference between those results and ours may be that a different flowering pathway operates in the *ctr1* mutant and in our *acs* mutants.

The antagonistic effect of the *acs6-1* and *acs7-1* mutations on flowering, together with the flowering time of plants overexpressing *ACS6* and *ACS9* reveal the operation of a communication network among ACS proteins that may cause local changes in ethylene production. We think that the late-flowering phenotype of the *acs6-1acs7-1* double mutant may be due to ethylene overproduction in the leaf primordial/SAM region brought about by alteration in the relative ratio of various active and inactive ACS isoforms.

Ethylene and plant pathogens: Ethylene plays an important role in plant pathogen responses associated with disease resistance or disease susceptibility, depending on the type of pathogen and plant species. Ethylene has been proposed to be more effective against necrotrophic pathogens, such as *B. cinerea* than against biotrophic pathogens. Ethylene-insensitive mutants *ein2*, *ein3*, and *etr1* show enhanced susceptibility to *B. cinerea* (Thomma *et al.* 1999; Ferarri *et al.* 2003). Plants that overexpress transcription factors involved in the ethylene and JA pathways exhibit an increased resistance to several necrotrophs (Berrocal-Lobo *et al.* 2002; Berrocal-Lobo and Molina 2004; Pré *et al.* 2008). Overexpression of *AP2C1* in Arabidopsis, which encodes a Ser/Thr protein type 2C phosphatase, reduces ethylene production and compromises resistance to the necrotrophic pathogen *B. cinerea* (Schweighofer *et al.* 2007). We observed that the high order *acs* mutants have enhanced susceptibility to necrotrophic pathogen *B. cinerea*, which suggests that ethylene is important for nonhost resistance to *B. cinerea* in Arabidopsis, and our gene expression profiling results support this proposition. We have also examined the responses of these mutants to bacterial pathogens, *Xanthomonas campestris* pv. *vesicatoria* (*Xcv*), and *X. campestris* pv. *campestris* (*Xcc*). No significant changes of bacterial growth were observed in these mutants as compared with that in the wt (data not shown), suggesting that ethylene production has no obvious effect in biotrophs or hemibiotrophs. Several *B. cinerea*-induced genes [AtGenExpress; response to *B. cinerea* infection, provided by Ferrari *et al.* (2007)], including genes encoding a putative NADP-

dependent oxidoreductase (At5g16980), a serine carboxypeptidase S28 family protein (At5g22860), two APS reductases (APR1 and APR3), and a cytochrome P450 gene *CYP71A12*, were suppressed in at least one of the high order *acs* mutants (Table S5 and Table S9). By contrast, a group of *B. cinerea*-repressed genes was induced in the mutants. Among them, a glutaredoxin family gene (At3g62950) was induced in all four mutants (Table S4 and Table S8). Two *B. cinerea*-repressed beta-ketoacyl-CoA synthase genes, *KCS12* and *KCS16*, were also induced in at least two of the mutants (Table S4 and Table S8). Thus, inhibition of ethylene synthesis alters expression of many *B. cinerea*-responsive genes and represses defense related genes, which leads to the enhanced susceptibility to *B. cinerea* infection.

Is ACC a primary plant growth regulator? The most obvious interpretation of our inability to recover a truly null ACS mutant is that the ethylene biosynthetic pathway is required for Arabidopsis embryo and/or gametophytic development. We know ethylene regulates key genes involved in auxin biosynthesis and transport (Stepanova *et al.* 2007, 2008; Swarup *et al.* 2007; Tao *et al.* 2008; Chandler 2009), processes known to have a central role in embryo patterning and development (Tanaka *et al.* 2006; Vanneste and Friml 2009). It is also possible that ethylene may regulate DNA methylation, which is critical for Arabidopsis embryogenesis and seed viability (Xiao *et al.* 2006). However, there is a potential conflict with such an interpretation. While the *octuple acs* mutant causes embryonic lethality, single or double *ein2* and *ctr1* mutants, which are missing key components of the signaling apparatus are viable (Kieber *et al.* 1993; Roman *et al.* 1995; Alonso *et al.* 1999) This suggests that ethylene is not required for Arabidopsis viability and embryo development. Since inactivation of all *ACS* genes eliminates the production of ethylene and inhibits the biosynthesis of its precursor, ACC, the prospect arises that ACC is a primary plant growth regulator responsible for embryo development, as it may be for cell expansion mediated by the FEI/SOS pathway (Xu *et al.* 2008). Perhaps the alternative MKK9-MPK3/6 dependent pathway of ACC synthesis is responsible for embryo development (Yoo *et al.* 2008). However, since the *ctr1ein2* double mutant is not embryonic lethal, this alterative pathway cannot be responsible for embryo development. If there is an alternative signaling pathway responsible for embryo development, it should branch from the linear pathway at the receptor level, above the CTR1-catalyzed step. Construction of a *heptuple* mutant, *etr1ers1etr2ein4ers2ctr1ein2* that inactivates all five receptors plus CTR1 and EIN2 has the potential to offer a definitive answer to the question of whether ACC is a primary growth regulator. Furthermore, the construction of a null ACO mutant has the potential to shine light to this intriguing possibility. There are 17 annotated *ACO* genes in the Arabidopsis genome (Arabidopsis Genome Initiative 2000), but whether all of them encode genuine ACC oxidase remains to be determined.

While we have presented above the rationale for ACC being a signaling molecule in its own right, another interpretation of the data is possible. Specifically, the elimination of the ACS-mediated pathway may affect the flux through the AdoMet pathway leading to increased levels of other metabolites that may cause embryo lethality.

"The *Arabidopsis* ACS symphony orchestra": Our results can be interpreted to indicate that ACC production, and, by extension, ethylene evolution, is a product of the collective action of the members of the ACS protein family. We view the ACS protein family as a "symphony orchestra" (45-member when all nine genes are expressed in a cell) that regulates ethylene-mediated processes by generating appropriate amounts of ACC in the proper spatial and temporal manner through their harmonious interplay. At any given moment, the orchestra is tuned by various inducers to produce ACC sufficient to mediate myriad ethylene responses (Figure 10). Each ACS dimeric isoform can be viewed as a particular instrument that interacts with its colleagues to produce the "melody" that coordinates plant growth development together with those of other hormonal and light regulatory networks. Disturbances in the tuning of the orchestra caused by mutations in the *acs* genes result in phenotypic cacophonies. Such disturbances can also be caused by expressing exogenous family members in a tissue-specific manner, as we saw in the complementation of the *acs6-1* and *acs9-1* single mutants. The number of players in each cell will depend on the number of genes expressed there. There are potentially 511 ($N = 2^9 - 1$) harmonies in the ACS orchestra in the 5×10^5 cells of a 10-day-old light-grown Arabidopsis seedling (assuming that the seedling volume is 4 μl because its average weight is ~4 mg and the density $\rho = 1$ g/ml; the cell size is 20 μm × 20 μm × 20 μm; the cell volume 8×10^{-15} m^3). The relative abundance of the players in the orchestras will depend on mRNA abundance, protein stability of various homo- and heterodimeric isoforms as well as on the K_d's of the various ACS polypeptides. The capacity of the various isozymes to form active heterodimers together with their C terminus heterogeneity provides vast biochemical diversity among the 511 harmonies capable of operating under a very broad spectrum of AdoMet concentration during the plant cycle. This diversity provides the molecular basis for explaining the pleiotropic effects of ethylene. The *ACS* family is a paradigm for the concept that gene redundancy provides biochemical and metabolic flexibility (Graur and Li 2000). The combinatorial complexity among the ACS family members is reminiscent of the auxin signaling apparatus, in which the multiple *Aux/IAA*, *ARF*, and *TIR/AFB* gene family members collaborate in the

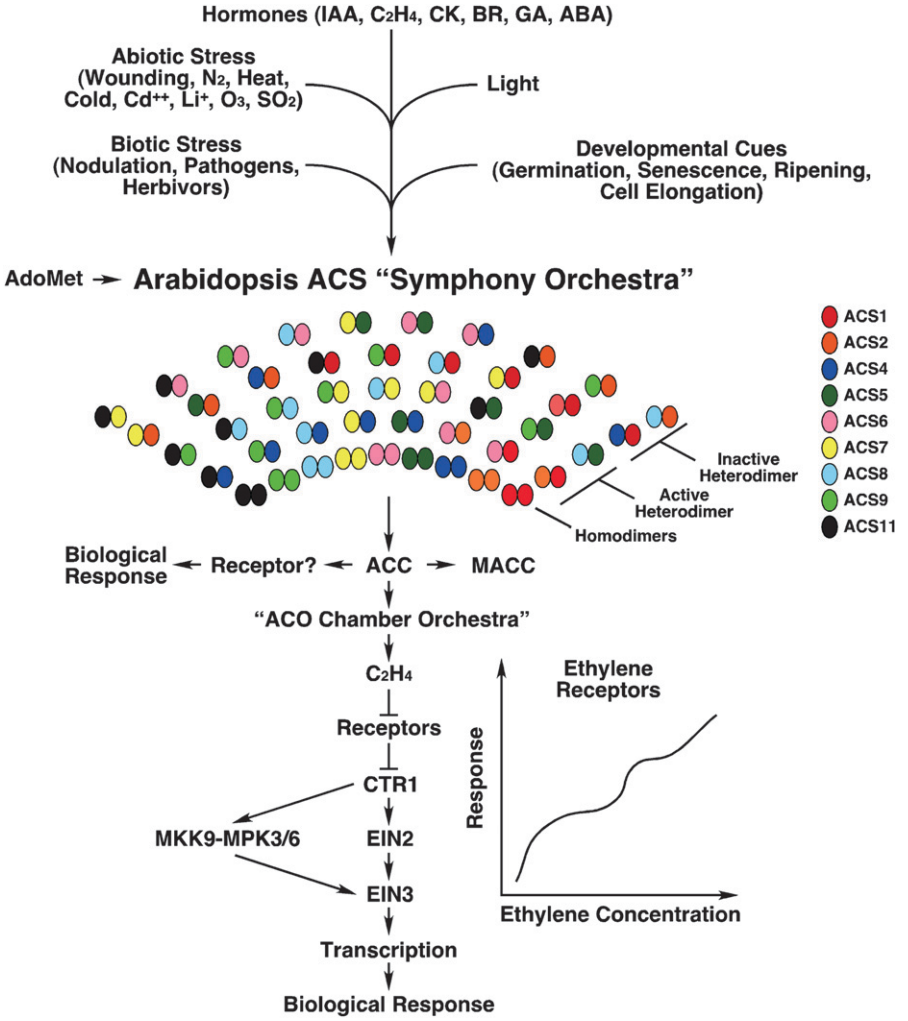

FIGURE 10.—"The Arabidopsis ACS Symphony Orchestra."

pleiotropic effects of auxin (MOCKAITIS and ESTELLE 2008).

The view presented in Figure 10 also indicates that the final biological outcome depends not only on the ACS family. ACC produced by the *ACS* family is processed by at least a 10-member ACO family, whose members act as monomers (DONG *et al.* 1992). Very little is known about its biochemical diversity and expression patterns during plant growth. Finally, ethylene is sensed by five different receptors that have the capacity to heterodimerize (GREFEN *et al.* 2008) and form 5 homo- and 15 heterodimeric isoforms. The combinatorial interplay among the receptor isoforms in a spatial and temporal manner coupled with potential differences in their affinity for ethylene *in vivo* may provide the molecular basis for cell- and tissue-specific ethylene responses (HALL *et al.* 2007; STEPANOVA *et al.* 2008; TAO *et al.* 2008). Furthermore, differences in spatial and temporal expression of different receptor isoforms with different affinities for ethylene may act as a shield during its diffusion through neighboring cells to prevent undesired biological responses.

Conclusions and future directions: Our results provide strong support for the hypothesis that the "Yang" ethylene biosynthetic pathway is the only route of ethylene production in Arabidopsis. The ethylene precursor ACC, may be a signaling molecule, regulating a variety of yet unidentified processes. Ethylene evolution is regulated by combinatorial interplay of the ACS polypeptides that serves as a rheostat controlling unique sets of genes that mediate the myriad ethylene-mediated processes during plant development. We still need to know and understand how the ACS symphony orchestra of each cell is coordinated with those in all the other Arabidopsis cells. Understanding how Arabidopsis coordinates the activity (output) of each ACS orchestra in each cell with those in the rest of the cells is a task for the future. More important, how the ethylene biosynthetic and signaling machineries are coordinated with the other hormonal and light networks to regulate plant growth is a major challenge for the future.

Knowledge of the temporal and spatial concentrations of substrates and intermediates of the ethylene biosynthetic pathway, together with the biochemical

parameters of its enzymes promises to greatly advance our understanding of the regulation of the *ACS* gene family. The development of single cell biosensors using riboswitches (Lai 2003) and Biophotonics (West and Halas 2003) for detecting AdoMet, ACC, or even ethylene may provide some of the tools for achieving this goal. Furthermore, single cell protein profiling will advance our understanding of the *ACS* family. Determining the protein stability and the biochemical properties of the various homo- and heterodimeric forms will require new technological innovations. The mutants generated for this study may be valuable for analysis to elucidate the post-translational regulation of the various ACS polypeptides. Finally, establishing whether ACC is a primary plant growth regulator should be a major goal for the future because it will augment the repertoire of plant growth regulators used by plants to control their growth.

Note: Any questions regarding the mutants and transgenic lines that have been deposited to ABRC should be addressed to Atsunari Tsuchisaka at atsunari@nature.berkeley.edu.

We thank Rebecca Schwab and Detlef Weigel for designing the specific amiRNA sequences to inhibit *ACS8* and *ACS11* gene expression and for their generous gift of *pRS300* plasmid containing the amiRNA backbone; Leor Eshed Williams for her advice and discussions regarding the amiRNA experiments; and Jennifer Fletcher and Pablo Leivar for useful discussions during the course of this work. This research was supported by the U.S. Department of Agriculture-Agricultural Research Service (CRIS 5335-21430-005-00D) (to A.T.).

LITERATURE CITED

Abeles, F. B., P. W. Morgan and M. E. Saltveit, Jr., 1992 *Ethylene in Plant Biology*. Academic Press, New York.

Achard, P., W. H. Vriezen, D. Van Der Straeten and N. P. Harberd, 2003 Ethylene regulates Arabidopsis development via the modulation of DELLA protein growth repressor function. Plant Cell **15:** 2816–2825.

Achard, P., H. Cheng, L. D. Grauwe, J. Decat, H. Schoutteten *et al.*, 2006 Integration of plant responses to environmentally activated phytohormonal signals. Science **311:** 91–94.

Achard, P., M. Baghour, A. Chapple, P. Hedden, D. Van Der Straeten *et al.*, 2007 The plant stress hormone ethylene controls floral transition via DELLA-dependent regulation of floral meristem-identity genes. Proc. Natl. Acad. Sci. USA **104:** 6484–6489.

Alabadí, D., and M. A. Blázquez, 2009 Molecular interactions between light and hormone signaling to control plant growth. Plant Mol. Biol. **69:** 409–417.

Alonso, J. M., T. Hirayama, G. Roman, S. Nourizadeh and J. R. Ecker, 1999 *EIN2*, a bifunctional transducer of ethylene and stress responses in *Arabidopsis*. Science **284:** 2148–2152.

Arabidopsis Genome Initiative, 2000 Analysis of the genome sequence of the flowering plant *Arabidopsis thaliana*. Nature **408:** 796–815.

Argueso, C. T., M. Hansen and J. J. Kieber, 2007 Regulation of ethylene biosynthesis. J. Plant Growth Regul. **26:** 92–105.

Bäurle, I., and C. Dean, 2006 The timing of developmental transitions in plants. Cell **125:** 655–664.

Berrocal-Lobo, M., A. Molina and R. Solano, 2002 Constitutive expression of ETHYLENE-RESPONSE-FACTOR1 in *Arabidopsis* confers resistance to several necrotrophic fungi. Plant J. **29:** 23–32.

Berrocal-Lobo, M., and A. Molina, 2004 Ethylene response factor 1 mediates *Arabidopsis* resistance to the soilborne fungus *Fusarium oxysporum*. Mol. Plant-Microbe Interact. **17:** 763–770.

Blázquez, M. A., and D. Weigel, 2000 Integration of floral inductive signals in *Arabidopsis*. Nature **404:** 889–892.

Bleecker, A. B., and H. Kende, 2000 Ethylene: a gaseous signal molecule in plants. Annu. Rev. Cell Dev. Biol. **16:** 1–18.

Boss, P. K., R. M. Bastow and J. S. Mylne, 2004 Multiple pathways in the decision to flower: Enabling, promoting, and resetting. Plant Cell **16:** S18–S31.

Broekaert, W. F., S. L. Delaure, M. F. C. De Bolle and B. P. A. Cammue, 2006 The role of ethylene in host-pathogen interactions. Annu. Rev. Phytopathol. **44:** 393–416.

Capitani, G., E. Hohenester, L. Feng, P. Storici, J. F. Kirsch *et al.*, 1999 Structure of 1-aminocyclopropane-1-carboxylate synthase, a key enzyme in the biosynthesis of the plant hormone ethylene. J. Mol. Biol. **294:** 745–756.

Chandler, J. W., 2009 Local auxin production: a small contribution to a big field. BioEssays **31:** 60–70.

Chang, C., S. F. Kwok, A. B. Bleecker and E. M. Meyerowitz, 1993 *Arabidopsis* ethylene-response gene *ETR1*: similarity of product to two-component regulators. Science **262:** 539–544.

Chen, M., J. Chory and C. Fankhauser, 2004 Light signal transduction in higher plants. Annu. Rev. Genet. **38:** 87–117.

Cheng, Y., G. Qin, X. Dai and Y. D. Zhao, 2007 NPY1, a BTB-NPH3-like protein, plays a critical role in auxin-regulated organogenesis in *Arabisopsis*. Proc. Natl. Acad. Sci. USA **104:** 18825–18829.

Chory, J., C. A. Peto, M. Ascbaugh, H. R. Saganic, L. H. Pratt *et al.*, 1989 Different roles for phytochrome in etiolated and green plants deduced from characterization of *Arabidopsis thaliana* mutants. Plant Cell **1:** 867–880.

Davies, P. J., 2004 *Plant Hormones: Biosynthesis, Signal Transduction, Action!* Kluwer Academic Publishers, Dordrecht, The Neitherlands.

De Paepe, A., M. Vuylsteke, P. Van Hummelen, M. Zabeau and D. Van Der Straeten, 2004 Transcriptional profiling by cDNA-AFLP and microarray analysis reveals novel insights into the early response to ethylene in *Arabidopsis*. Plant J. **39:** 537–559.

Domagalska, M. A., F. M. Schomburg, R. M. Amasino, R. D. Vierstra, F. Nagy *et al.*, 2007 Attenuation of brassinosteroid signaling enhances *FLC* expression and delays flowering. Development **134:** 2841–2850.

Dong, J. G., J. C. Fernández-Maculet and S. F. Yang, 1992 Purification and characterization of 1-aminocyclopropane-1-carboxylate oxidase from apple fruit. Proc. Natl. Acad. Sci. USA **89:** 9789–9793.

Dugardeyn, J., and D. Van Der Straeten, 2008 Ethylene: fine-turning plant growth and development by stimulation and inhibition of elongation. Plant Sci. **175:** 59–70.

Ferarri, S., D. Vairo, F. M. Ausubel, F. Cervone and G. De Lorenzo, 2003 Tandemly duplicated Arabidopsis genes that encode polygalacturonase-inhibiting proteins are regulated coordinately by different signal transduction pathways in response to fungal infection. Plant Cell **15:** 93–106.

Ferrari, S., R. Galletti, C. Denoux, G. De Lorenzo, F. M. Ausubel *et al.*, 2007 Resistance to *Botrytis cinerea* in Arabidopsis by elicitors is independent of salicylic acid, ethylene, or jasmonate signaling but requires *PHYTOALEXIN DEFICIENT3*. Plant Physiol. **144:** 367–379.

Fu, X., and N. P. Harberd, 2003 Auxin promotes *Arabidopsis* root growth by modulating gibberellin response. Nature **421:** 740–743.

Graur, D., and W.-H. Li, 2000 Gene duplication, exon shuffling, and concerted evolution, pp.249–322 in *Fundamentals of Molecular Evolution*, Ed. 2. Sinauer Associates, Sunderland, MA.

Grefen, C., K. Städele, K. Ruzicka, P. Obrdlik, K. Harter *et al.*, 2008 Subcellular localization and in vivo interactions of the *Arabidopsis thaliana* ethylene receptor family members. Mol. Plant **1:** 308–320.

Guo, H., and J. R. Ecker, 2004 The ethylene signaling pathway: new insights. Curr. Opin. Plant Biol. **7:** 40–49.

Hall, B. P., S. N. Shakeel and G. E. Schaller, 2007 Ethylene receptor: ethylene perception and signal transduction. J. Plant Growth Regul. **26:** 118–130.

Hansen, M., H. S. Chae and J. J. Kieber, 2008 Regulation of ACS protein stability by cytokinin and brassinosteroid. Plant J. **57:** 606–614.

Harper, R. M., E. M. Stowe-Evans, D. R. Luesse, H. Muto, K. Tatematsu *et al.*, 2000 The NPH4 locus encodes the auxin response factor ARF7, a conditional regulator of differential growth in aerial Arabidopsis tissue. Plant Cell **12:** 757–770.

Hu, C. D., Y. Chinenov and T. K. Kerppola, 2002 Visualization of interactions among bZIP and Rel family proteins in living cells using bimolecular fluorescence complementation. Mol. Cell **9:** 1694–1696.

Imaizumi, T., and S. A. Kay, 2006 Photoperiodic control of flowering: not only by coincidence. Trends Plant Sci. **11:** 550–558.

Jiao, Y., O. S. Lau and X. W. Deng, 2007 Light-regulated transcriptional networks in higher plants. Nat. Rev. Genet. **8:** 217–230.

Kieber, J. J., M. Rothenberg, G. Roman, K. A. Feldmann and J. R. Ecker, 1993 *CTR1*, a negative regulator of the ethylene response pathway in Arabidopsis, encodes a member of the Raf family of protein kinases. Cell **72:** 427–441.

Lai, E. C., 2003 RNA sensors and riboswitches: self-regulating messages. Curr. Biol. **13:** R285–R291.

Li, H., P. Johnson, A. Stepanova, J. M. Alonso and J. R. Ecker, 2004 Convergence of signaling pathways in the control of differential cell growth in Arabidopsis. Dev. Cell **7:** 193–204.

Li, J., P. Nagpal, V. Vitart, T. C. McMorris and J. Chory, 1996 A role for brassinosteroids in light-dependent development of *Arabidopsis*. Science **272:** 398–401.

Michaels, S. D., and R. M. Amasino, 1999 *FLOWERING LOCUS C* encodes a novel MADS domain protein that acts as a repressor of flowering. Plant Cell **11:** 949–956.

Michaels, S. D., and R. M. Amasino, 2001 Loss of *FLOWERING LOCUS C* activity eliminates the late-flowering phenotype of *FRIGIDA* and autonomous pathway mutations but not responsiveness to vernalization. Plant Cell **13:** 935–941.

Michael, T. P., G. Breton, S. P. Hazen, H. Priest, T. C. Mockler *et al.*, 2008 A morning-specific phytohormone gene expression program underlying rhythmic plant growth. PLos Biol. **6:** e225.

Mockaitis, K., and M. Estelle, 2008 Auxin receptors and plant development: a new signaling paradigm. Annu. Rev. Cell Dev. Biol. **24:** 55–80.

Neljubow, D., 1901 Uber die horizonate Nutation der Stengel von *Pisum sativum* und einiger anderen Pflanzen. Beith. Bot. Zentralbl. **10:** 128–139.

Nemhauser, J. L., F. Hong and J. Chory, 2006 Different plant hormones regulate similar processes through largely nonoverlapping transcriptional responses. Cell **126:** 467–475.

Oeller, P. W., L.-M. Wong, L. P. Taylor, D. A. Pike and A. Theologis, 1991 Reversible inhibition of tomato fruit senescence by antisense RNA. Science **254:** 437–439.

Pedmale, U. V., and E. Liscum, 2007 Regulation of phototropic signaling in *Arabisopsis* via phosphorylation state changes in the phototropin 1-interacting protein NPH3. J. Biol. Chem. **282:** 19992–20001.

Penfield, S., A. D. Gilday, K. J. Halliday, I. A. Graham, 2006 DELLA-mediated cotyledon expansion breaks coat-imposed seed dormancy **16:** 2366–2370.

Pien, S., D. Fleury, J. S. Mylne, P. Crevillen, D. Inze *et al.*, 2008 ARABIDOPSIS TRITHORAX1 dynamically regulates *FLOWERING LOCUS C* ACTIVATION via histone 3 lysine 4 trimethylation. The Plant Cell **20:** 580–588.

Pré, M., M. Atallah, A. Champion, M. De Vos, C. M. J. Pieterse *et al.*, 2008 The AP2/ERF domain transcription factor ORA59 integrates jasmonic acid and ethylene signals in plant defense. Plant Physiol. **147:** 1347–1357.

Roman, G., B. Lubarsky, J. J. Kieber, M. Rothenberg and J. R. Ecker, 1995 Genetic analysis of ethylene signal transduction in *Arabidopsis thaliana*: five novel mutant loci integrated into a stress response pathway. Genetics **139:** 1393–1409.

Samach, A., H. Onouchi, S. E. Gold, G. S. Ditta, Z. Schwarz-Sommer *et al.*, 2000 Distinct roles of CONSTANS target genes in reproductive development of *Arabidopsis*. Science **288:** 1613–1616.

Schwab, R., S. Ossowski, M. Riester, N. Warthmann and D. Weigel, 2006 Highly specific gene silencing by artificial microRNAs in *Arabidopsis*. Plant Cell **18:** 1123–1133.

Schwechheimer, C., 2008 Understanding gibberellic acid signaling: are we there yet? Curr. Opin. Plant Biol. **11:** 9–15.

Schwechheimer, C., and B. C. Willige, 2009 Shedding light on gibberellic acid signaling. Curr. Opin. Plant Biol. **12:** 57–62.

Schweighofer, A., V. Kazanaviciute, E. Scheikl, M. Teige, R. Doczi *et al.*, 2007 The PP2C-type phosphatase AP2C1, which negatively regulates MPK4 and MPK6, modulates innate immunity, jasmonic acid, and ethylene levels in Arabidopsis. Plant Cell **19:** 2213–2224.

Searle, I., Y. He, F. Turck, C. Vincent, F. Fornara *et al.*, 2006 The transcription factor FLC confers a flowering response to vernalization by repressing meristems competence and systemic signaling in Arabidopsis. Genes Dev. **20:** 898–912.

Smalle, J., M. Haegman, J. Kurepa, M. Van Montagu and D. Van Der Straeten, 1997 Ethylene can stimulate *Arabidopsis* hypocotyls elongation in the light. Proc. Natl. Acad. Sci. USA **94:** 2756–2761.

Smith, H., and G. C. Whitelam, 1997 The shade avoidance syndrome: multiple responses mediated by multiple phytochromes. Plant Cell Environ. **20:** 840–844.

Stepanova, A. N., J. Yun, A. V. Likhacheva and J. M. Alonso, 2007 Multilevel interactions between ethylene and auxin in Arabidopsis roots. Plant Cell **19:** 2169–2185.

Stepanova, A. N., J. M. Hoyt, J. Yun, L. M. Benavente, D.-Y Xie *et al.*, 2008 *TAA1*-mediated auxin biosynthesis is essential for hormone crosstalk and plant development. Cell **133:** 177–191.

Sun, T.-P., H. M. Goodman and F. M. Ausubel, 1992 Cloning the Arabidopsis *GA1* locus by genomic subtraction. Plant Cell **4:** 119–128.

Swarup, R., P. Paula, D. Hagenbeek, D. Van Der Straeten, G. T. S. Beemster *et al.*, 2007 Ethylene upregulates auxin biosynthesis in *Arabidopsis* seedlings to enhance inhibition of root cell elongation. Plant Cell **19:** 2186–2196.

Talbert, P. B., H. T. Adler, D. W. Parks and L. Comai, 1995 The *REVOLUTA* gene is necessary for apical meristem development and for limiting cell divisions in the leaves and stems of *Arabidopsis thaliana*. Development **121:** 2723–2735.

Tanaka, H., P. Dhonukshe, P. B. Brewer and J. Friml, 2006 Spatiotemporal asymmetric auxin distribution: a means to coordinate plant development. Cell. Mol. Life Sci. **63:** 2738–2754.

Tao, Y., J.-L. Ferrer, K. Ljung, F. Pojer, F. Hong *et al.*, 2008 Rapid synthesis of auxin via new tryptophan-dependent pathway is required for shade avoidance in plants. Cell **133:** 164–176.

Tarun, A. S., and A. Theologis, 1998 Complementation analysis of mutants of 1-aminocyclopropane-1-carboxylate synthase reveals the enzyme is a dimer with shared active sites. J. Biol. Chem. **273:** 12509–12514.

Terao-Morita, M., and M. Tasaka, 2004 Gravity sensing and signaling. Curr. Opin. Plant Biol. **7:** 712–718.

Thain, S. C., F. Vandenbussche, L. J. J. Laarhoven, M. J. Dowson-Day, Z.-Y. Wang *et al.*, 2004 Circadian rhythms of ethylene emission in Arabidopsis. Plant Physiol. **136:** 3751–3761.

Thomann, A., E. Lecher, M. Hansen, E. Dumbliauskas, Y. Parmentier *et al.*, 2009 Arabidopsis *CULLIN3* genes regulate primary root growth and patterning by ethylene-dependent and –independent mechanisms. PLoS Genet. **5:** e1000328.

Thomma, B. P. H. J., K. Eggermont, K. F. M. J. Tierens and W. F. Broekaert, 1999 Requirement of functional *Ethylene-Insensitive 2* gene for efficient resistance of Arabidopsis to infection by *Botrytis cinerea*. Plant Physiol. **121:** 1093–1101.

Thomma, B. P. H. J., I. A. M. A. Penninckx, W. F. Broekaert and B. P. A. Cammue, 2001 The complexity of disease signaling in *Arabidopsis*. Curr. Opin. Immun. **13:** 63–68.

Tsuchisaka, A., and A. Theologis, 2004a Heterodimeric interactions among the 1-amino-cyclopropane-1-carboxylate synthase polypeptides encoded by the *Arabidopsis* gene family. Proc. Natl. Acad. Sci. USA **101:** 2275–2280.

Tsuchisaka, A., and A. Theologis, 2004b Unique and overlapping expression patterns among the arabidopsis 1-amino-cyclopropane-1-carboxylate synthase gene family members. Plant Physiol. **136:** 2982–3000.

Vandenbussche, F., J.-P. Verbelen and D. Van Der Straeten, 2005 Of light and length: regulation of hypocotyls growth in *Arabidopsis*. BioEssays **27:** 275–284.

Vanneste, S., and J. Friml, 2009 Auxin: a trigger for change in plant development. Cell **136:** 1005–1016.

Wang, K. L. C., H. Yoshida, C. Lurin and J. R. Ecker, 2004 Regulation of ethylene gas biosynthesis by the *Arabidopsis* ETO1 protein. Nature **428:** 945–950.

West, J. L., and N. J. Halas, 2003 Engineered nanomaterials for biophotonics applications: improving sensing, imaging, and theraoeutics. Ann. Rev. Biomed. Eng. **5:** 285–292.

Wigge, P. A., M. C. Kim, K. E. Jaeger, W. Busch, M. Schmid *et al.*, 2005 Integration of spatial and temporal information during floral induction in *Arabidopsis*. Science **309:** 1056–1059.

Xiao, W., K. D. Custard, R. C. Brown, B. E. Lemmon, J. J. Harada *et al.*, 2006 DNA methylation is critical for Arabidopsis embryogenesis and seed viability. Plant Cell **18:** 805–814.

Xu, S.-L, A. Rahman, T. I. Baskin and J. J. Kieber, 2008 Two leucine-rich repeat receptor kinases mediate signaling linking cell wall biosynthesis and ACC synthase in *Arabidopsis*. Plant Cell **20:** 3065–3079.

Yamagami, T., A. Tsuchisaka, K. Yamada, W. F. Haddon, L. A. Harden *et al.*, 2003 Biochemical diversity among the 1-amino-cyclopropane-1-carboxylate synthase isozymes encoded by the *Arabidopsis* gene family. J. Biol. Chem. **278:** 49102–49112.

Yang, S. F., and N. E. Hoffman, 1984 Ethylene biosynthesis and its regulation in higher plants. Ann. Rev. Plant Physiol. **35:** 155–189.

Yip, W.-K., J.-G. Dong, J. W. Kenny, G. A. Thompson and S. F. Yang, 1990 Characterization and sequencing of the active site of 1-aminocyclopropane-1-carboxylate synthase. Proc. Natl. Acad. Sci. USA **87:** 7930–7934.

Yoo, S.-D., Y.-H. Cho, G. Tena, Y. Xiong and J. Sheen, 2008 Dual control of nuclear EIN3 by bifurcate MAPK cascade in C_2H_4 signaling. Nature **451:** 789–795.

Zhao, Y., 2008 The role of local biosynthesis of auxin and cytokinin in plant development. Curr. Opin. Plant Biol. **11:** 16–22.

Zhong, R., and Z.-H. Ye, 2001 Alteration of auxin polar transport in the Arabidopsis *ifl1* mutants. Plant Physiol. **126:** 549–563.

Communicating editor: B. Bartel

GENETICS

Supporting Information
http://www.genetics.org/cgi/content/full/genetics.109.107102/DC1

A Combinatorial Interplay Among the 1-Aminocyclopropane-1-Carboxylate Isoforms Regulates Ethylene Biosynthesis in *Arabidopsis thaliana*

Atsunari Tsuchisaka, Guixia Yu, Hailing Jin, Jose M. Alonso, Joseph R. Ecker, Xiaoming Zhang, Shang Gao and Athanasios Theologis

DOI: 10.1534/genetics.109.107102

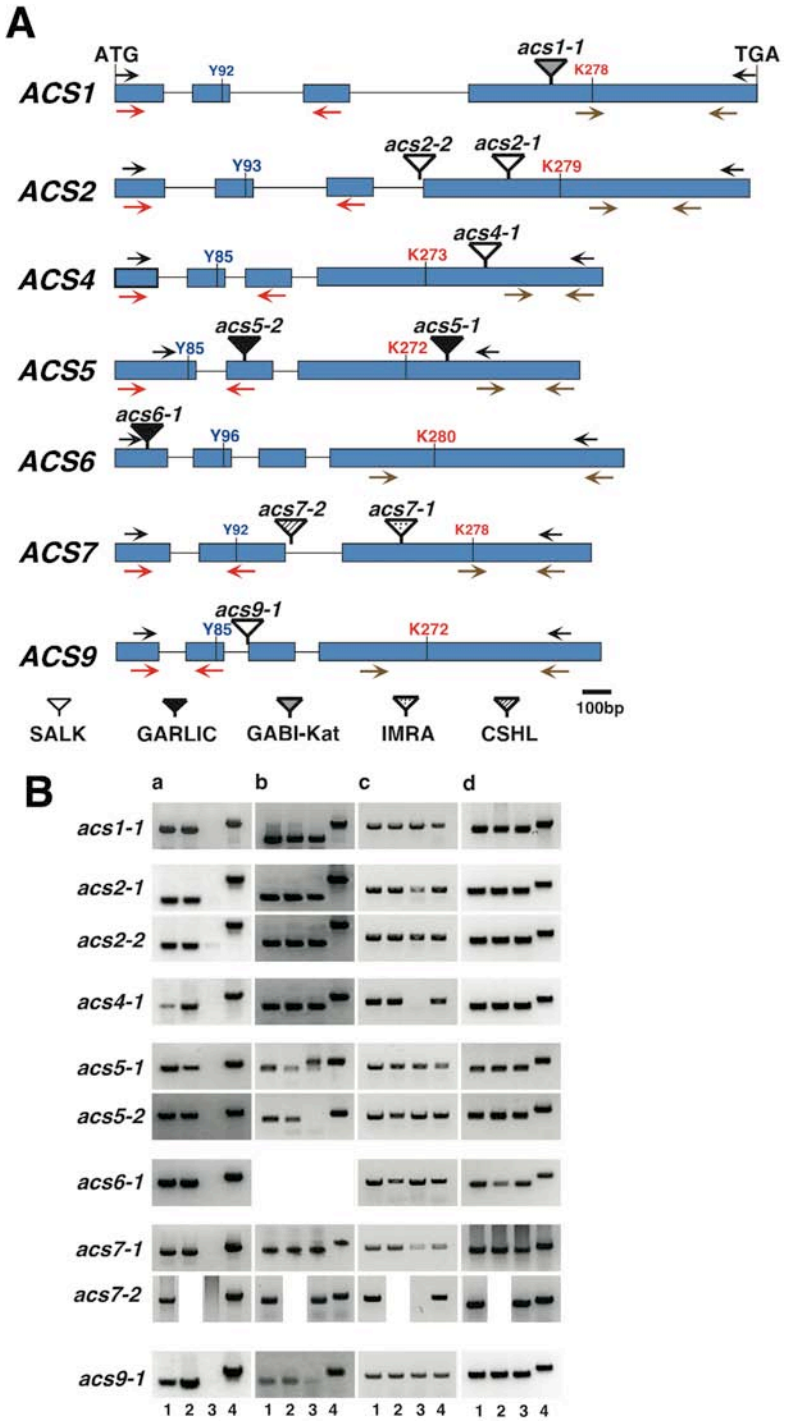

FIGURE S1.—T-DNA insertions in the *ACS* gene family members. The location of insertions in seven *ACS* gene family members is shown in (A). Boxes and lines connecting the boxes represent exons and introns, respectively. White, black, gray, point, and slash triangles denote SALK, GARLIC, GABI-Kat, IMRA, and CSHL lines, respectively. Black, Red and Green arrows indicate the location of primers used for RT-PCR. The Y and K residues participate in enzyme catalysis. The effect of the insertions on *ACS* gene expression is shown in (B). The expression of each inactivated *ACS* gene was accessed by RT-PCR using mRNA from CHX treated 7-day old etiolated seedlings. (See Materials and Methods). The lanes are: 1. wt; 2. homozygous w/o T-DNA; 3. homozygous for the T-DNA insertion; 4. genomic DNA. a. RT-PCR analysis with the "black set of primers" shown in A. b. RT-PCR analysis with the "red set of primers" shown in A. c. RT-PCR analysis with the "green set of primers" shown in A. d. RT-PCR analysis with ACT8 primers. The *ACT8* gene was used as a non-differential expressed gene.

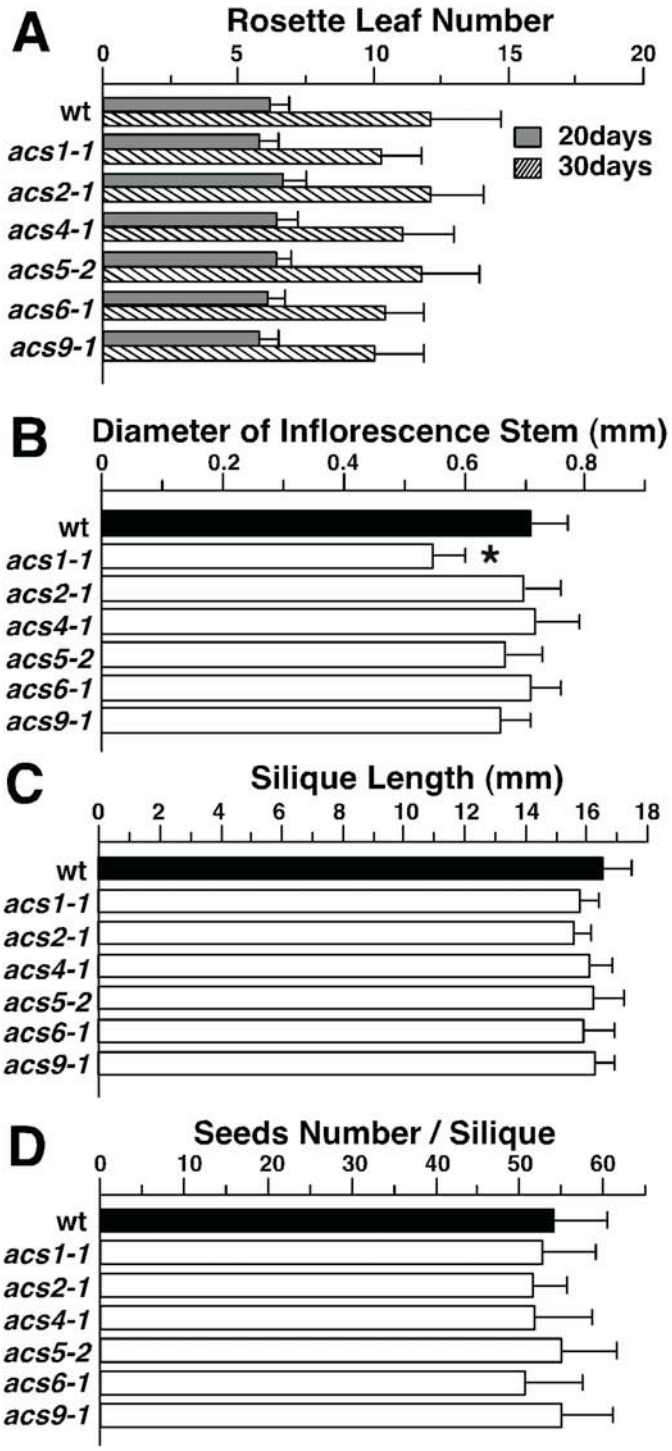

FIGURE S2.—Effect of the *acs* single mutants on various morphological characteristics of adult plants. Comparison of the rosette-leaf number among wt and *acs* single mutants in 20- and 30-days old light-grown plants is shown in (A; N= 20). Comparison of the inflorescence stem diameter among wt and *acs* single mutants in 40-day old light-grown plants is shown in (B; N= 10). Comparison of the length of mature siliques among wt and *acs* single mutants in 50-day old light-grown plants is shown in (C; N= 10). Comparison of the seed number/silique among wt and *acs* single mutants is shown in (D; N= 10). Bars represent the standard deviation (SD). The asterisk (*) above the bars indicates statistically significant difference between the mutant and the wt ($P < 0.01$). The absence of an asterisk indicates statistically insignificant difference between the mutant and the wt ($P > 0.05$).

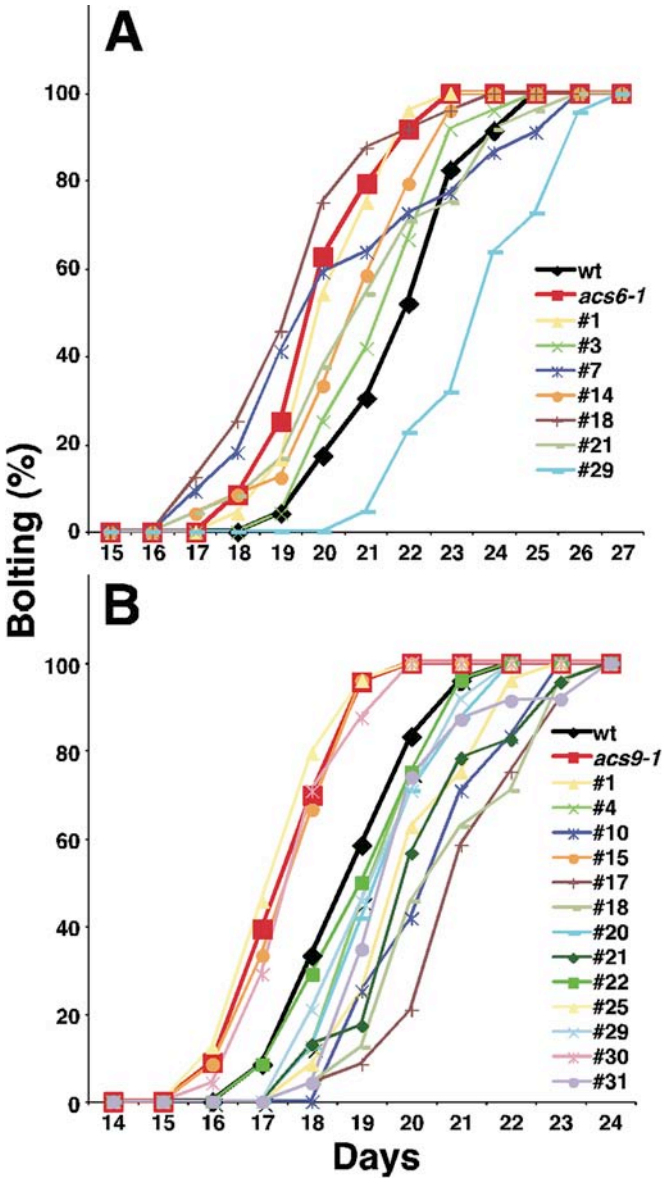

FIGURE S3.—Flowering time of the *acs6-1* and *acs9-1* complementation lines. Complementation lines of *acs6-1* with the *ACS6 cDNA* (A) and of *acs9-1* with the *ACS9 cDNA* (B). The flowering times of wt and single mutants are compared to those of several complementation lines shown in (A) and (B) respectively.

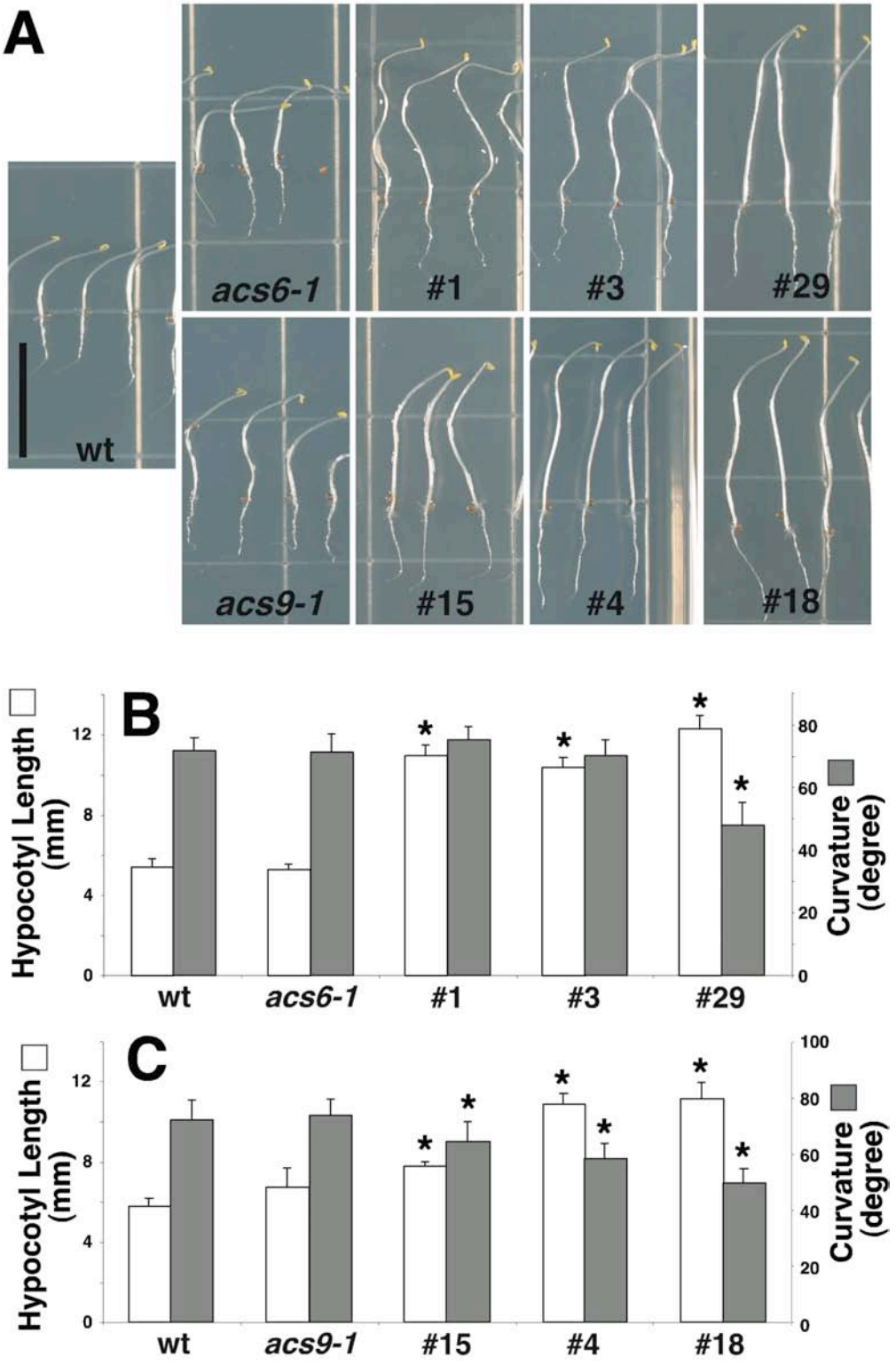

FIGURE S4.—Hypocotyl length and response to gravity of the *acs6-1* and *acs9-1* complementation lines. The gravitotropic responses of the wt, *acs6-1*, *acs9-1* and complementation lines in 3-day old etiolated seedlings after 24 hr of gravitostimulation are shown in (A). Bar= 1cm. Comparison of the hypocotyl length (white box) and gravitotropic response (gray box) among wt, *acs6-1* and complementation lines #1, #3, and #29 in 3-day old etiolated seedlings is shown in (B; N= 10). Similar comparison among wt, *acs9-1* and complementation lines #15, #4, and #18 in 3-day old etiolated seedlings is shown in (C; N= 10). Bars represent the standard deviation (SD). The asterisk (*) has been defined in the legend of Figure S2.

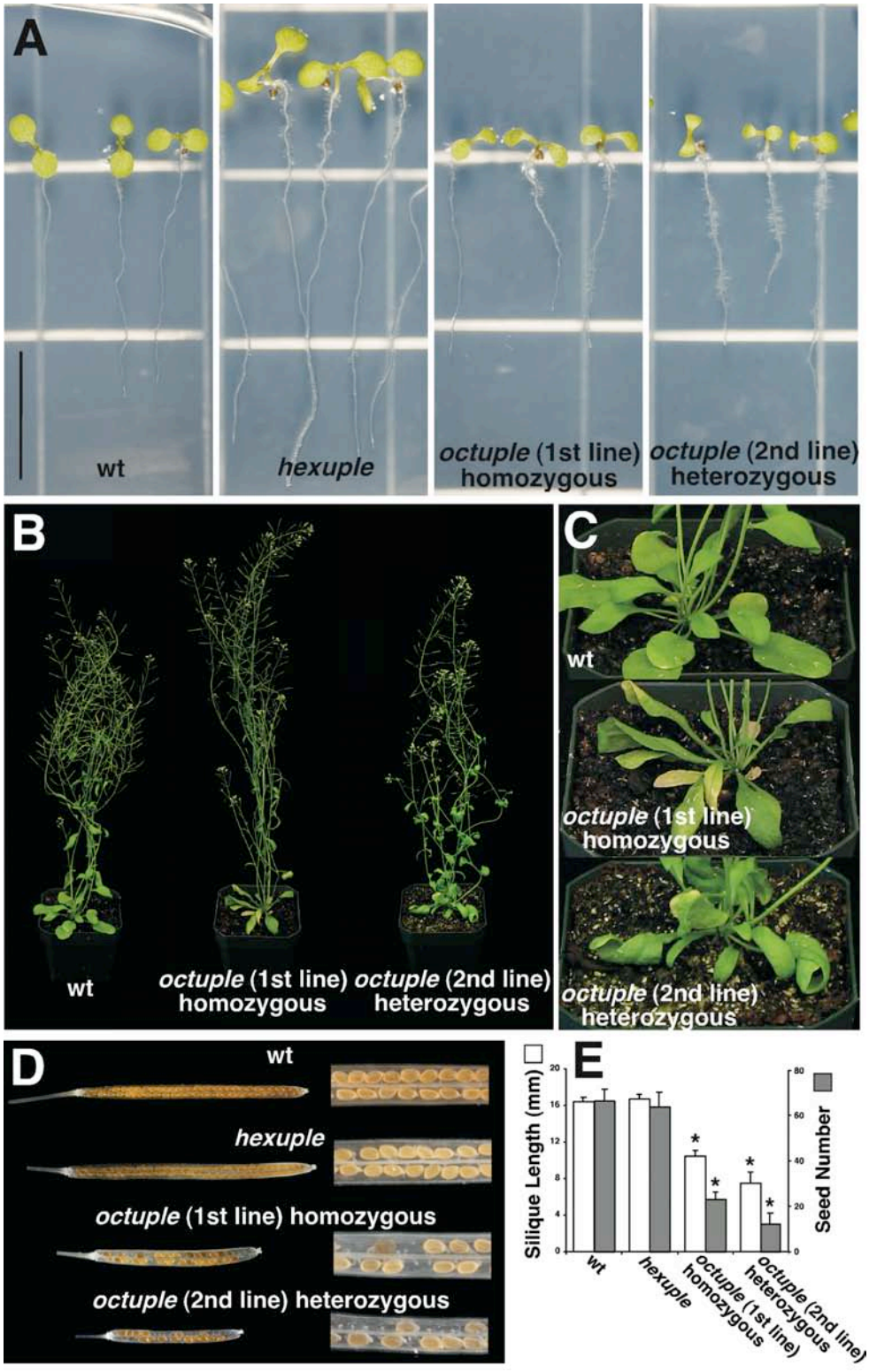

FIGURE S5.—Phenotypic comparison between the two *octuple* (*amiR*) lines. The phenotype of 5-day old light-grown seedlings is shown in (A). The phenotype of 50-day old plants is shown in (B) and leaf morphology is shown in (C). The silique morphology and seed content of the *octuple* (*amiR*) lines are shown in (D). Their silique length and seed number are shown in (E: N= 5). Bars represent the standard deviation (SD). The asterisk (*) has been defined in the legend of Figure S2.

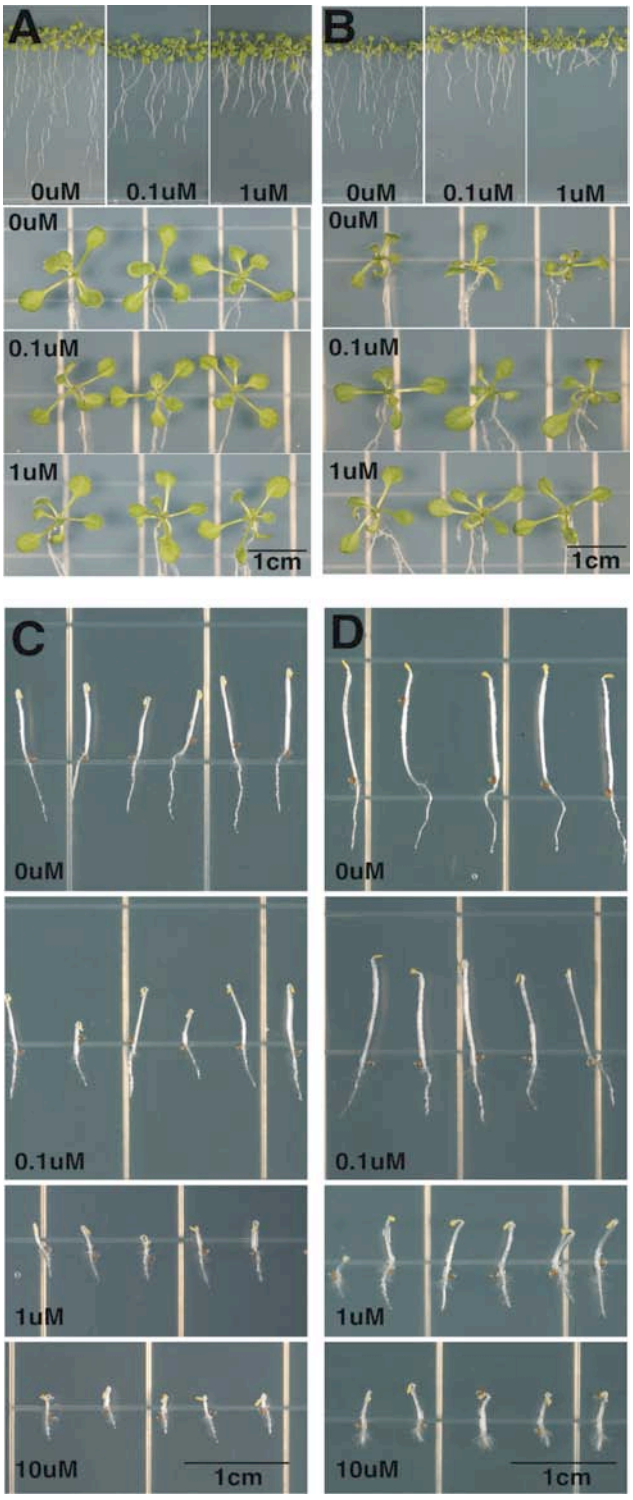

FIGURE S6.—Effect of exogenous ACC on the *octuple* seedling phenotype. The phenotypes of 10-day old light-grown wt and *octuple* seedlings treated with various concentrations of ACC are shown in panels (A) and (B), respectively. Similar comparison with 3-day old etiolated wt and *octuple* seedlings grown on plates containing different concentrations of ACC is shown in panels (C) and (D), respectively.

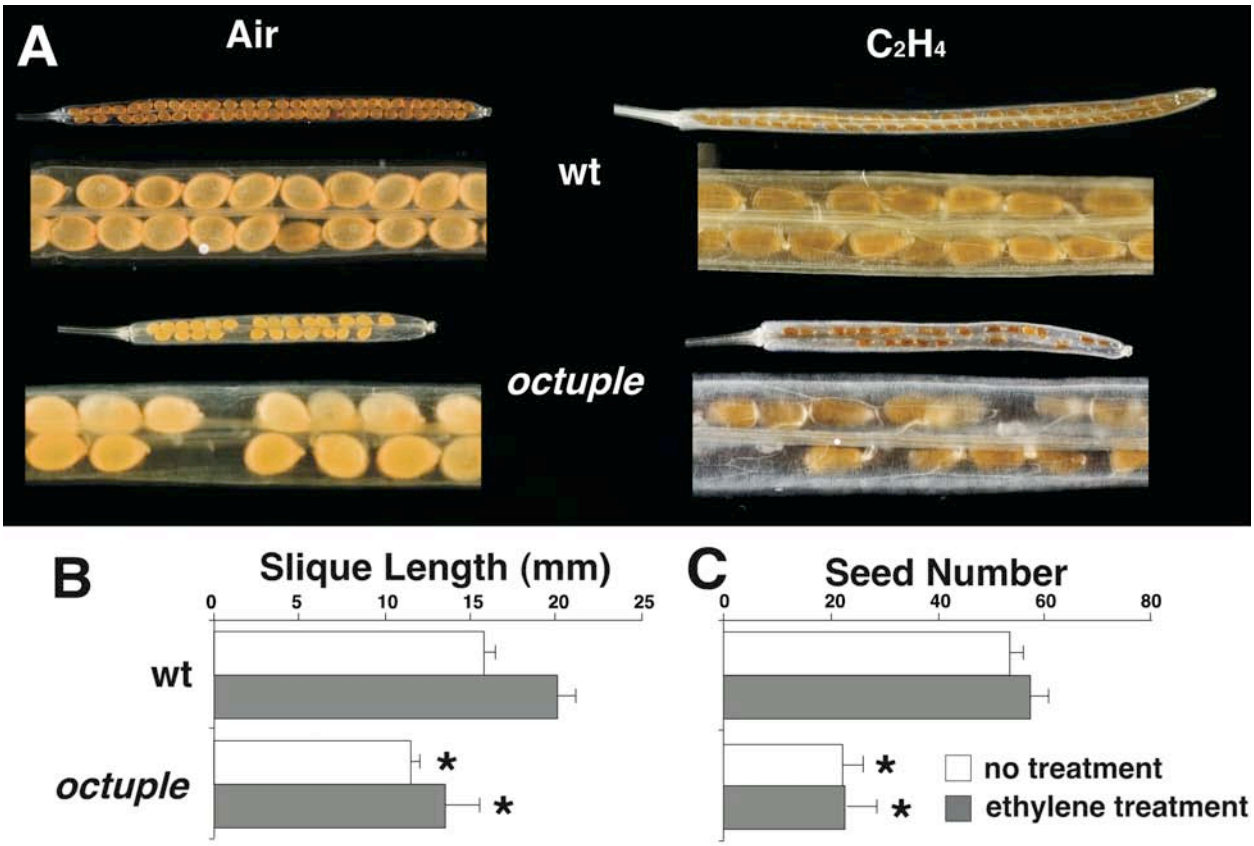

FIGURE S7.—Effect of exogenous ethylene on the *octuple* silique phenotype. Comparison of the silique phenotype of 40-day old wt with that of *octuple* plant after treatment with air (control) or with 10ppm exogenous ethylene is shown in (A). Quantitative comparison of the silique length (B) and seed number / silique (C) of wt and *octuple* mutant are shown below panel (A). (N= 5 in B and C). Bars represent the standard deviation (SD). The asterisk (*) has been defined in the legend of Figure S2.

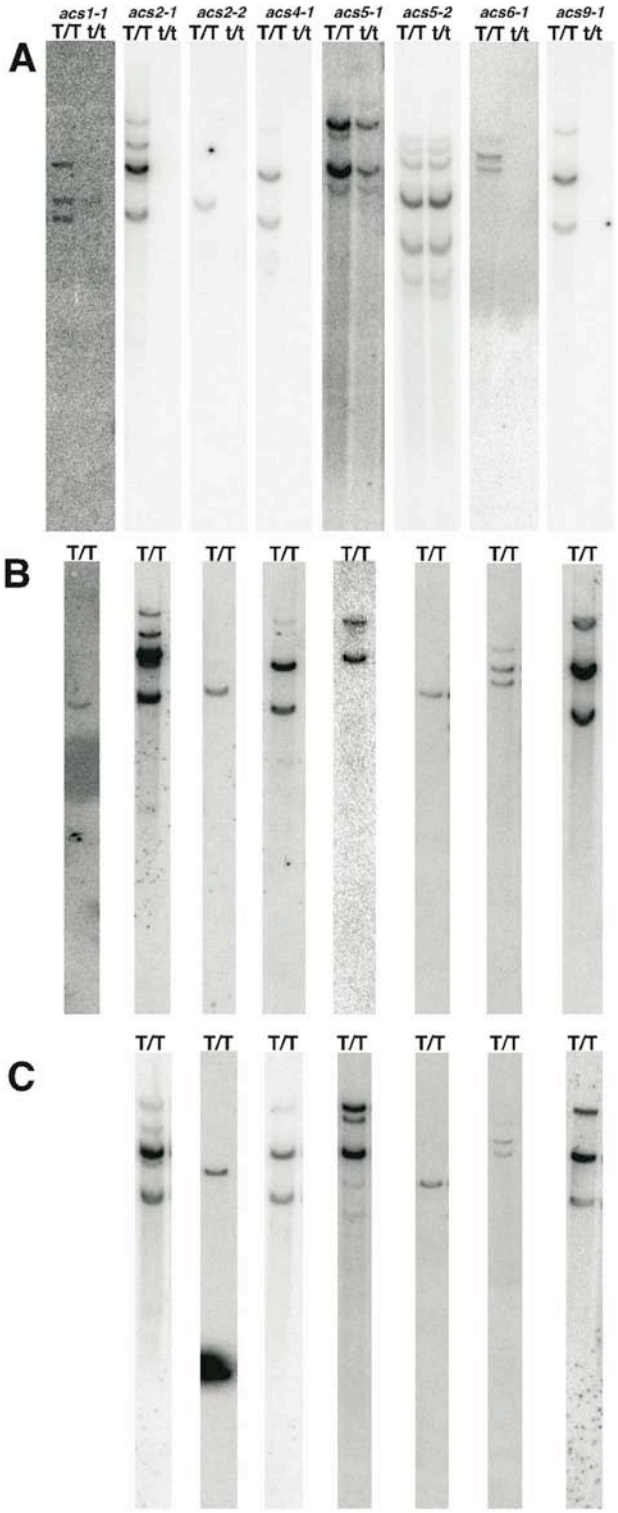

FIGURE S8.—Integration pattern of T-DNA in the single insertion lines accessed by southern blot analysis (See Supporting Experimental Procedures). No backcross (A), 1st backcross (B), 2nd backcross (C); T/T; homozygous for T-DNA, t/t; homozygous for no T-DNA.

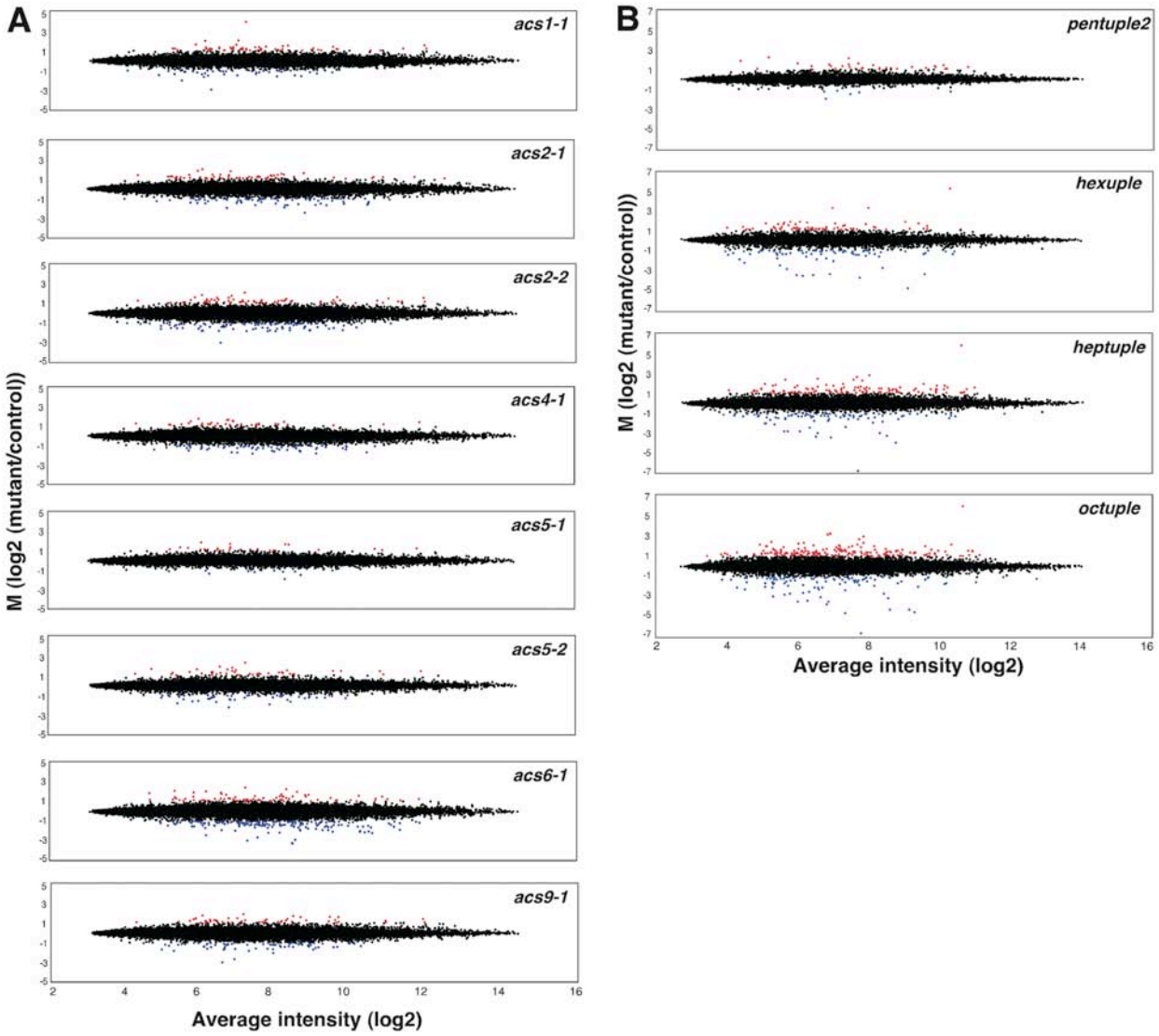

FIGURE S9.—Global gene expression profiling of the *acs* mutants. *M-A* plots (DUDIOT *et al.* 2002) showing changes in gene expression levels in the eight single mutants compared to the wt control are shown in (A). Each plot represents the log ratio of the average of the mutant (I) to the control samples (C) ($M = \log_2 (I / C)$), versus overall average intensity ($A = \log_2 \sqrt{(I*C)}$). The genes induced by each mutation ($M > 1$) are highlighted in red and the genes repressed by the mutation ($M < -1$) are highlighted in blue. Similar *M-A* plots for the four high order mutants are shown in (B). The data were further analyzed for variance to extract statistically valid regulated genes as described in Supporting Experimental Procedures.

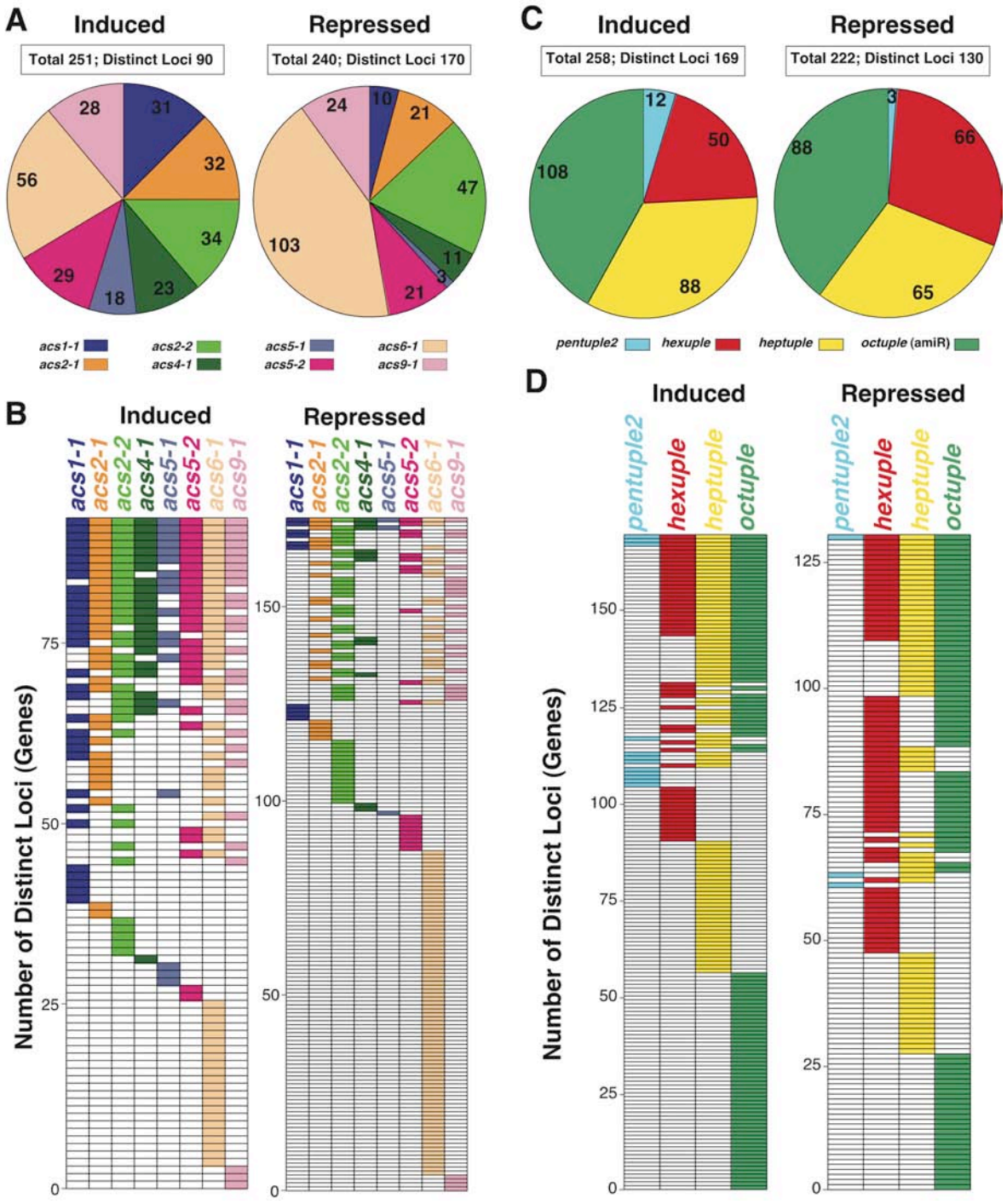

FIGURE S10.—Global Gene Expression Profiling. A Comparative analysis of genes differentially regulated by the single mutants is shown in (A). Each section of the pie diagram indicates the numbers of total genes with induced or repressed level of expression in each type of mutant. Genes with greater than two-fold increase were analyzed. The unique and overlapping patterns of gene expression among the induced and repressed genes in the single mutants are shown in (B). The lists of induced and repressed genes are shown in Tables S2 and S3, respectively. A similar comparative analysis of genes differentially regulated by the high order mutants is shown in panels (C) and (D). The lists of induced and repressed genes are shown in Tables S4 and S5, respectively. Seedling age; 10-day old light-grown *seedlings* for all mutants.

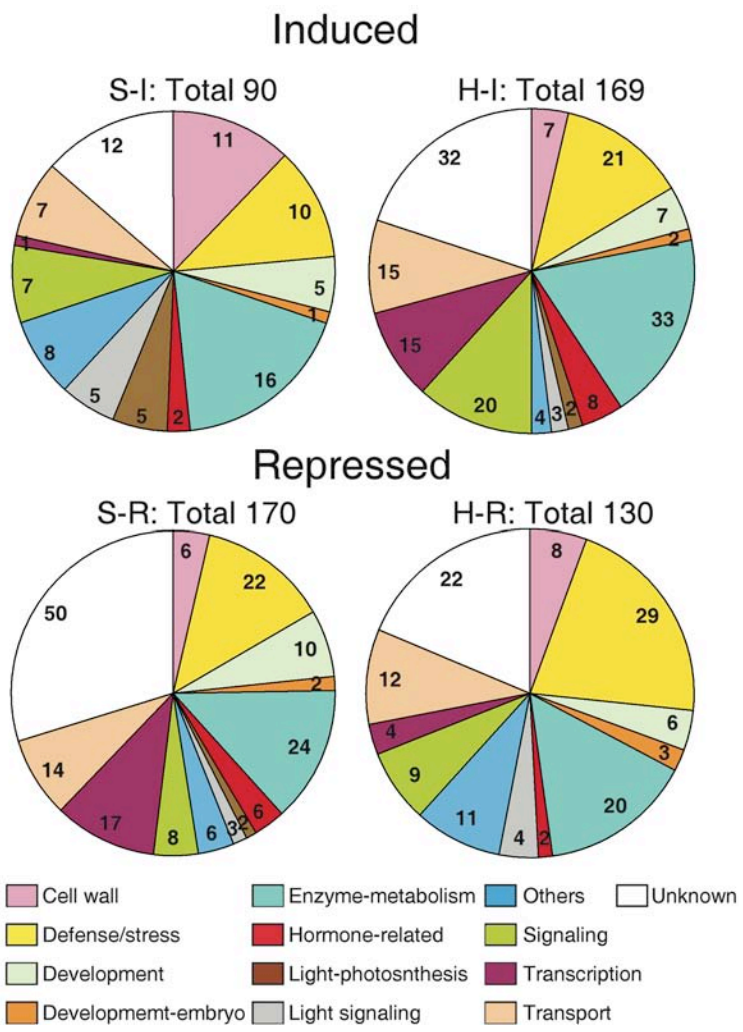

FIGURE S11.—Functional classification of Induced and Repressed genes in the single and high order mutants (S-I; induced in single mutants, S-R; repressed in single mutants, H-I; induced in high order mutants, H-R; repressed in high order mutants).

FILE S1

Supporting Materials and Methods

Strains and Transformation Vectors:

E. coli DH5α (*supE*44, *hsdR*17, *recA*1, *endA*1, *gyrA*1, *thi*-1, *relA*1, *lacU*169, *80lacZ* M15) was used for most transformations. The *pBS SK*- and *pTrc99a* vectors (Amersham Pharmacia Biotech Inc, Piscataway, NJ) were used for sub-cloning. The binary vector *pPZP122* (HAJDUKIEWICS *et al.* 1994) and *pPZP132* (this study) were used for plant transformation in the *Agrobacterium tumefaciens* strain GV3101. Standard protocols were followed for DNA manipulation described in SAMBROOK *et al.* (1989). Standard protocols for DNA sequencing were used to confirm the accuracy of the DNA constructs.

Plant Material and Growth Conditions:

Arabidopsis thaliana ecotype Columbia (Col) was used throughout this study. Seeds were surface sterilized for 8min in 5% sodium hypochlorite, 0.15% Tween 20, excessively rinsed in distilled water, and germinated on MS medium (0.8% Select Agar (Life Technologies, Inc., Rockville, MD), 0.5X Murashige-Skoog (MS) salts (Life Technologies, Inc.), 0.5mM MES, pH5.7, 1% sucrose, 1X B5 vitamins. After cold treatment at 4 °C for 2 days, the plates were incubated at 25 °C under 16h light / 8h dark (light grow seedlings) or under the dark (etiolated seedlings) for 3 to 10 days. Light-grown seedlings were transferred to soil and grown at 25 °C under 16 h light / 8h dark condition. Light-grown or etiolated wt and *octuple* seedlings were treated with exogenous ACC by placing seeds on top of MS plates containing various concentration of ACC. The plates were incubated for 10 days (light-grown seedlings) or 3 days (etiolated seedlings) under the conditions described above. Siliques from ethylene treated wt and *octuple* plants were obtained by treating 30-day old plants that had flowers with 10ppm ethylene for 48 hrs in a growth chamber under the conditions described above. Wild-type plants of the same age were treated with air under identical conditions. Subsequently, the ethylene treated plants were placed in the greenhouse and grown under the conditions described above until the siliques were ready for harvest.

Identification and Characterization of T-DNA Insertion Alleles:

We initiated this study using a PCR-based screening approach to identify T-DNA insertion mutants for the *ACS* gene family members. A total of 80,000 T-DNA insertion line populations in the Columbia ecotype (ALONSO *et al.* 2003) were initially screened using *ACS* gene and T-DNA specific primers (see below). Four lines were identified with insertions in the coding regions of *ACS2*, *4* and *9*. We named these insertion lines, *acs2-1*, *acs2-2*, *acs4-1* and *acs9-1*, respectively (Figure S1A). Subsequently, the laboratory participated in generating the GARLIC lines in collaboration with the former Torrey Mesa Research Institute and three additional lines were isolated (SESSIONS *et al.* 2002). We named these insertion lines, *acs5-1*, *acs5-2* and *acs6-1*, respectively

(Figure S1A). More recently, we isolated one insertion line in the coding region of *ACS1* from the GABI-kat collection and two lines in the coding region of *ACS7* from the INSTITUT NATIONAL DE LA RECHERCHE AGRONOMIQUE (INRA) and Cold Spring Harbor Laboratory (CSHL) collections, respectively. We named these insertion lines, *acs1-1*, *acs7-1* and *acs7-2*, respectively. Two additional lines were also identified in the SALK collection, in the *ACS7* and *ACS10* genes, respectively, but they were not included in this study. The insertion in *ACS7* is located 678bp upstream from the translation initiation codon and does not inactivate its gene expression (data not shown); the insertion in *ACS10* is in a non-authentic *ACS* gene; the gene annotated as *ACS10* encodes an aminotransferase (YAMAGAMI *et al.* 2003). All insertions lines are in Col-0 background except for *acs7-1* and *acs7-2,* which are in Ws-4 and Ler-0 backgrounds, respectively. All lines in the Col-0 background were backcrossed twice and Southern analysis of sibling plants that are either homozygous for the T-DNA insertion or homozygous for no T-DNA is shown in the Figure S8. The integration pattern of T-DNA becomes simpler in some lines after two backcrosses (Figure S8; compare panel A with panels B and C). The *acs7-1* line (Ws-4) was backcrossed eight times to the wild-type Col-0 background and used for some experiments reported in this study. The *acs7-2* line (Ler-0) was not used during this work.

1. Screening for T-DNA Insertions: The identification of insertion mutants utilizes a PCR-based screen. For each gene, a forward [F] primer annealing to 100-150 bp 5' of the ATG and a reverse [R] primer annealing to 100-150 bp 3' of the translation stop codon were designed. The size of the genomic products ranged from 3 to 1 kb. Eight sets of DNA template derived from 10,000 plants each (80,000 lines total) were screened. Each set of template contained 40 tubes of DNA (10 each of DNA combined from column, row, plate, and individual super pools). Identification of an individual requires a PCR product in each of the 4 super pools. A total of 1,280 PCR reactions (4 x 40 x 8 = 1,280) were carried out per gene using all combinations of F and R primers annealing to the left (LB) and right boarders (RB) of the T-DNA. All operations were adapted to a 384-well format and handling of samples performed with a BioMek robot. The products were analyzed by Southern blotting to allow increased sensitivity of detection and assess the specificity of screening. Subsequent to this screen, two large databases containing sequence of DNA flanking T-DNA inserts in 100,000 and 20,000 independent lines have been screened *in silico*. Data for the 100,000 lines were generated in a collaboration of U.C. Berkeley with the Torrey Mesa Research Institute and the 20,000 lines have been obtained by SIGNAL (http://signal.salk.edu/cgi-bin/tdnaexpress).

2. Confirmation of T-DNA Lines: The nature and location of the T-DNA insertion was confirmed by sequencing PCR products. Once the location of the T-DNA insertion line was confirmed, we designed gene specific PCR primers that flank the T-DNA for use in a co-dominant genotyping analysis. By performing two sets of PCR, one using the gene specific primer pair and the other using a gene specific primer and the T-DNA boarder primer, we could determine whether the individual is homozygous for no T-DNA insertion, heterozygous for the T-DNA insertion, or homozygous for the T-DNA insertion.

The oligonucleotides primers used for screening the SALK lines were:

ACS1: F; 5'-TGTCTCAGGGTGCATGTGAGAATCAACTT-3'

ACS1: R; 5'-AGCTCGAAGCAATGGTGAATGAGGAGACA-3'

ACS2: F; 5'-GCGACTAACAATCAACACGGAG-3'

ACS2: R; 5'-ACATTATCCCTGGAGACGAGAGAC-3'

ACS4: F; 5'-CCAAGTCTCTTCGTATTTCCTT-3'

ACS4: R; 5'-TAGTCGGAAAACCCAGTTAGAGAC-3'

ACS5: F; 5'-GTTCTCTCCTTCACCCACATTAGT-3'

ACS5: R; 5'-GGTACAATACACACAAACGT-3'

ACS6: F; 5'-AATTGATAGACCTGACGGAGTTAT-3'

ACS6: R; 5'-TCATAGTTGTTGCAGCCATCGGTTTA-3'

ACS7: F; 5'- CTAGTTCCCACACCGTATTATCCA-3'

ACS7: R; 5'- AGAACACTTTGGAGATTGCGTTGA-3'

ACS8: F; 5'-GATCCAGTGTAAGAGTGCAAACGGTT-3'

ACS8: R; 5'-CGTGAACCCGAGGAACGATAG-3'

ACS9: F; 5'-GGATGGGAAGAATACGAGAAGAACCC-3'

ACS9: R; 5'-ATCACTCTTCTACTATCTGTTGACTC-3'

ACS11: F; 5'-GTACACAATTTCCAAACTTTTGTTTATCGGTTGTTGTTTCC-3'

ACS11: R; 5'-AGAGGAAAGCTTGGAGACCCATTTGTTGATAAGAG-3'

The oligonucleotides primers used for identifying homozygous T-DNA lines were:

acs1-1: F; 5'-TAGACAGGCGATTGCGACGTTTATGGAGAGA-3'

acs1-1: R; 5'-GCCAGGAGAGACATTAATACTGAC-3'

acs2-1: F; 5'-TTTCCGCAGATTTGATAGAGACTTGA-3'

acs2-1: R; 5'-TCTGCTTTCTTGATCCCCGTGGTAAA-3'

acs2-2: F; 5'-GCGACTAACAATCAACACGGAG-3'

acs2-2: R, 5'-ACATTATCCCTGGAGACGAGAGAC-3'

acs4-1: F; 5'-GACAACAACCCAAACCGAACTCAACA-3'

acs4-1: R; 5'-CTCTTTTGGCATCTTCTACTTGAG-3'

acs5-1 and *acs5-2*: F; 5'-CCAGCTATGTTTCGATCTAATCGAGTCATGGTTAAC-3'

acs5-1 and *acs5-2*: R; 5'-GAGGTCAAGCTCTGCTTCAAATGTGTTTGTGTCCA-3'

acs6-1: F; 5'-ATGGTGGCTTTTGCAACAGAGAAGAAGCA-3'

acs6-1: R; 5'-AAGGCTTCCACCGTAATCTTGAACCCATT-3'

acs7-1: F; 5'-AACAACAACAACGTCGAGCTTTCTCGAGT-3'

acs7-1: R; 5'-AGATCCCGGAGATATATTCAGGTTCAGCT-3'

acs9-1: F; 5'-GGATGGGAAGAATACGAGAAGAACCC-3'

acs9-1: R; 5'-ATCACTCTTCTACTATCTGTTGACTC-3'

3. Molecular characterization of the T-DNA lines: To determine the number of T-DNA inserts present in the lines, we compared the Southern hybridization patterns arising from sibling plants that were either homozygous for the T-DNA insertion or homozygous for no T-DNA. To remove additional T-DNA loci from the lines of interest, backcrosses to wild-type Columbia were performed and plants homozygous for the T-DNA insertion were again identified.

Southern Analysis:

Genomic DNA was isolated from flower buds as described by LIU *et al.* (1995). Five ug of genomic DNA was digested with *Xba*I

(SALK, GARLIC and GABI lines). These restriction enzymes does not cut the T-DNA. The digested genomic DNA was separated on a 0.8% agarose gel transferred to Hybond-N+ membrane (Amersham Biosciences), and hybridized with T-DNA specific probes. The SALK lines were hybridized with a *Bam*HI/*Nhe*I fragment obtained from *pBIN19*, the GARLIC lines were hybridized with a *Pvu*II fragment obtained from *pBluescript KS*+, the GABI line was hybridized with a *Afl*III/*Ssp*I fragment obtained from *pUC18*. After hybridization, the filters were analyzed using a phosphoimager (Molecular Dynamics).

Construction of Higher Order Mutants:

We used the strategy outlined below for constructing higher order mutations.

Construction of double mutants:

Cross: (1×2) → identify 1 + 2 by screening 61 F2 seedlings.

(1×3) → identify 1 + 3 by screening 61 F2 seedlings.

(1×4) → identify 1 + 4 by screening 61 F2 seedlings.

(1×5) → identify 1 + 5 by screening 61 F2 seedlings.

The number of seedlings to be screened is calculated using the equation: $N = \log (1-P)/\log [1-(1/4^n)]$ where, N is the number of plants that need to be screened, P is the desired probability, and n is number of genes being considered. With P = 0.98 and n = 2, 61 plants to be screened.

Construction of triple mutants: (and so on)

Cross-: (1 + 2) × (1 + 3) → identify 1 + 2 + 3 by screening 61 F2 seedlings.

(1 + 2) × (1 + 4) → identify 1 + 2 + 4 by screening 61 F2 seedlings.

(1 + 2) × (1 + 5) → identify 1 + 2 + 5 by screening 61 F2 seedlings.

The strategy is always based on screening for a double mutation. The generation and analysis of high order insertion lines is facilitated by the co-dominant PCR method described above.

Inactivation of the *ACS8* and *ACS11* gene expression with an artificial microRNA (*amiR*):

An artificial microRNA (*amiR*) containing transgene that specifically inhibit both *ACS8* and *ACS11* gene expression was constructed by overlapping PCR using the *pRS300* plasmid as template containing the MIR319a (SCHWAB *et al.* 2006). The PCR products were subcloned into the *pBS-SK-* vector. The primers used for preparing the *amiR* are shown below

I; 5'-GATAGTCTCGTTAGCCGGGGTTGTCTCTCTTTTGTATTCC-3'

II; 5'-GAGGCGTGCGAACTATATACTCATCAAAGAGAATCAATGA-3'

III; 5'-GACACCCCCGGCTAAGGAGACTTTCACAGGTCGTGATATG-3'

IV; 5'-GAAAGTCTCCTTAGCCGGGGGTGTCTACATATATATTCCT-3'

The specific sequences present in both *ACS8* and *ACS11* genes are underlined. DNA sequencing was used to confirm that no spurious mutations were introduced during mutagenesis.

Subsequently, the *pPZP122-35S-GUS-NOS* was modified for subcloning the *amiR* construct: the *GUS* gene was removed by *Xba*I/*Sac*I digestion and a linker containing useful restriction sites was ligated for subcloning the *amiR* into *pPZP122-35S-NOS*. The *amiR* gene were subcloned into the *Sal*I/*Bam*HI sites of *pPZP122-35S-NOS*. giving rise to *pPZP122-35S-amiR-NOS*. The linker sequences used are:

Sense; 5'- CTAGACTCGAGTCGACCGCGGATCCGAGCT-3'

Antisense; 5'- CGGATCCGCGGTCGACTCGAGT-3'

The *pPZP122-35S-amiR-NOS* was introduced into the *hexuple* mutant by transformation. The primers used for identifying the homozygous *octuple* line (1st line) were:

F; 5'-TCAACAAACTTTTAGGGGGTGTTATTGGTTCCA-3'

R; 5'-TTCATVAGGAAGTTAGCTGCCCAGTCCACGATT-3'

The primers used for identifying the heterozygous *octuple* line (2nd line) were:

F; 5'-TATACTGGTATCCTCATGAATGCTGGTGTTGGT-3'

R; 5'-ACATTGTGTTTGGCATGTGGCTGTGTAGACGTT-3'

Complementation of the *amiR* lines:

The *amiR* target sequences of the *ACS8* and ACS*11* ORFs were mutated by site-directed mutagenesis giving rise to *ACS8m* and *ACS11m* ORFs that encode functional proteins. The *pQE80-ACS8* and *pQE801-ACS11* plasmids (TSUCHISAKA and THEOLOGIS 2004b) were used as templates. The primers used are:

ACS8m: 5'- TGGTGCTACTCCAGCGAATGAAACGCTCATGTTTTGTCT-3'

ACS11m: 5'- AGCTGGATCAACCTCAGCCAATGAAACGTTAATGTTCTGT-3'

The mutant codon is underlined. DNA sequencing was used to confirm that no spurious mutations were introduced during mutagenesis.

Subsequently, the *ACS8m* and *ACS11m* ORFs were subcloned into the *Bam*HI (blunted)/*Sac*I sites of *pPZP132-35S-NOS* as *EcoRI* (blunted)/*SacI* fragments. A double gene constructs expressing both *ACS8m* and *ACS11m* was constructed by subcloning the *35S-ACS11m-NOS* gene into the *Bsi*WI/*Pme*I sites of *pPZP132-35S-ACS8m-NOS* as a *Bsi*WI/*Fsp*I fragment. The double gene construct was introduced into the *octuple* (*amiR*) mutant by transformation.

The primers used for identifying homozygous lines expressing *ACS8m* and *ACS11m* were:

Line#8: F; 5'-ACCAAAATCAGAGATCTGGGTACTTACGAGTCT-3'

Line#8: R; 5'-ACAGTGTAAAAGCTTCGAGAGACGCGAGAGGAA-3'

Line#10: F; 5'-AAGACAGCGAGATATAAGACGCATATGGCTCAA-3'

Line#10: R; 5'-ATGTACAAGAAGGTTCACGCAGCTATCCGAGCA-3'

Line#14: F; 5'-TATGAGTTGTTTGGCATTCTGGCCAGATCCAGA-3'

Line#14: R; 5'-ATGATGGTAACTGTACTGACGTAAACGAGAGCT-3'

Mapping the Insertion Sites of the *amiR, amiR* complementation and BiFC transgenes:

We used thermal asymmetric interlaced (TAIL) PCR for mapping the integration sites of the *amiR*, *amiR* complementation and BiFC transgenic lines following the procedure described by LIU *et al.* (1995). The primers used were:

Arbitrary primers:

TAIL-1; 5'-[A/C/G/T]GTCGA[C/G][A/T]GA[A/C/G/T]A[A/T]GAA-3'

TAIL-2; 5'-GT[A/C/G/T]CGA[C/G][A/T]CA[A/C/G/T]A[A/T]GTT-3'

TAIL-3; 5'-[A/T]GTG[A/C/G/T]AG[A/T]A[A/C/G/T]CA[A/C/G/T]AGA-3'

TAIL-4; 5'-TG[A/T]G[A/C/G/T]AG[C/G]A[A/C/G/T]CA[C/G]AGA-3'

TAIL-5; 5'-[A/C/G/T]TCGA[C/G]T[A/T]T[C/G]G[A/T]GTT-3'

TAIL-6; 5'-AG[A/T]G[A/C/G/T]AG[A/T]A[A/C/G/T]CA[A/T]AGG-3'

TAIL-7; 5'-[C/G]TTG[A/C/G/T]TA[C/G]T[A/C/G/T]CT[A/C/G/T]TGC-3'

T-DNA border-specific primers:

TL-1; 5'-CTAGAGTCGATCGACATCGAGTTTC-3'

TL-2; 5'-TGTGTGAGTAGTTCCCAGATAAGGG-3'

TL-3; 5'-GTACATTAAAAACGTCCGCAATGTG-3'

TL-1, TL-2 and TL-3 were used for primary, secondary, and tertiary TAIL-PCR reactions, respectively. The amplified fragments were isolated by using QIAquick® Gel Extraction Kit (QIAGEN, Valencia, CA) and sequenced. The chromosomal locations were determined by BLAST using V5.0 of the Arabidopsis chromosome (NCBI, http://www.ncbi.nlm.nih.gov/). The insertion was verified by PCR using TL-2 primers and the gene specific primers described above.

Complementation of the *acs6-1* and *acs9-1* mutants:

Both mutants were complemented by expressing the *ACS6* and *ACS9* ORFs from their own promoters (2.5kb). The *3'UTR*s of each gene (1kb) was also included in the constructs to ensure appropriate tissue specific expression (DIETRICH *et al.* 1992). The promoter regions and *3'UTR*s of *ACS6* and *ACS9* were obtained from the *pPZP122-ACS6 promoter-3'* and *pPZP122-ACS9 promoter-3'* plasmids, respectively (TSUCHISAKA and THEOLOGIS 2004b). The *ACS6* and *ACS9* ORFs were obtained from *pQE801-ACS6* and *ACS9* (TSUCHISAKA and THEOLOGIS 2004a) by *Nde*I (blunt-end)/*Sac*I digestion and were subcloned into the *pPZP122-ACS6 promoter-3'* and *pPZP122-ACS9 promoter-3'* as *Sma*I/*Sac*I fragments, respectively.

The primers used for identifying homozygous *acs6* complementation lines were:

Line#1: F; 5'-TGGTTATTGCAGTCCATCCAGTAGCATTCGA-3'

Line#1: R; 5'-AGTATTTTAGTTCGTTGCCCGTGAATCAGCT-3'

Line#3: F; 5'-AACTGCAACTAGGTTTGGGACACCGAGGTTT-3'

Line#3: R; 5'-ACATATGCAGATATAGAGGCGGCGTATGAGTGT-3'

Line#7: F; 5'-TCTGAAACGTTAAGGTTATGGGACTGGACATCT-3'

Line#7: R; 5'-TGCTTTAATCCATCTCCCTGAAGCTCCCATTCT-3'

Line#14: F; 5'-TACGTGGACTTATTGGTTGCAGGTATGGCCA-3'

Line#14: R; 5'-TTTCAACATGCTCCTACCAAACGCCCTGAGT-3'

Line#18: F; 5'-TAATTGACCATAGAGGGCATACTCTGGAGCCAA-3'

Line#18: R; 5'-AAACGACTCAAGATTGGGTATCTCGTCTCGGT-3'

Line#21: F; 5'-AAGCATAAGTTACCCTGAAGGTTGGGACGGT-3'

Line#21: R; 5'-ATGGTATGGGTTCAACAGTGGCGAGATTCGA-3'

Line#29: F; 5'-ACGACATCGTTTTAATGGTCATCGGGACCCTCT-3'

Line#29: R; 5'-ATTCTAGTGGATTGACGCTCCCCAGTTACCA-3'

The primers used for identifying homozygous *acs9* complementation lines were:

Line#1: F; 5'-AGGTCCCATTAACAAGAGTCGGTCCAAGACT-3'

Line#1: R; 5'-AACAACAAACCCAAGCTCTGCAACAGCTCGA-3'

Line#4: F; 5'-AGCTAAGATCAGGATAAGGCATATCGCAGCAGT-3'

Line#4: R; 5'-TTGAGAAACATCTGAGTAGGGTTTGGTCGAGGA-3'

Line#10: F; 5'-AGAGGTGAGAATAGAGTCTCCTCCGTTGACA-3'

Line#10: R; 5'-ACAATGATGATCACGAGCTTTGAAGCCATTGCG-3'

Line#15: F; 5'-TTCCTATCAGCACTCTGAACCTCAGGCAGAA-3'

Line#15: R; 5'-AGCAATTGAGTATCGCATGGTGGTCCTTCCGTT-3'

Line#17: F; 5'-ATTAAGAGGCTTTGAGAGCCATGCGAAGGGA-3'

Line#17: R; 5'-TCCTAATCTCCACTTAATCCGGAACACCCCA-3'

Line#18: F; 5'-AAGGATCAAAGACTGGTTGGTTAGCCATGTCTC-3'

Line#18: R; 5'-AAGAAGGCTAGTGTTAGCGCAAATCACAGGACA-3'

Line#20: F; 5'-AAAACCGTTCAAAGGTTGCTAGCGTGCTTGCGA-3'

Line#20: R; 5'-TTGAGGACAAAGTTACGTTTGGACGGCAGGA-3'

Line#21: F; 5'-AAAGTATAGAGTCCCCTACCGTTGCGACAATGA-3'

Line#21: R; 5'-TTTGAAAGCAGTTCGTGACTCCATAGCTGAGCA-3'

Line#22: F; 5'-TTGCGATGAAGAAGAAGATACTCGGAGTGGTGA-3'

Line#22: R; 5'-TAAAAGAATGGCGTCTCTGTGCCTTTCTCTCCA-3'

Line#25: F; 5'-AATTGACCTCCTCTCAAAGTGTTCACCTACCCA-3'

Line#25: R; 5'-AAGATCTTCTCCTCCCTCTTCCCCTTTAGGA-3'

Line#29: F; 5'-AACTGCTAGAAACCTGACCTCCTTCGTTCCT-3'

Line#29: R; 5'-TCTCTATACGAGTACAACAGATCCAGAGGATGA-3'

Line#30: F; 5'-AAGGTTTTGTTTGATAAGGGAAAGTCGGCATGAGA-3'

Line#30: R; 5'-TATGAGTTTTAGACCTAAACCTGGAGCATGAAGCT-3'

Line#31: F; 5'-TTTGGTACGGAAGGAGACAACGATACAGGCCTA-3'

Line#31: R; 5'-ATCTTCAAGGTTCCAGGTTGTTGCCTCAAGGAA-3'

Characterization of Mutant Phenotypes:

Hypocotyl-length measurements were carried out with light-grown seedlings grown on vertical plates for 10 days. Shoot-length measurements were made with light-grown plants grown on soil for 30 to 100 days. The lengths were determined by taking pictures of individual seedlings or plants. The photographs were analyzed using the image analysis software (NIH image 1.63 program; http://rsb.info.nih.gov/nih-image/download.html). The gravitotropic response was determined with dark-grown seedlings grown on vertical plates for 3 days and subsequently rotated by 90 degrees for 24hr. The response was determined by taking pictures of individual seedlings. The photographs were analyzed using the image analysis software. Hypocotyl-length and hook curvature measurements were carried out with dark-grown seedlings grown on vertical plates for 3 days. Flowering time initiation was determined when the bolt was ~1cm. Hypocotyl cell size was determined as described by YADEGARI *et al.* (1994). The fixed tissue was viewed and photographed with an Axioplan Zeiss Microscopy System with QCapture Suite v2.68.6 (Quantitative Imaging Corp., Burnaby, BC, Canada V5C 6C6). The silique morphology of the *octuple* (*amiR*) lines was also determined as described by YADEGARI *et al.* (1994). The fixed tissue was viewed and photographed.

Ethylene Production:

Ethylene production was determined in 5- or 10-day old light grown seedlings and 30- or 40-day old light grown plants (only the aerial parts were used). Twenty seedlings were placed in 4 ml vials and ethylene accumulation was determined after 24 hrs of incubation (16hr light/8hr dark) at 25 °C. Mature plants were placed in 250 ml jars and ethylene accumulation was determined under similar conditions as described above. The ethylene concentration in the headspace of the vials/jars was determined by gas chromatography (5890A HEWLETT PACKARD GAS Chromatograph, Palo Alto, CA).

Histochemical GUS Assay:

The *ACSpromoter-GUS* constructs reported by TSUCHISAKA and THEOLOGIS (2004b) were used to determine the *ACS* gene expression in the shoot apical meristem (SAM) of young light-grown Arabidopsis seedlings. Histochemical assays of GUS activity in transgenic lines were performed as described (JEFFERSON *et al.* 1987). Five days old light grown seedlings were incubated in 100 mM sodium phosphate pH7.5 – 0.5 mM potassium ferrocyanide – 0.5 mM potassium ferricyanide – 10 mM EDTA – 0.1% triton X-100 containing 1 mM 5-bromo-4-chloro-β-D-gluconide at 37 °C for 12hr following vacuum infiltration. Subsequently, the samples were then transferred to 70% ethanol to remove the chlorophyll.

Longitudinal sections were prepared as follows: stained samples were infiltrated with a series of ethanol / Histoclear (National Diagnostics, Atlanta, GA) / Paraplast X-tra (KENDALL, Mansfield, MA) solutions as previously described (JACKSON 1991). Ribbons of 8μm sections were cut on a rotary microtome (MICROM HM340), floated on 42 °C water in the water bass for about 10min, and transferred to slides and dried overnight on a 42 °C block. Sections were dewaxed with Histoclear and mounted permanently with Hydromount Aqueous Non-Fluorescing Mounting Media (National Diagnostics).

RT-PCR Analysis for *ACS* and Flowering Gene Expression:

ACS gene expression in the T-DNA lines (except *ACS1* which does not respond to CHX, YAMAGAMI *et al.* 2003) was determined with total RNA isolated from treated with 50 uM CHX 7-day old etiolated seedlings using RNeasy (Qiagen, Valencia, CA). *ACS1* expression was determined with total RNA isolated from 7-day old light-grown seedlings using RNeasy. *ACS* gene expression in the *acs6-1* and *acs9-1* complementation lines was determined with total RNA or polyA$^+$-RNA isolated from 5-day old light-grown seedlings. Five-day old light grown seedlings were used for all the amiR experiments. Flowering gene expression was determined with total RNA isolated from 3-, 7- or 9-day old light-grown seedlings using RNeasy. PolyA$^+$-RNA was purified from total RNA using Oligotex (Qiagen). Genomic DNA was removed by treating 2 ug total RNA or 1 ug polyA$^+$-RNA with 10U of RNase-free DNase I (Roche Applied Science, Indianapolis, IN) for 15 min at 37 °C in 10 ul of 1X DNase I buffer (50 mM Tris-HCl (pH7.5), 10 mM $MgCl_2$) containing 40U of RNase inhibitor (Ambion, Inc., Austin, TX). The reaction

was stopped by adding 1 ul of 50 mM EDTA (pH8.0), subsequently, 1 ul of 100-pmol/ml oligo (dT) (Operon), were added and incubated at 70 °C for 10 min. First strand synthesis was carried out by adding 4 ul of 5X 1st strand buffer, 2 ul of 0.1M DTT, and 1ul 10 mM dNTP mix, and incubated at 42 °C for 2 min. Add 10U of SuperScript2 reverse transcriptase (Invitrogen), and incubate at 25 °C for 10 min followed by 42 °C for 50 min. Finally, the enzyme was inactivated by heating at 70 °C for 15 min. The 1st strand cDNA was purified by QIAquick Gel Extraction Kit (Qiagen) and Polymerase chain reaction (PCR) was carried with 1 ul of 1st strand cDNA, 0.5 ul each primer solution (10 mM), 1 ul 10X PCR buffer, 0.8 ul dNTP mix, and 0.1 ul ExTaq enzyme (Takara) in 10 ul total reaction volume. The PCR conditions were: 94 °C for 2 min (hot-start), one cycle; 94 °C for 15 sec, 56-60 °C for 15 sec, and 72 °C for 2 min for 25-45 cycles; followed by one cycle of incubation at 72 °C for 3 min.

The primers used for *ACS* gene expression are listed below. Primers designated b is for long size PCR product ("black arrows" in Fig.1A); r primers are for short size PCR product in before T-DNA insertion ("red arrows" in Fig. 1A); g primers are for short size PCR product in after T-DNA insertion ("green arrows" in Fig. 1A).

ACS1 b: F; 5'-TGTCTCAGGGTGCATGTGAGAATCAACTT-3'

ACS1 b: R; 5'-AGTGTGTCTTCGTCCATATTAGCAAAGCAGA-3'

ACS1 r: F; 5'-TGTCTCAGGGTGCATGTGAGAATCAACTT-3'

ACS1 r: R; 5'-TCTCTCCATAAACGTCGCAATCGCCTGTCTA-3'

ACS1 g: F; 5'-TACTCTTACAACGATGTTGTTGTGTCCTGCGCA -3'

ACS1 g: R; 5'-TGACCTAACATGTTCCTCGTACCTCATCGAAGA -3'

ACS2 b: F; 5'-GCGACTAACAATCAACACGGAG-3'

ACS2 b: R; 5'-ACATTATCCCTGGAGACGAGAGAC-3'

ACS2 r: F; 5'-AGATAGCGACTAACAATCAACACGGAGAGAACT-3'

ACS2 r: R; 5'-AGAACATGATTGTTTCATTGGCTCCGGTGGCT-3'

ACS2 g: F; 5'-CTTCGATGTTGTCCGATGATCAGTTTGTGGATAAT-3'

ACS2 g: R; 5'-GTCCATGTTGGCAAAGCAAATCCTAAACCATC-3'

ACS4 b: F; 5'-CCAAGTCTCTTCGTATTTCCTT-3'

ACS4 b: R; 5'-TAGTCGGAAAACCCAGTTAGAGAC-3'

ACS4 r: F; 5'-AAAGCTACATGCAACAGCCATGGCCAAGT-3'

ACS4 r: R; 5'-ACATTAGAGTCTCGTTTGCGGAAGTGGCT-3'

ACS4 g: F; 5'-CTCCTTAGATCTAAAACGTTCGAAGCGGAAATGGATC-3'

ACS4 g: R; 5'-AACCCAGTTAGAGACATTTGACATCGTCTTCTTCCTC-3'

ACS5 b: F; 5'-CCAGCTATGTTTCGATCTAATCGAGTCATGGTTAAC-3'

ACS5 b: R; 5'-TCCATGAAACCCGGAAAACCCAGTTAGAGACTGTC-3'

ACS5 r: F; 5'-TGACAAGCAATGGTCATGGACAAGACTCATCCT-3'

ACS5 r: R; 5'-ACGGTTTCCTCTTATCTCTTCCATAAACTCAGCCA-3'

ACS5 g: F; 5'-TGGACACAAACACATTTGAAGCAGAGCTTGACCTC-3'

ACS5 g: R; 5'-TCCATGAAACCCGGAAAACCCAGTTAGAGACTGTC-3'

ACS6 b: F; 5'-TGACGGTCACGGCGAGAATTCCTCTTATT-3'

ACS6 b: R; 5'-CCTGAGGTTACTCTGCCAACACTTCTTCT-3'

ACS6 g: F; 5'-AGTGTTGCGGAAGTAATCGAGGAGATCGA-3'

ACS6 g: R; 5'-AACCTGAGGTTACTCTGCCAACACTTCTT-3'

ACS7 b: F; 5'-AACAACAACAACGTCGAGCTTTCTCGAGT-3'

ACS7 b: R; 5'-AGATCCCGGAGATATATTCAGGTTCAGCT-3'

ACS7 r: F; 5'-AACAACAACAACGTCGAGCTTTCTCGAGT-3'

ACS7 r: R; 5'-TCCATGAAACTAGCCATGGCTTGTCTGAA-3'

ACS7 g: F; 5'-ACAACGATAATGTTGTTCGGACAGCGAGA-3'

ACS7 g: R; 5'-AGATCCCGGAGATATATTCAGGTTCAGCT-3'

ACS8: F; 5'-CGATCTCATTGAGTCATGGCTTGCTAAGA-3'

ACS8: R; 5'-ACGGTCCATCAACGAACCTCTTCAATCTA-3'

ACS9 b: F; 5'-GGATGGGAAGAATACGAGAAGAACCC-3'

ACS9 b: R; 5'-ATCACTCTTCTACTATCTGTTGACTC-3'

ACS9 r: F; 5'-TTCCTACTTCTTGGGATGGGAAGAATACGAGAAGA-3'

ACS9 r: R; 5'-TTCTTGAATTCGGGTAGGCCATGATAGTCTTGA-3'

ACS9 g: F; 5'-TGGGTTTGAACAGTTTGTAAGTGTCATGGATGTCT-3'

ACS9 g: R; 5'-TCACTCTTCTACTATCTGTTGACTCTACGTACTCT-3'

ACS11: F; 5'-AACCTCGGCTAACGAGACTCTAATGTTCT-3'

ACS11: R; 5'-ATGACACGATGAGCCTGGAGAGATGTTAA-3'

The primers used for flowering gene expression are listed below.

FT: F; 5'-TACGAAAATCCAAGTCCCACTG-3'

FT: R; 5'-AAACTCGCGAGTGTTGAAGTTC-3' (ABE *et al.* 2005)

SOC1: F; 5'-TGAGGCATACTAAGGATCGAG-3'

SOC1: R; 5'-GCGTCTCTACTTCAGAACTTGGGC-3' (ABE *et al.* 2005)

CO: F; 5'-TCACCACCAAAGCGAGAAAA-3'

CO: R; 5'-TGGCTTGCAGGGTCAGGTTG-3' (CHENG and WANG 2005)

FLC: F; 5'-TTCTCCAAACGTCGCAACGGTCT-3'

FLC: R; 5'-GATTTGTCCAGCAGGTGACATCTC-3' (CHENG and WANG 2005)

ACT8 gene specific primers described by AN *et al.* (1996) were used for control amplification. Quantification of the gene expression was determined using the image analysis software (NIH image 1.63 program; http://rsb.info.nih.gov/nih-image/download.html).

Bimolecular Fluorescence Complementation (BiFC) *in planta:*

The homo- and heterodimeric interaction among the various subunits of the *ACS* gene family members were determined *in planta* by BiFC. The Citrine YFP was used for the assay (GRIESBECK *et al.* 2001) in which the mutation Q69M confers a much lower pKa (5.7) than for other YFP forms making it less sensitive to fluctuations in intercellular pH. Arabidopsis transgenic lines were constructed expressing YNQ69M- and YC-ACS N-terminus fusion proteins driven by their own *ACS* promoter. The *3'UTR* of each *ACS* gene was also included in each construct to ensure the correct tissue specific expression (DIETRICH *et al.* 1992). The T7 and His tags were also included in the YNQ69M-ACS and YC-ACS constructs, respectively (See construct design below).

The *YC-ACS* constructs were introduced into the *pPZP122* transformation vector that confers Gentamicine resistance (*GenR*). The *YNQ69M-ACS* constructs were introduced into the *pPZP132* transformation vector that confers Hygromycin resistance (*HygR*).

1. Construction of *pPZP132*:

The hygromycine resistance gene was isolated by PCR using *pIG121-Hm* as template (AKAMA *et al.* 1992) and was subcloned as a *Nco*I (blunted) / *Eco*RV fragment into the *Bgl*II (blunted) sites of *pPZP122*.

The following oligonucleotides were used for preparing the hygromycine resistance gene.

F; 5'-TGACAAGCTTCCATGGAAATGAAAAAGCCTGAACTCACCGCGACGTCT-3'

R; 5'-GTACGAATTCGATATCTATTTCTTTGCCCTCGGACGAGTGCT-3'

DNA sequencing was used to confirm that no spurious mutations were introduced during PCR.

2. Construct Design:

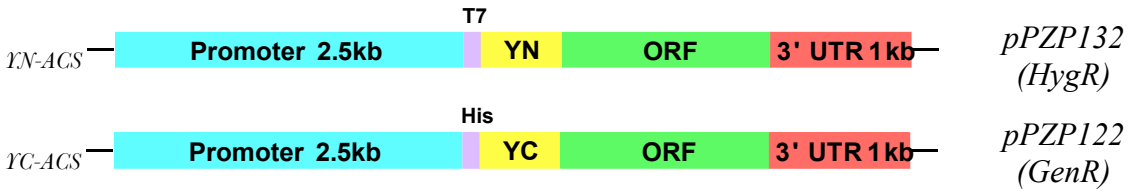

3. Plasmids used for constructing the *ACS Promoter-YC/YNQ69M-ACS-3'* transgenes:

The promoter regions and *3'UTRs* of *ACS1*, *2*, *4*, *5*, *6*, *7*, *8*, *9* and *11* were obtained from the following plasmids; *pPZP122-ACS1 promoter-3'*, *pPZP122-ACS2 promoter-3'*, *pPZP122-ACS4 promoter-3'*, *pPZP122-ACS5 promoter-3'*, *pPZP122-ACS6 promoter-3'*, *pPZP122-ACS7 promoter-3'*, *pPZP122-ACS8 promoter-3'*, *pPZP122-ACS9 promoter-3'* and *pPZP122-ACS11 promoter-3'*, (TSUCHISAKA and THEOLOGIS 2004b). The *ACS1*, *2*, *4*, *5*, *6* and *7* ORFs were obtained from the *pQE801-ACS1*, *2*, *4*, *5*, *6* and *7* plasmids (TSUCHISAKA and THEOLOGIS 2004a). The *ACS8*, *9* and *11* ORFs were obtained from the *pET-ACS8*, *9* and *11* plasmids (YAMAGAMI *et al.* 2003).

The *YNQ69M* was prepared by site directed mutagenesis using *pQE801-YN* as template (TSUCHISAKA and THEOLOGIS 2004a). The mutagenesis primer was

YN Q69M; 5'- CCACCTTCGGCTACGGCCTGATGTGCTTCGCCCGCTACCCCGACC-3'

The mutant codon is underlined. DNA sequencing was used to confirm that no spurious mutations were introduced during mutagenesis.

The *YC* and *YNQ69M* gene were isolated by PCR using *pQE80-YC* (TSUCHISAKA and THEOLOGIS 2004a) and *pQE801-YNQ69M* as templates and were subcloned into the *pBS SK-* vector. The T7 or His tags were introduced into the N-

terninus of the *YN Q69M* and *YC* cDNAs by PCR using the *pQE801-YN Q69M* and *pQE80-YC* plasmids as templates giving rise to *pBS SK--YNQ69M* and *pBS SK--YC* plasmids, respectively.

The following oligonucleotides were used

YN: F; 5'-GCATGGATCCATGGCTAGCATGACTGGTGGACAGCAAAT-3'

YC: F; 5'-GCATGGATCCATGAGAGGATCGCATCACCATCACCATCA-3'

YN/YC: R; 5'-TCGATCTAGACATATGAGATCCACCTCCACCAGATCCACCT-3'

The *ACS* ORFs were fused into the *YNQ69M* and *YC* fragments by the linker peptide GGSGGSGGSGGSGGS. DNA sequencing was used to confirm that no spurious mutations were introduced during mutagenesis.

4. Construction details:

35S-YC/YNQ69M-NOS (negative control)

The *35Spromoter-GUS-NOS* gene were isolated from *pBI121* and subcloned into the *HindIII/EcoRI* sites of *pPZP122* or *pPZP132* giving rise to *pPZP122-35S-GUS-NOS*, *pPZP132-35S-GUS-NOS*. Subsequently, the *YNQ69M* and *YC* genes was subcloned into the *BamHI/SacI* sites of *pPZP132-35S-GUS-NOS* and *pPZP122-35S-GUS-NOS* respectively giving rise to *pPZP132-35S- YNQ69M – NOS* and *pPZP122-35S-YC-NOS* plasmids used for transformation.

35S-bFosYC/bJunYN-NOS (positive control)

The *bJunYN* and *bFosYC* genes was isolated from *pQE801-bJunYN* and *pQE80-bFosYC* (TSUCHISAKA and THEOLOGIS 2004a) and subcloned into the *Bam*HI (blunted)/*Sac*I sites of *pPZP122-35S-GUS-NOS* and *pPZP132-35S-GUS-NOS* as *Eco*RI (blunted)/*Sac*I fragments giving rise to *pPZP132-35S-JunYN-NOS* and *pPZP122-35S-FosYC-NOS* plasmids used for transformation.

ACS1 promoter-YC/YNQ69M-ACS1-3'

The *ACS1* ORF was subcloned into the *NdeI/SacI* sites of *pBS-YC* or *pBS-YNQ69M*. The *YC-ACS1* gene was subcloned into the *Bam*HI sites of *pPZP122-ACS1 promoter-3'*. The *ACS1 promoter-3'* gene was subcloned into the *Hind*III/*Eco*RI sites of *pPZP132*. The *YNQ69M-ACS1* gene was subcloned into the *Bam*HI site of *pPZP132-ACS1 promoter-3'*.

ACS2 promoter-YC/YNQ69M-ACS2-3'

The *ACS2* ORF was subcloned into the *Nde*I/*Sac*I sites of *pBS-YC* or *pBS-YNQ69M*. The *YC-ACS2* gene was subcloned into the *Pst*I/*Sac*I sites of *pPZP122-ACS2 promoter-3'*. The *ACS2 promoter-3'* gene was subcloned into the *Hind*III/*Pme*I sites of *pPZP132*. The *YNQ69M-ACS2* gene was subcloned into the *Pst*I/*Sac*I sites of *pPZP132-ACS2 promoter-3'*.

ACS4 promoter-YC/YNQ69M-ACS4-3'

The *ACS4* ORF was subcloned into the *Nde*I/*Sac*I sites of *pBS-YC* or *pBS-YNQ69M*. The *YC-ACS4* gene was subcloned into the *Pst*I/*Sac*I sites of *pPZP122-ACS4 promoter-3'*. The *ACS4 promoter-3'* gene was subcloned into the *Bst*XI/*Pme*I sites of *pPZP132*. The *YNQ69M-ACS4* gene was subcloned into the *Pst*I/*Sac*I sites of *pPZP132-ACS4 promoter-3'*.

ACS5 promoter-YC/YNQ69M-ACS5-3'

The *ACS5* ORF was subcloned into the *Nde*I/*Sac*I sites of *pBS-YC* or *pBS-YNQ69M*. The *YC-ACS5* gene was subcloned into the *Bam*HI site of *pPZP122-ACS5 promoter-3'*. The *ACS5 promoter-3'* gene was subcloned into the *Hind*III/*Sph*I sites of *pPZP132*. The *YNQ69M-ACS5* gene was subcloned into the *Bam*HI site of *pPZP132-ACS5 promoter-3'*.

ACS6 promoter-YC/YNQ69M-ACS6-3'

The *ACS6* ORF was subcloned into the *Nde*I/*Sac*I sites of *pBS-YC* or *pBS-YNQ69M*. The *YC-ACS6* gene was subcloned into the *Bam*HI/*Sac*I sites of *pPZP122-ACS6 promoter-3'*. The *ACS6 promoter-3'* gene was subcloned into the *Pst*I/*Pme*I sites of *pPZP132*. The *YNQ69M-ACS6* gene was subcloned into the the *Bam*HI/*Sac*I sites of *pPZP132-ACS6 promoter-3'*.

ACS7 promoter-YC/YNQ69M-ACS7-3'

The *ACS7* ORF was subcloned into the *Nde*I/*Not*I *(blunted)* sites of *pBS-YC* or *pBS-YNQ69M* as a *Nde*I (partial)/*Pvu*II fragment. The *YC-ACS7* gene was subcloned into the *Bam*HI/*Sma*I sites of *pPZP122-ACS7 promoter-3'* as a *Bam*HI/*Sal*I (blunted) fragment. The *ACS7 promoter-3'* gene was subcloned into the *Hind*III/*Eco*RI sites of *pPZP132*. The *YNQ69M-ACS7* gene was subcloned into the *Bam*HI/*Sma*I sites of *pPZP132-ACS7 promoter-3'* as a *Bam*HI/*Sal*I (blunted) fragment.

ACS8 promoter-YC/YNQ69M-ACS8-3'

The *ACS8* ORF was subcloned into the *Nde*I/*Not*I sites of *pBS-YC* or *pBS-YNQ69M*. The *YC-ACS8* gene was subcloned into the *Pst*I/*Sal*I sites of *pPZP122-ACS8 promoter-3'*. The *ACS8 promoter-3'* gene was subcloned into the *Hind*III/*Sph*I sites of *pPZP132*. The *YNQ69M-ACS8* gene was subcloned into the *Pst*I/*Sal*I sites of *pPZP132-ACS8 promoter-3'*.

ACS9 promoter-YC/YNQ69M-ACS9-3'

The *ACS9* ORF was subcloned into the *Nde*I/*Sac*I sites of *pBS-YC* or *pBS-YNQ69M*. The *YC-ACS9* gene was subcloned into the *Bam*HI/*Sac*I sites of *pPZP122-ACS9 promoter-3'*. The *ACS9 promoter-3'* gene was subcloned into the *Pst*I/*Pme*I sites of *pPZP132*. The *YNQ69M-ACS9* gene was subcloned into the *Bam*HI/*Sac*I sites of *pPZP132-ACS9 promoter-3'*.

ACS11 promoter-YC/YNQ69M-ACS11-3'

The *ACS11* ORF was subcloned into the *Nde*I/*Not*I sites of *pBS-YC* or *pBS-YNQ69M*. The *YC-ACS11* gene was subcloned into the *Bam*HI/*Sma*I sites of *pPZP122-ACS11 promoter-3'* as a *Bam*HI/*Not*I (blunted) sites fragment. The *ACS11 promoter-3'* gene was subcloned into the *Bgl*II/*Xmn*I sites of *pPZP132* as a *Bgl*II/*Pml*I fragment. The *YNQ69M-ACS11* gene was subcloned into the *BamHI/SmaI* sites of *pPZP132-ACS11 promoter-3'* as a *Bam*HI/*Not*I (blunted) fragment.

The *ACSpromoter-YC/YNQ69M-3'* transgenes were introduced into the Arabidopsis genome by transformation of the *pentuple2* mutant and homozygous lines were identified using the following primers.

YC: F; 5'-AGAGGTTTGATGTGGAACACTGTCAGCGTCA-3'

YC: R; 5'-TCCGATGTCAATGGACTGCTTTGGTAGACCT-3'

YC-ACS1: F; 5'-ATATACATGCGTCTCGCGTCTCCTTTCAAGT-3'

YC-ACS1: R; 5'-TTAGACGTCTAGCTTTTGTTTGTCCAAGGCA-3'

YC-ACS2: F; 5'-AATCTTTAACAAAGGGCAAACGAGACGGCCT-3'

YC-ACS2: R; 5'-AAAATAAATTGTTCTCGCGGTGTACCGCGGA-3'

YC-ACS4: F; 5'-TACCAGATGATGACGAGATGGAGTCTTGCCT-3'

YC-ACS4: R; 5'-TTTTGCTAGCCGATTCATGCAGACTGCAGCA-3'

YC-ACS5: F; 5'-TGAATAGATTCGGCTGATGGATTGGTAGGGA-3'

YC-ACS5: R; 5'-TTCATCTTTTTCCATGGTCAGTTGGCCCCAT-3'

YC-ACS6: F; 5'-TATTATTCTAGTGAGCGTCCTCTGTGCGTGA-3'

YC-ACS6: R; 5'-TTCAGCTGCTTTCGTGTTCGACAAGGAACCT-3'

YC-ACS7: F; 5'-ACAAAGTCGTAGCCACATACCTTCTTGCCCA-3'

YC-ACS7: R; 5'-TTTAGCAAGTGTTGCCACTCCAGATGTCCCA-3'

YC-ACS8: F; 5'-TTGAAATCTGAGTTTCCTTGTTGGGGCGTGA-3'

YC-ACS8: R; 5'-ACAAGAGATGATCCAAGCCATAAGCTCTCCT-3'

YC-ACS9: F; 5'-ACCGATAAATTTTCTCGTGCTCCATGTTGGG-3'

YC-ACS9: R; 5'-ATATTGGAGACTTTGTGGAGGAAGCACTCGT-3'

YC-ACS11: F; 5'-TTGAAGGGAATGATCATGCACAGCGCGAAGT-3'

YC-ACS11: R; 5'-ATGTTAACATGTGCGGCCACTCCTCAACACA-3'

YN Q69M: F; 5'-ATGTTTCTCTTCTCTCAACCGGTGTATCGGT-3'

YN Q69M: R; 5'-TGCATAACAAGAGCACAGAGGAAGCACAGCA-3'

YN Q69M-ACS1: F; 5'-ATTTACGAGTCTACCCATACCGGTGAGACGA-3'

YN Q69M-ACS1: R; 5'-TATACTTGTTGCGTGAGGAGGAAACTCCGGA-3'

YN Q69M-ACS2: F; 5'-AAGAAGACATTGATGCAGCAAACAGAGAACGCT-3'

YN Q69M-ACS2: R; 5'-ATCCAGCTTTTACATGGAATCTGTACATGTCCA-3'

YN Q69M-ACS4: F; 5'-CCAGTGAATTGTAATACGACTCACTATAGGGCG-3'

YN Q69M-ACS4: R; 5'-ACAATAGCATAATTCTCACAGCAGCACCGTAGA-3'

YN Q69M-ACS5: F; 5'-ATCACACTGTCACATGGAGAACAGCAAGCGA-3'

YN Q69M-ACS5: R; 5'-ATTCTGTGTAATGCCAACTTGATGCTGCCCA-3'

YN Q69M-ACS6: F; 5'-TAATACGTTCCAAGTTCGATCTACCTGATGC-3'

YN Q69M-ACS6: R; 5'-AGAAGTTGGAAGTCAAAGGATAGCCAGAAGA-3'

YN Q69M-ACS7: F; 5'-TTACTTCTGCTTGTACTATTGGGTCCGCGGT-3'

YN Q69M-ACS7: R; 5'-AATTAGAGCGCGTGAATCTCACATCGCGACA-3'

YN Q69M-ACS8: F; 5'-AGAAACACAAATAAGAGTGAGGCCTAGGCGT-3'

YN Q69M-ACS8: R; 5'-TCCTTCGAGCCAACATCTAATGAGGTCGTGA-3'

YN Q69M-ACS9: F; 5'-AGCAAATCTCGTTTCTCGCTTGAATCCCTGCA-3'

YN Q69M-ACS9: R; 5'-AATATCATTGTCCTCCTTGGCTCTCTCCTGGT-3'

YN Q69M-ACS11: F; 5'-TAACAAGGCTTCATGGCGTGGAATTGACGTG-3'

YN Q69M-ACS11: R; 5'-ATAAACCTCTGGAGCCATATATCGCCCTGCT-3'

The single *YC-ACS* lines were crossed to the various single *YNQ69M-ACS* lines and double lines were generated expressing all the possible combinations of ACS homo- and heterodimers.

5. Imaging of Yellow Fluorescence in *Planta*:

Three-day old etiolated seedlings of the various double lines were placed on MS medium containing 50 μM NAA and incubated at 25 °C for 24 h in the dark. The fluorescence of the root tip was monitored using a Zeiss AxioObserver Z1 for Live-Cell fluorescence imaging system with Hamamatsu 9100-13 EMCCD camera. The excitation filter was HQ500/20, the emission filter was HQ520lp, and the beamsplitter was Q515lp (CHROMA).

Pathogen Infection Assay:

Arabidopsis plants were grown at 24 ºC under a 12 hour light/12 hour dark cycle for 4 weeks before the pathogen inoculation. The *Botrytis cinerea* (strain BO5-10, from Dr. Mike Coffey from UC Riverside) was cultured on 2x V8 agar (36% V8 juice, 0.2% $CaCO_3$, and 2% Bacto-agar) and incubated at 20 to 25°C. Plants were inoculated by spraying spore suspension at a concentration of 2 X 10^5 spores/ml and kept under high humidity as described in (MENGISTE *et al.* 2003). The growth and inoculation of *Alternaria brassicicola* (from Dr. Shunyuan Xiao at University of Maryland Biotechnology Institute) was performed as described in (THOMMA *et al.* 1999). Spore suspension of 1 X 10^6 spores/ml was used. The growth, inoculation and population measurement of bacteria *Xcv* (strain 85-10) and *Xcc* (strain 2669) (from Dr. Brian Staskawicz at UC Berkeley) were conducted as described in (WHALEN *et al.* 1988; BENT *et al.* 1992). Rosette leaves were infiltrated with *Xcv* suspension of OD_{600} 0.002 (approximately 2 X 10^6 cfu/ml) or *Xcc* suspension of OD_{600} 0.0002 (approximately 2 X 10^5 cfu/ml) for bacteria growth measurement. Bacterial populations in leaves were sampled from inoculated leaves of 5 individual plants for each time point at 0 DPI and 4DPI.

Microarray Analysis:

To determine how the single and high order mutations affect the molecular phenotype of young Arabidopsis seedlings, we carried out global gene expression analysis. Two independent experiments were carried out; one with the eight single mutants (**Single**

Expt; 27 chips including wt control) and another with the four high order mutants (**High Order Expt;** 15 chips including wt control). Each experiment was performed in triplicate with biotin-labeled cRNA samples prepared with total RNA from 10-day old light-grown seedlings. Seeds were surface sterilized for 8min in 5% sodium hypochlorite, 0.15% Tween 20, excessively rinsed in distilled water, and germinated on MS medium (0.8% Select Agar (Life Technologies, Inc., Rockville, MD), 0.5X Murashige-Skoog (MS) salts (Life Technologies, Inc.), 0.5mM MES, pH5.7, 1% sucrose, 1X B5 vitamins. After cold treatment at 4 °C for 2 days, the plates were incubated at 25 °C under 16h light / 8h for 10 days. Total RNA was prepared using RNAqueous RNA isolation kit with Plant RNA isolation aid (Ambion, Austin, TX). After LiCl precipitation, RNA was purified using RNeasy columns (Qiagen, Valencia, CA) and re-precipitated with LiCl. RNA pellets were washed with 70% EtOH (three times), and resuspended in DEPC-treated water. Ten micrograms of total RNA was used for biotin-labeled cRNA probe synthesis. cRNA probe synthesis were performed according to the manufacturer's protocols (Affymetrix, Inc., Santa Clara, CA). Hybridization, washing, and scanning and detection of array images were performed at UC Berkeley's Functional Genomics Laboratory.

Data Analysis:

The hybridization data of the two experiments (Single Expt. and High Order Expt.) were processed and analyzed separately. Affymetrix GeneChip Microarray Suite version 5.0 software was used to obtain signal values for individual genes. The data files containing the probe level intensities (cell files) were used for background correction and normalization using the $\log_2$ scale robust multi-array analysis (RMA) procedure (IRIZARRY *et al.* 2003). The "R" environment (IHAKA and GENTLEMAN 1996) was used for running the RMA program. Data analysis and statistical extraction were performed using $\log_2$ converted expression intensity data within Microsoft Excel (Microsoft, Redmond, WA). We used an *M-A* plot (DUDIOT *et al.* 2002) to represent the difference between two data sets. $M = \log_2 (X/Y)$ and $A = \log_2 \sqrt{X*Y}$ (X and Y are the average expression levels for X and Y data sets), respectively. Also, a *t* value (DUDIOT *et al.* 2002) cutoff was used to identify the statistically valid differentially regulated genes among the two data sets. The *t* value was calculated using the following formulas; $t = M/SE$ ($SE^2 = 1/n^2 (var_1 + var_2 ... + var_n)$; *var* is the variance of the expression intensity of the triplicate experiments, n is the number of data sets). A high *t* value corresponds to low variability (high confidence) data, whereas a low *t* value corresponds to high variability (low confidence) data. We use 7 as the cutoff *t*-value; data with $|t| < 7$ were excluded from our differentially regulated gene list. Venn diagrams were drawn using *VENNY*; (OLIVEROS 2007, http://bioinfogp.cnb.csic.es/tools/venny/index.htm).

SUPPORTING RESULTS AND DISCUSSION

Global Gene Expression Analysis

To determine how the single and high order mutations affect the phenotype of young Arabidopsis seedlings, we profiled their gene expression as described in the Supporting Materials and Methods A cursory examination of the scatter plots representing the

transcriptional profiles of the single mutants demonstrates that the loss of individual *ACS* gene family members causes small changes in gene expression compared to wt (Figure S9A). The loss of multiple gene family members progressively enhances the degree of alteration of gene expression compared to wt, suggesting that ethylene-mediated transcriptional regulation is globally altered in the high order mutants (Figure S9B).

We identified the differentially regulated genes in each mutant as described in the Experimental Procedures. Figure S9 shows the number of genes that met the criteria for 2-fold induction (Induced genes) and for > 2-fold repression (Repressed genes) compared to the wt for every single and high order mutant analyzed. Among the induced or repressed genes there are genes whose expression is altered in more than one mutant (overlapping set of target genes), as well as genes whose expression is altered only in one mutant (non-overlapping set of target genes). Among the 251 genes induced in the single mutants, 90 (36%) represent distinct loci whose expression is induced in one or more single mutants. Similarly, 170 of the 240 repressed genes (71%) represent distinct loci (Figure S10A). The same is true for the high order mutants. Among the 258 genes induced in the high order mutants, 169 (65%) represent distinct loci whose expression is induced in one or more high order mutants. Similarly, 130 of the 222 repressed genes (58%) represent distinct loci (Figure S10C). The expression patterns of the single and high order mutants are unique and overlapping (Figure S10B and D). The results of Figure S10 represent an ethylene dose response curve of the transcriptional output in young seedlings and demonstrate the unique and redundant functions of the *ACS* gene family members. A complete list of the Induced and Repressed genes shown in Figure S10 can be found in Tables S2 and S3 (single mutants) and Tables S4 and S5 (high order mutants)

The genes identified as induced or repressed were functionally categorized to determine the possible metabolic and biological processes affected by the mutations. Approximately 80% of them are currently annotated as encoding proteins of known or putative function (Figure S11). A wide range of cellular and metabolic processes are affected by loss of *ACS* gene function. Various classes of genes involved in disease and stress resistance, cell wall biosynthesis, light signaling, biosynthesis of secondary metabolites, transport, development and transcription show altered gene expression in the mutants. Tables S6, S7 (single mutants) and S8, S9 (high order mutants) list the Induced and Repressed genes according to their functional classification, respectively.

Highlights of the Genome Expression Profiling Analysis: Table S10, part A lists the genes most highly induced and repressed in the high order mutants. Three genes involved in the glucosinolate biosynthetic pathway are among the most affected genes: *ESP* (*EPITHIOSPECIFIER PROTEIN*) and *IMS2/MAM-L/MAM3 (METHYLTHIOALKYLMALATE SYNTHASE-LIKE)* are induced; *ESM1* (*EPITHIOSPECIFIER MODIFIER 1*) is repressed. Glucosinolates are plant metabolites with antimicrobial and insect-deterring properties (CLAY *et al.* 2009; GRUBB and ABEL 2006). A thionin gene of the pathogen response (PR-13) gene family (STEC 2006) is repressed more than 70-fold (Table S10, part A), but few other genes involved in plant defense responses are among the list of repressed genes. Notably, a set of NBS-LRR type disease resistance genes, At1g56510, At1g59218 and

At1g63880, are repressed in at least two of the high order mutants (Table S10, part A). Numerous genes encoding proteases and protease inhibitors are induced or repressed by the mutants (Tables S4 and S5). The biological function of most of these genes is unknown. A subtilisin-like serine protease encoded by the '*STOMATAL DENSITY AND DISTRIBUTION*' (*SDD1*) gene is induced in the *octuple* mutant (Table S10A). *SDD1* regulates stomata density in Arabidopsis leaves (BERGER and ALTMANN 2009), raising the prospect that stomata density is defective (lower) in the *octuple* mutant. The expression of the *SQP1* (*SQUALENE MONOOXYGENASE 1*) gene involved in brassinosteroid biosynthesis (FUJIOKA and YOKOTA 2003) is reduced in the mutants. A gene of unknown function involved in embryo development, *MEE14* (*MATERNAL EFFECT EMBRYO ARREST 14*), (PAGNUSSAT *et al.* 2005) is among the highly induced genes in all four mutants. Finally the list the *AT-E1* gene which encodes one of the subunits of the puruvate-dehydrogenase complex, is down regulated by the mutants; a Histone H3 gene and two genes of unknown function that encode ZW9 and a meprin/TRAF domain containing protein are among the highly repressed genes (Table S10, part A).

Light-Related Genes: A significant number of genes (Table S10, part B) such as *CSA1* (*CONSTITUTIVE SHADE AVOIDANCE 1*), *LHY* (*LATE ELONGATED HYPOCOTYL*), *CRY3* (*CRYPTOCHROME 3*), *ELIP* (*EARLY LIGHT-INDUCIBLE PROTEIN*), *FKF1* (*FLAVIN-BINDING*, *KELCH REPEAT*, *F-BOX*) and *GCN5* involved in light perception, signaling, photoperiodic control and chloroplast biogenesis are repressed more than two-fold in the high order gene mutants (CHEN *et al* 2004; JIAO *et al.* 2007; IMAIZUMI and KAY 2006). Among the induced genes the list includes: two of the phototropin-responsive *NPH3* gene family members involved in blue light signaling (MOTCHULSKI and LISCUM 1999), *HLH1/PAR1* (*PHY RAPIDLY REGULATED 1*) which encodes a transcriptional repressor of the auxin regulated *SAUR* genes and is responsible for integrating shade avoidance and auxin transcriptional networks (ROIG-VILLANOVA *et al.* 2007) and two genes, *PORA* and *PORB* (*PHOTOCHLOROPHYLLIDE OXIDOREDUCTASE A* or *B*) which are involved in chlorophyll biosynthesis and their expression is regulated by *PIF1* (HUQ *et al.* 2004).

SUPPORTING REFERENCES

ABE, M., Y. KOBAYASHI, S. YAMAMOTO, Y. DAIMON, A. YAMAGUCHI, Y. IKEDA, H. ICHINOKI, M. NOTAGUCHI, K. GOTO and T. ARAKI, 2005 FD, a bZIP protein mediating signals from the floral pathway integrator FT at the shoot apex. Science **309:** 1052-1056.

AKAMA, K., H. SHIRAISHI, S. OHTA, K. NAKAMURA, K. OKADA and Y. SHIMURA, 1992 Efficient transformation of *Arabidopsis thaliana*: comparison of the efficiencies with various organs, plant ecotypes and *Agrobacterium* strains. Plant Cell Rep. **12:** 7-11.

ALONSO, J. M. A., A. N. A. STEPANOVA, T. J. A. LEISSE, C. J. A. KIM, H. A. CHEN, P. A. SHINN, D. K. A. STEVENSON, J. A. ZIMMERMAN, P. A. BARAJAS, R. A. CHEUK, C. A. GADRINAB, C. A. HELLER, A. A. JESKE, E. A. KOESEMA, C. C. A. MEYERS, H. A. PARKER, L. A. PREDNIS, Y. A. ANSARI, N. A. CHOY, H. A. DEEN, M. A. GERALT, N. A. HAZARI, E. A. HOM, M. A. KARNES, C. A. MULHOLLAND, R. A. NDUBAKU, I. A. SCHMIDT, P. A. GUZMAN, L. A. AGUILAR-HENONIN, M. A. SCHMID, D. A. WEIGEL, D. E. A. CARTER, T. A. MARCHAND, E. A. RISSEEUW, D. A. BROGDEN, A. A. ZEKO, W. L. A. CROSBY, C. C. A. BERRY and J. R. ECKER, 2003 Genome-wide insertional mutagenesis of *Arabidopsis thaliana*. Science **301:** 653-657.

AN, Y. Q., J. M. MCDOWELL, S. R. HUANG, E. C. MCKINNEY, S. CHAMBLISS and R. B. MEAGHER, 1996 Strong, constitutive expression of the *Arabidopsis ACT2/ACT8* actin subclass in vegetative tissues. Plant J. **10:** 107-121.

BERGER, D., and T. ALTMANN, 2000 A subtilisin-like serine protease involved in the regulation of stomatal density and distribution in Arabidopsis thaliana. Genes Dev. **14:** 1119-1131.

BENT, A. F., R. W. INNES, J. R. ECKER and B. J. STASKAWICZ, 1992 Disease development in ethylene-insensitive *Arabidopsis-thaliana* infected with virulent and avirulent *Pseudomonas* and *Xanthomonas* pathogens. Mol. Plant-Microbe Interact. **5:** 372-378.

CHEN, M., J. CHORY and C. FANKHAUSER, 2004 Light signal transduction in higher plants. Annu. Rev. Genet. **38:** 87-117.

CHENG, X.-F., and Z.-Y. WANG, 2005 Overexpression of *COL9*, a *CONSTANS-LIKE* gene, delays flowering by reducing expression of *CO* and *FT* in *Arabidopsis thaliana*. Plant J. **43:** 758-768.

CLAY, N. K., A. M. ADIO, C. DENOUX, G. JANDER and F. M. AUSUBEL, 2009 Glucosinolate metabolites required for an *Arabidopsis* innate immune response. Science **323:** 95-101.

DIETRICH, R. A., S. E. RADKE and J. J. HARADA, 1992 Downstream DNA sequences are required to activate a gene expressed in the root cortex of embryos and seedlings. Plant Cell **4:** 1371-1382.

DUDIOT, S., Y. H. YANG, M. J. CALLOW and T. P. TERRY, 2002 Statistical methods for identifying differentially expressed genes in replicated cDNA microarray experiments. Statistics Sinica **12:** 111-139.

FUJIOKA, S., and T. YOKOTA, 2003 Biosynthesis and metabolism of brassinosteroids. Annu. Rev. Plant Biol. **54:** 137-164.

GRIESBECK, O., G. S. BAIRD, R. E. CAMPBELL, D. A. ZACHARIAS and R. Y. TSIEN, 2001 Reducing the environmental sensitivity of yellow fluorescent protein. J. Biol. Chem. **276:** 29188-29294.

GRUBB, C. D., and S. ABEL, 2006 Glucosinolate metabolism and its control. Trends Plant Sci. **11:** 89-100.

HAJDUKIEWICZ, P., Z. SVAB and P. MALIGA, 1994 The small, versatile *pPZP* family of *Agrobacterium* binary vectors for plant transformation. Plant Mol. Biol. **25:** 989-994.

HUQ, E., B. AL-SADY, M. HUDSON, C. KIM, K. APEL and P. H. QUAIL, 2004 PHYTOCHROME-INTERACTING FACTOR 1 is a critical bHLH regulator of chlorophyll biosynthesis. Science **305:** 1937-1941.

IHAKA, R., and R. GENTLEMAN, 1996 R: A language for data analysis and graphics. J. Comput. Graph. Stat. **5:** 299-314.

IMAIZUMI, T., and S. A. KAY, 2006 Photoperiodic control of flowering: not only by coincidence. Trends Plant Sci. **11:** 550-558.

IRIZARRY, R. A., B. M. BOLSTAD, F. COLLIN, L. M. COPE, B. HOBBS and T. P. SPEED, 2003 Summaries of affymetrix GeneChip probe level data. Nucleic Acids Res. **31:** E15.

JACKSON, D. P., 1991 In situ hybridization in plants, pp.163-174 in *Molecular Plant Pathology: A Practical Approach*, edited by D. J. BOWLES, S. J. GURR and M. MCPHERSON. Oxford Univ. Press, Oxford.

JEFFERSON, R. A., T. A. KAVANAGH and M. V. BEVAN, 1987 GUS fusions: ß-glucuronidase as a sensitive and versatile gene fusion marker in higher plants. EMBO J. **6:** 3901-3907.

JIAO, Y., O. S. LAU and X. W. DENG, 2007 Light-regulated transcriptional networks in higher plants. Nat. Rev. Genet. **8:** 217-230.

LIU, Y. G., N. MITSUKAWA, T. OOSUMI and R. F. WHITTIER, 1995 Efficient isolation and mapping of *Arabidopsis thaliana* T-DNA insert junctions by thermal asymmetric interlaced PCR. Plant J. **8:** 457-463.

MENGISTE, T., X. CHEN, J. SALMERON and R. DIETRICH, 2003 The *BOTRYTIS SUSCEPTIBLE1* gene encodes an R2R3MYB transcription factor protein that is required for biotic and abiotic stress responses in Arabidopsis. Plant Cell **15:** 2551-2565.

MOTCHOULSKI, A., and E. LISCUM, 1999 *Arabidopsis* NPH3: a NPH1 photoreceptor-interacting protein essential for phototropism. Science **286:** 961-964.

PAGNUSSAT, G. C., H.-J. YU, Q. A. NGO, S. RAJANI, S. MAYALAGU, C. S. JOHNSON, A. CAPRON, L.-F. XIE, D. YE and V. SUNDARESAN, 2005 Genetic and molecular identification of genes required for female gametophyte development and function in *Arabidopsis*. Development **132:** 603-614.

ROIG-VILLANOVA, I., J. BOU-TORRENT, A. GALSTYAN, L. CARRETERO-PAULET, S. PORTOLÉS, M. RODORÍGUEZ-CONCEPCIÓN and J. F. MARTÍNEZ-GARCÍA, 2007 Interaction of shade avoidance and auxin responses: a role for two novel atypical bHLH proteins. EMBO J. **26:** 4756-4767.

SAMBROOK, J., E. F. FRITSCH and T. MANIATIS, 1989 Molecular Cloning: A Laboratory Manual, 2nd edition. Cold Spring Harbor Laboratory Press, Cold Spring Harbor, New York.

SCHWAB, R., S. OSSOWSKI, M. RIESTER, N. WARTHMANN and D. WEIGEL, 2006 Highly specific gene silencing by artificial microRNAs in *Arabidopsis*. Plant Cell **18:** 1123-1133.

SESSIONS, A., E. BURKE, G. PRESTING, G. AUX, J. MCELVER, D. PATTON, B. DIETRICH, P. HO, J. BACWADEN, C. KO, J. D. CLARKE, D. COTTON, D. BULLIS, J. SNELL, T. MIGUEL, D. HUTCHISON, B. KIMMERLY, T. MITZEL, F. KATAGIRI, J. GLAZEBROOK, M. LAW and A. A. GOFF, 1997 A high-throughput Arabidopsis reverse genetics system. Plant Cell **14:** 2985-2994.

STEC, B., 2006 Plant thionins – the structural perspective. Cell. Mol. Life Sci. **63:** 1370-1385.

THOMMA, B. P. H. J., I. NELISSEN, K. EGGERMONT and W. F. BROEKAERT, 1999 Deficiency in phytoalexin production causes enhanced susceptibility of *Arabidopsis thaliana* to the fungus *Alternaria brassicicola*. Plant J. **19:** 163-171.

TSUCHISAKA, A., and A. THEOLOGIS, 2004a Heterodimeric interactions among the 1-amino-cyclopropane-1-carboxylate synthase polypeptides encoded by the *Arabidopsis* gene family. Proc. Natl. Acad. Sci. USA **101:** 2275-2280.

TSUCHISAKA, A., and A. THEOLOGIS, 2004b Unique and overlapping expression patterns among the arabidopsis 1-amino-cyclopropane-1-carboxylate synthase gene family members. Plant Physiol. **136:** 2982-3000.

WHALEN, M. C., R. E. STALL and B. J. STASKAWICZ, 1988 Characterization of a gene from a tomato pathogen determining hypersensitive resistance in non-host species and genetic analysis of this resistance in bean. Proc. Natl. Acad. Sci. USA **85:** 6743-6747.

YADEGARI, R., G. R. DE PAIVA, T. LAUX, A. M. KOLTUNOW, N. APUYA, J. L. ZIMMERMAN, R. L. FISCHER, J. J. HARADA and R. B. GOLDBERG, 1994 Cell differentiation and morphogenesis are uncoupled in Arabidopsis raspberry embryos. Plant Cell **6:** 1713-1729.

YAMAGAMI, T., A. TSUCHISAKA, K. YAMADA, W. F. HADDON, L. A. HARDEN and A. THEOLOGIS, 2003 Biochemical diversity among the 1-amino-cyclopropane-1-carboxylate synthase isozymes encoded by the *Arabidopsis* gene family. J. Biol. Chem. **278:** 49102-49112.

TABLE S1

Effect of the *pentuple2* Mutation on Various Phenotypic Characteristics of Plants Grown Under Various Conditions

Phenotype	Effect
Hypocotyl length of light and dark grown seedlings	Longer than wt
Cotyledon size	Larger than wt
Flowering time	Earlier than wt
Shoot length of mature plants	Longer than wt
Ethylene production	Lower than wt
Hook formation	Same as wt
Gravitotropic response	Same as wt
Rosette leaf number and size	Same as wt
Diameter of inflorescence stem	Same as wt
Flower form and size	Same as wt
Silique length	Same as wt
Seeds number/siliques and siliques size	Same as wt
Senescence	Same as wt
Cold treatment	Same as wt
Disease resistance*	Same as wt

*The following pathogens were tested: Two bacteria pathogens: *Xanthomonas campestris* pv. *vesicatoria* (*Xcv*), and *Xanthomonas campestris* pv. *campestris* (*Xcc*). A necrotropic fungus: *Alternaria brassicicola*. A susceptible virus pathogen: Oil rape mosaic virus (ORMV).

TABLE S2

List of genes induced by the single mutants. The color code denotes the gene whose expression has been induced by a particular mutation.

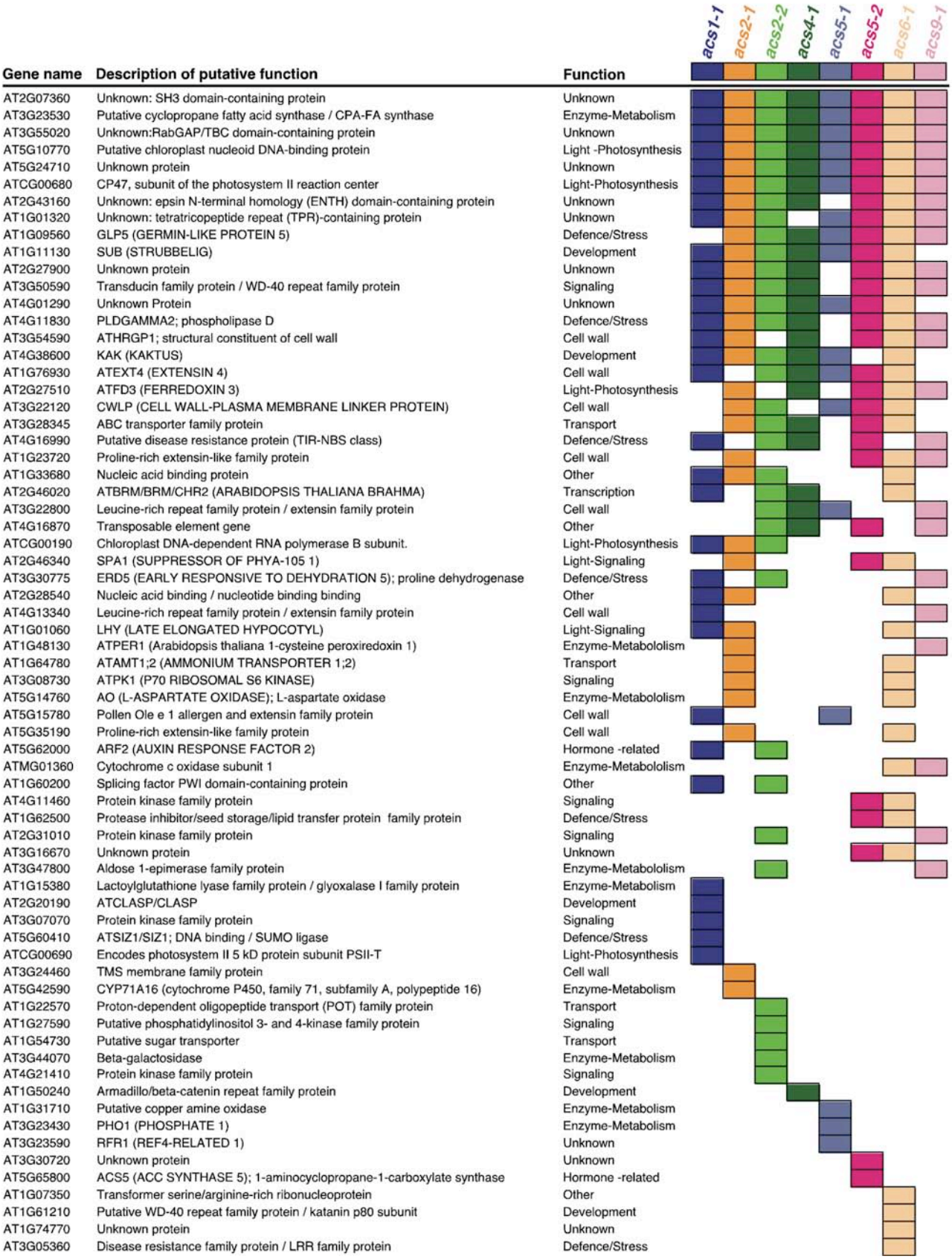

Gene name	Description of putative function	Function
AT2G07360	Unknown: SH3 domain-containing protein	Unknown
AT3G23530	Putative cyclopropane fatty acid synthase / CPA-FA synthase	Enzyme-Metabolism
AT3G55020	Unknown:RabGAP/TBC domain-containing protein	Unknown
AT5G10770	Putative chloroplast nucleoid DNA-binding protein	Light -Photosynthesis
AT5G24710	Unknown protein	Unknown
ATCG00680	CP47, subunit of the photosystem II reaction center	Light-Photosynthesis
AT2G43160	Unknown: epsin N-terminal homology (ENTH) domain-containing protein	Unknown
AT1G01320	Unknown: tetratricopeptide repeat (TPR)-containing protein	Unknown
AT1G09560	GLP5 (GERMIN-LIKE PROTEIN 5)	Defence/Stress
AT1G11130	SUB (STRUBBELIG)	Development
AT2G27900	Unknown protein	Unknown
AT3G50590	Transducin family protein / WD-40 repeat family protein	Signaling
AT4G01290	Unknown Protein	Unknown
AT4G11830	PLDGAMMA2; phospholipase D	Defence/Stress
AT3G54590	ATHRGP1; structural constituent of cell wall	Cell wall
AT4G38600	KAK (KAKTUS)	Development
AT1G76930	ATEXT4 (EXTENSIN 4)	Cell wall
AT2G27510	ATFD3 (FERREDOXIN 3)	Light-Photosynthesis
AT3G22120	CWLP (CELL WALL-PLASMA MEMBRANE LINKER PROTEIN)	Cell wall
AT3G28345	ABC transporter family protein	Transport
AT4G16990	Putative disease resistance protein (TIR-NBS class)	Defence/Stress
AT1G23720	Proline-rich extensin-like family protein	Cell wall
AT1G33680	Nucleic acid binding protein	Other
AT2G46020	ATBRM/BRM/CHR2 (ARABIDOPSIS THALIANA BRAHMA)	Transcription
AT3G22800	Leucine-rich repeat family protein / extensin family protein	Cell wall
AT4G16870	Transposable element gene	Other
ATCG00190	Chloroplast DNA-dependent RNA polymerase B subunit.	Light-Photosynthesis
AT2G46340	SPA1 (SUPPRESSOR OF PHYA-105 1)	Light-Signaling
AT3G30775	ERD5 (EARLY RESPONSIVE TO DEHYDRATION 5); proline dehydrogenase	Defence/Stress
AT2G28540	Nucleic acid binding / nucleotide binding binding	Other
AT4G13340	Leucine-rich repeat family protein / extensin family protein	Cell wall
AT1G01060	LHY (LATE ELONGATED HYPOCOTYL)	Light-Signaling
AT1G48130	ATPER1 (Arabidopsis thaliana 1-cysteine peroxiredoxin 1)	Enzyme-Metabololism
AT1G64780	ATAMT1;2 (AMMONIUM TRANSPORTER 1;2)	Transport
AT3G08730	ATPK1 (P70 RIBOSOMAL S6 KINASE)	Signaling
AT5G14760	AO (L-ASPARTATE OXIDASE); L-aspartate oxidase	Enzyme-Metabololism
AT5G15780	Pollen Ole e 1 allergen and extensin family protein	Cell wall
AT5G35190	Proline-rich extensin-like family protein	Cell wall
AT5G62000	ARF2 (AUXIN RESPONSE FACTOR 2)	Hormone -related
ATMG01360	Cytochrome c oxidase subunit 1	Enzyme-Metabololism
AT1G60200	Splicing factor PWI domain-containing protein	Other
AT4G11460	Protein kinase family protein	Signaling
AT1G62500	Protease inhibitor/seed storage/lipid transfer protein family protein	Defence/Stress
AT2G31010	Protein kinase family protein	Signaling
AT3G16670	Unknown protein	Unknown
AT3G47800	Aldose 1-epimerase family protein	Enzyme-Metabololism
AT1G15380	Lactoylglutathione lyase family protein / glyoxalase I family protein	Enzyme-Metabolism
AT2G20190	ATCLASP/CLASP	Development
AT3G07070	Protein kinase family protein	Signaling
AT5G60410	ATSIZ1/SIZ1; DNA binding / SUMO ligase	Defence/Stress
ATCG00690	Encodes photosystem II 5 kD protein subunit PSII-T	Light-Photosynthesis
AT3G24460	TMS membrane family protein	Cell wall
AT5G42590	CYP71A16 (cytochrome P450, family 71, subfamily A, polypeptide 16)	Enzyme-Metabolism
AT1G22570	Proton-dependent oligopeptide transport (POT) family protein	Transport
AT1G27590	Putative phosphatidylinositol 3- and 4-kinase family protein	Signaling
AT1G54730	Putative sugar transporter	Transport
AT3G44070	Beta-galactosidase	Enzyme-Metabolism
AT4G21410	Protein kinase family protein	Signaling
AT1G50240	Armadillo/beta-catenin repeat family protein	Development
AT1G31710	Putative copper amine oxidase	Enzyme-Metabolism
AT3G23430	PHO1 (PHOSPHATE 1)	Enzyme-Metabolism
AT3G23590	RFR1 (REF4-RELATED 1)	Unknown
AT3G30720	Unknown protein	Unknown
AT5G65800	ACS5 (ACC SYNTHASE 5); 1-aminocyclopropane-1-carboxylate synthase	Hormone -related
AT1G07350	Transformer serine/arginine-rich ribonucleoprotein	Other
AT1G61210	Putative WD-40 repeat family protein / katanin p80 subunit	Development
AT1G74770	Unknown protein	Unknown
AT3G05360	Disease resistance family protein / LRR family protein	Defence/Stress

AT3G22840	ELIP1 (EARLY LIGHT-INDUCABLE PROTEIN)	Light-Signaling
AT3G27170	CLC-B (chloride channel protein B); voltage-gated chloride channel	Transport
AT3G45450	Unknown protein	Unknown
AT3G50400	GDSL-motif lipase/hydrolase family protein	Enzyme-Metabolism
AT4G13410	ATCSLA15 (Cellulose synthase-like A15)	Cell wall
AT4G14690	ELIP2 (EARLY LIGHT-INDUCIBLE PROTEIN 2)	Light-Signaling
AT4G16140	Proline-rich family protein	Cell wall
AT4G19430	Unknown protein	Unknown
AT4G26850	VTC2 (VITAMIN C DEFECTIVE 2)	Defence/Stress
AT5G08640	FLS (FLAVONOL SYNTHASE)	Enzyme-Metabolism
AT5G12020	HSP17.6II (17.6 KDA CLASS II HEAT SHOCK PROTEIN)	Defence/Stress
AT5G13580	ABC transporter family protein	Transport
AT5G15950	Adenosylmethionine decarboxylase family protein]	Enzyme-Metabolism
AT5G24850	CRY3 (CRYPTOCHROME 3)	Light-Signaling
AT5G51440	23.5 kDa mitochondrial small heat shock protein (HSP23.5-M)	Stress
AT5G52640	HSP81-1 (HEAT SHOCK PROTEIN 81-1)	Stress
AT5G58760	DDB2 (DAMAGED DNA-BINDING 2); nucleotide binding	Other
AT5G62210	Embryo-specific protein-related	Development-embryo
AT5G02540	Short-chain dehydrogenase/reductase (SDR) family protein	Enzyme-Metabolism
ATCG00420	NADH dehydrogenase subunit J.	Enzyme-Metabolism
ATMG01270	Ribosomal protein S7 family protein	Other

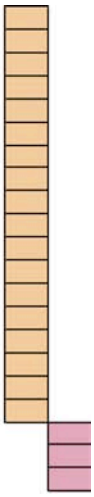

TABLE S3

List of genes repressed by the single mutants. The color code denotes the gene whose expression has been induced by a particular mutation.

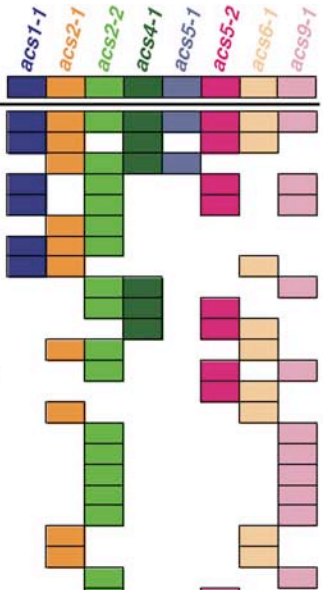

Gene name	Description of putative function	Function
ATCG00700	PSII low MW protein	Light-photosynthesis
AT2G42540	COR15A (COLD-REGULATED 15A)	Defence/stress
ATMG00290	Mitochondrial ribosomal protein S4	Other
AT3G49580	Unknown protein	Unknown
AT5G24660	Unknown protein	Unknown
AT1G76960	Unknown protein	Unknown
AT2G07708	Unknown protein	Unknown
AT2G43550	Putative trypsin inhibitor	Defence/stress
AT4G12970	Unknown protein	Unknown
AT4G14020	Rapid alkalinization factor (RALF) family protein	Transpost
AT4G33550	Lipid binding	Transpost
AT5G25190	Putative ethylene-responsive element-binding protein	Hormone-related
AT5G48850	Male sterility MS5 family protein	Development-embryo
AT1G02205	CER1 (ECERIFERUM 1)	Cell wall
AT1G12845	Unknown protein	Unknown
AT1G13650	Similar to 18S pre-ribosomal assembly protein gar2-related	Other
AT1G16410	CYP79F1 (SUPERSHOOT 1)	Development
AT1G62180	APR2 (5'ADENYLYLPHOSPHOSULFATE REDUCTASE 2)	Enzyme-metabolism
AT1G65870	Disease resistance-responsive family protein	Defence/stress
AT1G72910	Putative disease resistance protein (TIR-NBS class)	Defence/stress
AT2G15090	Putative fatty acid elongase	Enzyme-metabolism
AT2G28720	Putative histone H2B	Other
AT2G35960	NHL12 (NDR1/HIN1-like 12)	Defence/stress
AT2G40435	Transcription regulator	Transcription
AT2G40460	Proton-dependent oligopeptide transport (POT) family protein	Transpost
AT3G03840	Putative auxin-responsive protein	Hormone-related
AT3G06070	Unknown protein	Unknown
AT3G46600	Scarecrow transcription factor family protein	Development
AT3G47430	PEX11B	Light-signaling
AT3G53800	Armadillo/beta-catenin repeat family protein	Development
AT3G56400	WRKY70 (WRKY DNA-binding protein 70); transcription factor	Transcription
AT4G02075	PIT1 (PITCHOUN 1); protein binding / zinc ion binding	Transpost
AT4G04610	APR1 (PAPS REDUCTASE HOMOLOG 19)	Enzyme-metabolism
AT4G14270	Unknown: PAM2 motif containing protein	Unknown
AT4G21990	APR3 (APS REDUCTASE 3)	Enzyme-metabolism
AT4G27280	Calcium-binding EF hand family protein	Transpost
AT4G27440	PORB (PROTOCHLOROPHYLLIDE OXIDOREDUCTASE B)	Light-photosynthesis
AT5G05090	Myb family transcription factor	Transcription
AT5G22880	H2B/HTB2 (HISTONE H2B); DNA binding	Other
AT5G37770	TCH2 (TOUCH 2); calcium ion binding	Transpost
AT5G42200	Zinc finger (C3HC4-type RING finger) family protein	Transcription
AT5G66400	RAB18 (RESPONSIVE TO ABA 18)	Defence/stress
AT1G02820	Late embryogenesis abundant 3 family protein / LEA3 family protein	Defence/stress
AT1G23205	Invertase/pectin methylesterase inhibitor family protein	Cell wall
AT3G51750	Unknown protein	Unknown
AT5G58770	Putative dehydrodolichyl diphosphate synthase	Enzyme-metabolism
AT4G15620	Integral membrane family protein	Cell wall
AT2G02120	LCR70/PDF2.1 (Low-molecular-weight cysteine-rich 70); protease inhibitor	Defence/stress
AT1G47400	Unknown protein	Unknown
AT2G22190	Trehalose-phosphatase	Enzyme-metabolism
AT4G22212	Encodes a defensin-like (DEFL) family protein	Defence/stress
AT1G01240	Unknown protein	Unknown
AT2G23290	AtMYB70 (myb domain protein 70); DNA binding / transcription factor	Transcription
AT2G42190	Unknown protein	Unknown
AT5G23660	MTN3 (ARABIDOPSIS HOMOLOG OF MEDICAGO TRUNCATULA MTN3)	Development
AT5G67300	ATMYB44/ATMYBR1/MYBR1 (MYB DOMAIN PROTEIN 44)	Transcription
AT1G04770	Male sterility MS5 family protein	Development-embryo
AT1G24020	MLP423 (MLP-LIKE PROTEIN 423)	Defence/stress
AT2G27420	Putative cysteine proteinase	Enzyme-metabolism
AT1G36370	SHM7 (serine hydroxymethyltransferase 7); glycine hydroxymethyltransferase	Enzyme-metabolism
AT1G67865	Unknown protein	Unknown
AT2G23000	SCPL10 (serine carboxypeptidase-like 10)	Enzyme-metabolism
AT2G40000	Unknown protein	Unknown
AT3G10525	Unknown protein/similar to SIM (SIAMESE)	Unknown
AT3G16175	Thioesterase family protein	Enzyme-metabolism
AT4G09890	Unknown protein	Unknown
AT4G13800	Permease-related	Transpost
AT4G17090	CT-BMY (BETA-AMYLASE 3, BETA-AMYLASE 8)	Enzyme-metabolism

AT4G28290	Unknown protein	Unknown
AT5G51190	PutativeAP2 domain-containing transcription factor	Transcription
AT5G24150	SQP1 (Squalene monooxygenase 1)	Enzyme-metabolism
AT5G62140	Unknown protein	Unknown
AT2G38530	LTP2 (LIPID TRANSFER PROTEIN 2); lipid binding	Transport
AT3G47295	Unknown protein	Unknown
AT3G10520	AHB2 (NON-SYMBIOTIC HAEMOGLOBIN 2)	Development
AT4G14060	Major latex protein-related / MLP-related	Defence/stress
AT1G06100	Fatty acid desaturase family protein	Enzyme-metabolism
AT1G19960	Unknown protein	Unknown
AT2G33850	Unknown protein	Unknown
AT3G16360	AHP4 (HPT PHOSPHOTRANSMITTER 4); kinase	Signaling
AT3G47380	Invertase/pectin methylesterase inhibitor family protein	Cell wall
AT5G03350	Legume lectin family protein	Defence/stress
AT5G13170	Nodulin MtN3 family protein	Transport
AT5G24770	VSP2 (VEGETATIVE STORAGE PROTEIN 2); acid phosphatase	Enzyme-metabolism
AT1G02300	Putative cathepsin B-like cysteine protease	Defence/stress
AT1G02340	HFR1 (LONG HYPOCOTYL IN FAR-RED)	Light-signaling
AT1G21130	Putative O-methyltransferase	Enzyme-metabolism
AT1G25230	Purple acid phosphatase family protein	Enzyme-metabolism
AT1G25400	Unknown protein	Unknown
AT1G26800	Zinc finger (C3HC4-type RING finger) family protein	Transcription
AT1G33055	Unknown protein	Unknown
AT1G35612	Transposable element gene	Other
AT1G49500	Unknown protein	Unknown
AT1G53885	Unknown protein	Unknown
AT1G54740	Unknown protein	Unknown
AT1G56220	Dormancy/auxin associated family protein	Hormone-related
AT1G67050	Unknown protein	Unknown
AT1G68190	Zinc finger (B-box type) family protein	Transcription
AT1G70290	ATTPS8 (Arabidopsis thaliana trehalose phosphatase/synthase 8)	Enzyme-metabolism
AT1G74670	Putative gibberellin-responsive protein	Hormone-related
AT1G75190	Unknown protein	Unknown
AT1G77210	Putative sugar transporter	Transpost
AT1G80440	Kelch repeat-containing F-box family protein	Signaling
AT1G80920	J8; heat shock protein binding / unfolded protein binding	Defence/stress
AT2G02710	Unknown; PAC motif-containing protein	Unknown
AT2G02950	PKS1 (PHYTOCHROME KINASE SUBSTRATE 1)	Light-signaling
AT2G15890	MEE14 (maternal effect embryo arrest 14)	Development-embryo
AT2G15960	Unknown protein	Unknown
AT2G17450	RHA3A (RING-H2 finger A3A); protein binding / zinc ion binding	Transpost
AT2G17880	Putative DNAJ heat shock protein	Defence/stress
AT2G18300	basic helix-loop-helix (bHLH) family protein	Signaling
AT2G18670	Zinc finger (C3HC4-type RING finger) family protein	Transcription
AT2G24240	potassium channel tetramerisation domain-containing protein	Transpost
AT2G24550	Unknown protein	Unknown
AT2G25900	ATCTH (Arabidopsis thaliana Cys3His zinc finger protein); transcription factor	Transcription
AT2G27830	Unknown protein	Unknown
AT2G29300	Putative tropinone reductase	Enzyme-metabolism
AT2G29670	Unknown protein	Unknown
AT2G36050	ATOFP15/OFP15 (Arabidopsis thaliana ovate family protein 15)	Development
AT2G39400	Hydrolase, alpha/beta fold family protein	Enzyme-metabolism
AT2G40530	Unknown protein	Unknown
AT2G41430	ERD15 (EARLY RESPONSIVE TO DEHYDRATION 15)	Defence/stress
AT2G44130	Kelch repeat-containing F-box family protein	Signaling
AT2G46550	Unknown protein	Unknown
AT3G10020	Unknown protein	Unknown
AT3G11410	AHG3/ATPP2CA (ARABIDOPSIS THALIANA PROTEIN PHOSPHATASE 2CA)	Signaling
AT3G15630	Unknown protein	Unknown
AT3G19620	Glycosyl hydrolase family 3 protein	Enzyme-metabolism
AT3G26740	CCL (CCR-LIKE)	Development
AT3G29670	Transferase family protein	Enzyme-metabolism
AT3G47160	Unknown protein	Unknown
AT3G48360	BT2 (BTB AND TAZ DOMAIN PROTEIN 2); transcription regulator	Transcription
AT3G49790	ATPP2-A10 (Phloem protein 2-A10)	Signaling
AT3G52070	Unknown protein	Unknown
AT3G61060	ATPP2-A13 (Phloem protein 2-A13)	Defence/stress
AT3G62550	Universal stress protein (USP) family protein	Defence/stress
AT3G62950	Glutaredoxin family protein	Defence/stress
AT4G03510	RMA1 (Ring finger protein with Membrane Anchor 1)	Cell wall
AT4G04630	Unknown protein	Unknown
AT4G05070	Unknown protein	Unknown
AT4G10910	Unknown protein	Unknown

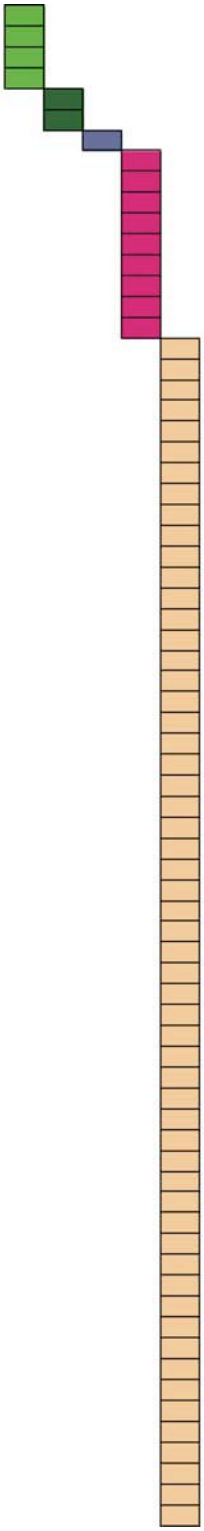

AT4G11280	ACS6 (1-AMINOCYCLOPROPANE-1-CARBOXYLIC ACID (ACC) SYNTHASE 6)	Hormone-related
AT4G12690	Unknown protein	Unknown
AT4G14550	IAA14 (SOLITARY ROOT)	Hormone-related
AT4G16000	Unknown protein	Unknown
AT4G23870	Unknown protein	Unknown
AT4G29190	Zinc finger (CCCH-type) family protein	Transcription
AT4G30650	Putative low temperature and salt responsive protein	Defence/stress
AT4G30660	Putativelow temperature and salt responsive protein	Defence/stress
AT4G30690	Translation initiation factor 3 (IF-3) family protein	Other
AT4G34250	Putative fatty acid elongase	Enzyme-metabolism
AT4G37260	AtMYB73/MYB73 (myb domain protein 73)	Transcription
AT5G11070	Unknown protein	Unknown
AT5G15160	bHLH family protein	Signaling
AT5G22270	Unknown protein	Unknown
AT5G22920	Zinc finger (C3HC4-type RING finger) family protein	Transcription
AT5G45340	CYP707A3 (cytochrome P450, family 707, subfamily A, polypeptide 3)	Defence/stress
AT5G45820	CIPK20 (CBL-INTERACTING PROTEIN KINASE 20)	Signaling
AT5G46710	Zinc-binding family protein	Transport
AT5G47240	ATNUDT8 (Arabidopsis thaliana Nudix hydrolase homolog 8)	Enzyme-metabolism
AT5G49450	ATBZIP1 (ARABIDOPSIS THALIANA BASIC LEUCINE-ZIPPER 1)	Transcription
AT5G50450	Zinc finger (MYND type) family protein	Transcription
AT5G51390	Unknown protein	Unknown
AT5G56100	Glycine-rich protein / oleosin	Development
AT5G57340	Unknown protein	Unknown
AT5G62350	Invertase/pectin methylesterase inhibitor family protein	Cell wall
AT3G52740	Unknown protein	Unknown
AT5G26220	ChaC-like family protein	Development
AT5G42180	Peroxidase 64 (PER64) (P64) (PRXR4)	Enzyme-metabolism
AT1G55960	Unknown protein	Unknown

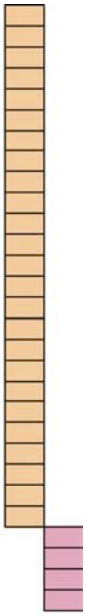

TABLE S4

List of genes induced by the high order mutants. The color code denotes the gene whose expression has been induced by a particular mutation.

Gene name	Description of putative function	Function
AT2G15890	MEE14 (maternal effect embryo arrest 14)	Development-embryo
AT3G15630	Unknown protein	Unknown
AT3G62950	Glutaredoxin family protein	Enzyme-Metabolism
AT1G50290	Unknown protein	Unknown
AT1G54040	ESP (EPITHIOSPECIFIER PROTEIN)	Defence/Stress
AT1G60810	ACLA-2 (ATP-citrate lyase A-2)	Enzyme-Metabolism
AT1G62290	Aspartyl protease family protein	Defence/Stress
AT1G72060	Serine-type endopeptidase inhibitor	Defence/Stress
AT2G28630	beta-ketoacyl-CoA synthase family protein	Enzyme-Metabolism
AT2G43620	Putative chitinase	Defence/Stress
AT3G10020	Unknown protein	Unknown
AT3G62550	Universal stress protein (USP) family protein	Defence/Stress
AT4G22280	F-box family protein	Signaling
AT4G22470	Protease inhibitor/seed storage/lipid transfer protein (LTP) family protein	Defence/Stress
AT5G15360	Unknown protein	Unknown
AT5G18840	Putative sugar transporter	Transport
AT5G19100	Extracellular dermal glycoprotein-related / EDGP-related	Cell wall
AT5G19250	Unknown protein	Unknown
AT5G23020	IMS2/MAM-L/MAM3 (METHYLTHIOALKYMALATE SYNTHASE-LIKE)	Enzyme-Metabolism
AT5G23570	SGS3 (SUPPRESSOR OF GENE SILENCING 3)	Defence/Stress
AT5G24240	Phosphatidylinositol 3- and 4-kinase family protein	Signaling
AT5G27660	Serine-type peptidase/ trypsin	Defence/Stress
AT5G32460	Transcriptional factor B3 family(pseudogene)	Transcription
AT5G47240	ATNUDT8 (Arabidopsis thaliana Nudix hydrolase homolog 8)	Enzyme-Metabolism
AT1G15040	Glutamine amidotransferase-related protein	Enzyme-Metabolism
AT5G15420	Unknown protein	Unknown
AT1G13260	RAV1 (Related to ABI3/VP1 1)	Hormone -related
AT1G13700	Glucosamine/galactosamine-6-phosphate isomerase family protein	Enzyme-Metabolism
AT1G25560	Putative AP2 domain-containing transcription factor	Transcription
AT1G56220	Dormancy/auxin associated family protein	Hormone-related
AT1G60270	Glycosyl hydrolase family 1(pseudogene)	Enzyme-Metabolism
AT1G64170	ATCHX16 (CATION/H+ EXCHANGER 16); monovalent cation:proton antiporter	Transport
AT1G64460	Phosphatidylinositol 3- and 4-kinase family protein	Signaling
AT1G64470	Ubiquitin family protein	Signaling
AT1G70820	Putative phosphoglucomutase	Enzyme-Metabolism
AT2G15960	Unknown protein	Unknown
AT2G39400	Hydrolase, alpha/beta fold family protein	Enzyme-Metabolism
AT3G19850	Phototropic-responsive NPH3 family protein	Light -Signaling
AT3G21080	ABC transporter-related	Transport
AT3G26200	CYP71B22 (cytochrome P450, family 71, subfamily B, polypeptide 22)	Defence/Stress
AT3G46280	Protein kinase-related	Signaling
AT3G47160	Unknown protein	Unknown
AT4G03510	RMA1 (Ring finger protein with Membrane Anchor 1)	Cell wall
AT4G16870	Transposable element gene	Other
AT4G12470	Protease inhibitor/seed storage/lipid transfer protein (LTP) family protein	Defence/Stress
AT4G14270	Unknown; contains PAM2 motif	Unknown
AT4G21510	F-box family protein	Signaling
AT4G23680	Major latex protein-related / MLP-related	Defence/Stress
AT4G34250	Putative fatty acid elongase	Enzyme-Metabolism
AT4G34770	Auxin-responsive family protein	Hormone -related
AT5G13200	GRAM domain-containing protein / ABA-responsive protein-related	Stress
AT5G22270	Unknown protein	Unknown
AT5G22920	Zinc finger (C3HC4-type RING finger) family protein	Transcription
AT5G27200	ACP5 (ACYL CARRIER PROTEIN 5); acyl carrier	Enzyme-Metabolism

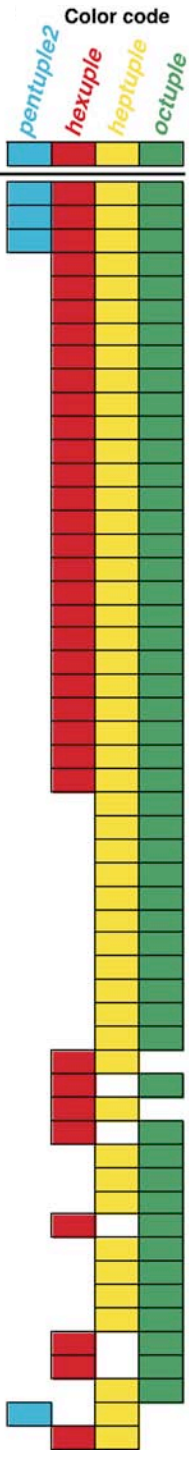

AT5G27280	Zinc finger (DNL type) family protein	Transcription
AT5G46050	ATPTR3/PTR3 (PEPTIDE TRANSPORTER PROTEIN 3)	Transport
AT5G47990	CYP705A5 (cytochrome P450, family 705, subfamily A, polypeptide 5)	Defence/Stress
AT5G48010	Putative pentacyclic triterpene synthase	Enzyme-Metabolism
AT5G49450	ATBZIP1 (ARABIDOPSIS THALIANA BASIC LEUCINE-ZIPPER 1)	Transcription
AT5G54190	PORA (Protochlorophyllide reductase A)	Light-photosynthesis
AT4G12550	AIR1 (Auxin-Induced in Root cultures 1)	Hormone -related
AT5G26270	Unknown protein	Unknown
AT5G42600	MRN (MARNERAL SYNTHASE)	Defence/Stress
AT5G42580	CYP705A12 (cytochrome P450, family 705, subfamily A, polypeptide 12)	Enzyme-Metabolism
AT5G65800	ACS5 (ACC SYNTHASE 5); 1-aminocyclopropane-1-carboxylate synthase	Hormone -related
AT1G24260	SEP3 (SEPALLATA3)	Development
AT1G65390	ATPP2-A5; carbohydrate binding protein	Signaling
AT2G14560	Unknown protein	Unknown
AT2G25470	Leucine-rich repeat family protein	Signaling
AT2G26440	Pectinesterase family protein	Cell wall
AT2G36690	Oxidoreductase, 2OG-Fe(II) oxygenase family protein	Enzyme-Metabolism
AT2G44080	ARL (ARGOS-LIKE)	Development
AT3G21020	Transposable element gene	Other
AT4G14365	Zinc finger (C3HC4-type RING finger) family protein	Transcription
AT4G26200	ACS7	Hormone -related
AT4G31570	Unknown protein	Unknown
AT5G16380	Unknown protein	Unknown
AT5G20150	Unknown; SPX (SYG1/Pho81/XPR1) domain-containing protein	Unknown
AT5G46330	FLS2 (FLAGELLIN-SENSITIVE 2)	Signaling
AT1G02660	Lipase class 3 family protein	Enzyme-Metabolism
AT1G33970	Putative avirulence-responsive protein	Defence/Stress
AT1G50280	Phototropic-responsive NPH3 family protein	Light -Signaling
AT1G53080	Legume lectin family protein	Defence/Stress
AT1G66800	Cinnamyl-alcohol dehydrogenase familyprotein	Enzyme-Metabolism
AT1G67810	Fe-S metabolism associated domain-containing protein	Enzyme-Metabolism
AT1G68190	Zinc finger (B-box type) family protein	Transcription
AT1G71030	ATMYBL2 (Arabidopsis myb-like 2)	Transcription
AT1G76410	ATL8; protein binding / zinc ion binding	Signaling
AT1G77210	Putative sugar transporter	Transport
AT1G80920	J8; heat shock protein binding	Defence/Stress
AT2G02710	Unknown protein	Unknown
AT2G29670	Unknown protein	Unknown
AT3G02550	LBD41 (LOB DOMAIN-CONTAINING PROTEIN 41)	Development
AT3G15450	Unknown protein	Unknown
AT3G26740	CCL (CCR-LIKE)	Development
AT3G49790	ATPP2-A10 (Phloem protein 2-A10)	Defence/Stress
AT3G61060	ATPP2-A13 (Phloem protein 2-A13)	Defence/Stress
AT4G05070	Unknown protein	Unknown
AT4G27440	PORB (PROTOCHLOROPHYLLIDE OXIDOREDUCTASE B)	Light-photosynthesis
AT4G27450	Unknown protein	Unknown
AT4G28040	Nodulin MtN21 family protein	Transport
AT4G37260	AtMYB73/MYB73 (myb domain protein 73)	Transcription
AT5G02540	Short-chain dehydrogenase/reductase (SDR) family protein	Enzyme-Metabolism
AT5G18130	Unknown protein	Unknown
AT5G20250	DIN10 (DARK INDUCIBLE 10); hydrolase	Defence/Stress
AT5G23220	NIC3 (NICOTINAMIDASE 3)	Enzyme-Metabolism
AT5G37980	Putative NADP-dependent oxidoreductase	Enzyme-Metabolism
AT5G38010	UDP-glucoronosyl/UDP-glucosyl transferase family protein	Enzyme-Metabolism
AT5G38020	S-adenosyl-L-methionine:carboxyl methyltransferase family protein	Enzyme-Metabolism
AT5G38550	Jacalin lectin family protein	Defence/Stress
AT5G38710	Putative proline oxidase	Enzyme-Metabolism
AT5G43440	Putative 2-oxoglutarate-dependent dioxygenase	Enzyme-Metabolism
AT5G44260	Zinc finger (CCCH-type) family protein	Transcription
AT1G04110	SDD1 (STOMATAL DENSITY AND DISTRIBUTION)	Development
AT1G05575	Unknown protein	Unknown
AT1G06160	Ethylene-responsive factor	Hormone -related

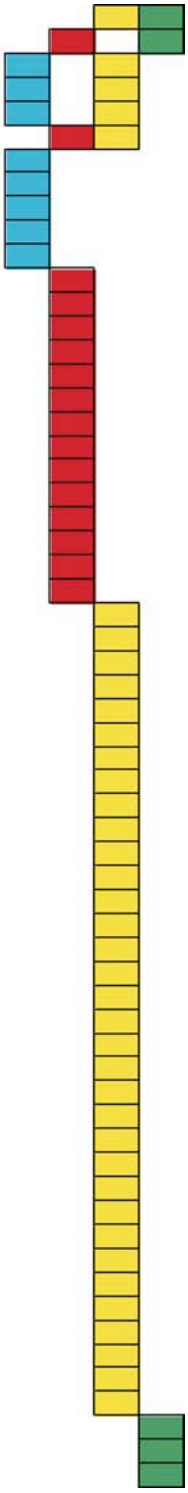

AT1G15670	Kelch repeat-containing F-box family protein	Signaling
AT1G16070	AtTLP8 (TUBBY LIKE PROTEIN 8)	Development
AT1G19380	Unknown protein	Unknown
AT1G20590	CYCB2;3 cyclin-dependent protein kinase regulator	Signaling
AT1G22890	Unknown protein	Unknown
AT1G60020	Transposable element gene	Other
AT1G61810	BGLU45; hydrolase, hydrolyzing O-glycosyl compounds	Enzyme-Metabolism
AT1G76540	CDKB2;1 (CYCLIN-DEPENDENT KINASE B2;1)	Signaling
AT1G76930	ATEXT4 (EXTENSIN 4)	Cell wall
AT1G78460	SOUL heme-binding family protein	Transport
AT2G18600	Putative RUB1-conjugating enzyme	Signaling
AT2G23170	GH3.3; indole-3-acetic acid amido synthetase	Hormone -related
AT2G25735	Unknown protein	Unknown
AT2G27970	CKS2 (CDK-SUBUNIT 2); cyclin-dependent protein kinase	Signaling
AT2G42870	HLH1/PAR1 (PHY RAPIDLY REGULATED 1); transcription regulator	Light-Signaling
AT3G07800	Putative thymidine kinase	Enzyme-Metabolism
AT3G12520	SULTR4;2 (sulfate transporter 4;2); sulfate transmembrane transporter	Transport
AT3G17680	Unknown protein	Unknown
AT3G18830	ATPLT5 (POLYOL TRANSPORTER 5);sugar transporter	Transport
AT3G22880	ATDMC1 (RECA-LIKE GENE); ATP binding / DNA-dependent ATPase	Other
AT3G23550	MATE efflux family protein	Transport
AT3G25760	AOC1 (ALLENE OXIDE CYCLASE 1)	Enzyme-Metabolism
AT3G27060	TSO2 ; ribonucleoside-diphosphate reductase	Enzyme-Metabolism
AT3G47800	Aldose 1-epimerase family protein	Enzyme-Metabololism
AT3G49580	Unknown protein	Unknown
AT4G02330	ATPMEPCRB; pectinesterase	Cell wall
AT4G02390	APP ; NAD+ ADP-ribosyltransferase	Enzyme-Metabolism
AT4G12480	pEARLI 1; lipid binding	Transport
AT4G12500	Protease inhibitor/seed storage/lipid transfer protein (LTP) family protein	Defence/Stress
AT4G21070	ATBRCA1 (BREAST CANCER SUSCEPTIBILITY1); ubiquitin-protein ligase	Signaling
AT4G22753	SMO1-3 (STEROL 4-ALPHA METHYL OXIDASE)	Enzyme-Metabolism
AT4G22960	Unknown protein	Unknown
AT4G28950	ARAC7/ATRAC7/ATROP9/RAC7/ROP9 ;RHO-RELATED PROTEIN	Signaling
AT4G36670	Putative mannitol transporter	Transport
AT4G37490	CYC1 (CYCLIN 1); cyclin-dependent protein kinase regulator	Signaling
AT5G03230	Unknown protein	Unknown
AT5G05180	Unknown protein	Unknown
AT5G06870	PGIP2 (POLYGALACTURONASE INHIBITING PROTEIN 2)	Cell wall
AT5G07100	WRKY26 (WRKY DNA-binding protein 26)	Transcription
AT5G13220	JAS1/JAZ10/TIFY9 (JASMONATE-ZIM-DOMAIN PROTEIN 10)	Defence/Stress
AT5G16990	Putative NADP-dependent oxidoreductase	Enzyme-Metabolism
AT5G17160	Unknown protein	Unknown
AT5G23910	Microtubule motor	Development
AT5G24280	Unknown protein	Unknown
AT5G48720	Unknown protein	Unknown
AT5G48850	Male sterility MS5 family protein	Development-embryo
AT5G52750	Heavy-metal-associated domain-containing protein	Transport
AT5G56580	ATMKK6 (ARABIDOPSIS NQK1); kinase	Signaling
AT5G60250	Zinc finger (C3HC4-type RING finger) family protein	Transcription
AT5G61590	AP2 domain-containing transcription factor family protein	Transcription
AT5G62550	Unknown protein	Unknown
AT5G64060	ANAC103 (Arabidopsis NAC domain containing protein 103)	Transcription
AT5G67480	BT4 (BTB AND TAZ DOMAIN PROTEIN 4)	Transcription

TABLE S5

List of genes repressed by the high order mutants. The color code denotes the gene whose expression has been induced by a particular mutation.

Gene name	Description of putative function	Function
AT4G11280	ACS6 (1-AMINOCYCLOPROPANE-1-CARBOXYLIC ACID (ACC) SYNTHASE 6)	Hormone-related
AT1G58270	ZW9	Development
AT1G65190	Protein kinase family protein	Signaling
AT1G65370	Unknown: meprin and TRAF homology domain-containing protein	Unknown
AT1G66100	Putative thionine	Defence/stress
AT4G25710	Kelch repeat-containing F-box family protein	Signaling
AT4G26150	CGA1 (CYTOKININ-RESPONSIVE GATA FACTOR 1); transcription factor	Hormone-related
AT5G03350	Legume lectin family protein	Defence/stress
AT5G05040	Cysteine protease inhibitor	Defence/stress
AT5G17880	CSA1 (CONSTITUTIVE SHADE-AVOIDANCE1)	Light-signaling
AT5G20380	Transporter-related	Transport
AT5G22510	Putative beta-fructofuranosidase	Enzyme-metabolism
AT5G22860	Serine carboxypeptidase S28 family protein	Defence/stress
AT5G24150	SQP1 (Squalene monooxygenase 1)	Enzyme-metabolism
AT5G26260	Unknown: meprin and TRAF domain-containing protein	Unknown
AT5G27270	EMB976 (EMBRYO DEFECTIVE 976)	Development-embryo
AT5G26270	Unknown protein	Unknown
AT5G35450	Putative disease resistance protein (CC-NBS-LRR class)	Defence/stress
AT5G35490	Unknown protein	Unknown
AT1G55960	Unknown protein	Unknown
AT2G27420	Putative cysteine proteinase	Enzyme-metabolism
AT1G01060	LHY (LATE ELONGATED HYPOCOTYL)	Light-signaling
AT1G53900	GTP binding / translation initiation factor	Other
AT1G54260	Histone H1/H5 family protein	Other
AT1G56510	Putative disease resistance protein (TIR-NBS-LRR class)	Defence/stress
AT1G58380	XW6; structural constituent of ribosome	Other
AT1G58807	Putative disease resistance protein (CC-NBS-LRR class)	Defence/stress
AT1G59218	Putative disease resistance protein (CC-NBS-LRR class)	Defence/stress
AT1G59900	AT-E1 ALPHA (pyruvate dehydrogenase complex E1 alpha subunit)	Enzyme-metabolism
AT1G62430	ATCDS1 (CDP-diacylglycerol synthase 1)	Enzyme-metabolism
AT1G63090	ATPP2-A11 (Phloem protein 2-A11); carbohydrate binding	Signaling
AT1G63880	Putative disease resistance protein (TIR-NBS-LRR class)	Defence/stress
AT1G02820	Late embryogenesis abundant 3 family protein / LEA3 family protein	Defence/stress
AT3G12110	ACT11 (ACTIN-11); structural constituent of cytoskeleton	Cell wall
AT3G14210	ESM1 (EPITHIOSPECIFIER MODIFIER 1); carboxylesterase	Defence/stress
AT3G14650	CYP72A11 (cytochrome P450, family 72, subfamily A, polypeptide 11)	Enzyme-metabolism
AT3G15310	Transposable element gene	Other
AT3G15590	Putative DNA-binding protein	Other
AT3G16450	Jacalin lectin family protein	Defence/stress
AT3G21950	S-adenosyl-L-methionine:carboxyl methyltransferase family protein	Enzyme-metabolism
AT3G22840	ELIP1 (EARLY LIGHT-INDUCABLE PROTEIN); chlorophyll binding	Light-signaling
AT3G24460	TMS membrane family protein	Cell wall
AT1G23205	Invertase/pectin methylesterase inhibitor family protein	Cell wall
AT4G24130	Unknown protein	Unknown
AT4G25810	XTR6 (XYLOGLUCAN ENDOTRANSGLYCOSYLASE 6)	Cell wall
AT4G31805	WRKY family transcription factor	Transcription
AT5G02270	ATNAP9 (Non-intrinsic ABC protein 9)	Transport
AT5G03340	(Cell division control protein 48 homolog E); ATPase	Development
AT5G06790	Unknown protein	Unknown
AT5G08600	U3 ribonucleoprotein (Utp) family protein	Other
AT5G10140	FLC (FLOWERING LOCUS C)	Development
AT5G10400	Histone H3	Other
AT5G11580	UVB-resistance protein-related / (RCC1) family protein	Defence/stress
AT5G15020	Unknown protein	Unknown

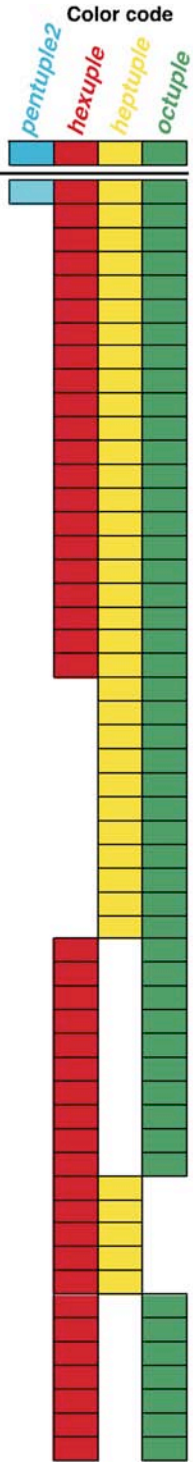

AT5G15960	KIN (COLD-RESPONSIVE 6.6)	Defence/stress
AT5G15980	Unknown:pentatricopeptide (PPR) repeat-containing protein	Unknown
AT5G16220	Unknown: octicosapeptide/Phox/Bem1p (PB1) domain-containing protein	Unknown
AT5G16980	Putative NADP-dependent oxidoreductase	Enzyme-metabolism
AT5G17890	LIM domain-containing protein / disease resistance protein-related	Defence/stress
AT5G23070	Putative thymidine kinase	Enzyme-metabolism
AT5G23410	Similar to FKF1 (FLAVIN-BINDING KELCH DOMAIN F BOX PROTEIN)	Signaling
AT5G28350	Unknown protein	Unknown
AT5G38910	Putative germin-like protein	Defence/stress
AT5G24850	CRY3 (CRYPTOCHROME 3)	Light-signaling
AT5G58770	Putative dehydrodolichyl diphosphate synthase	Enzyme-metabolism
AT1G58150	Unknown protein	Unknown
AT1G62150	Mitochondrial transcription termination factor-related / mTERF-related	Other
AT2G38530	LTP2 (LIPID TRANSFER PROTEIN 2); lipid binding	Transport
AT4G23300	Protein kinase family protein	Signaling
AT2G18150	Putative peroxidase	Enzyme-metabolism
AT1G20390	Transposable element gene	Other
AT1G74770	Unknown protein	Unknown
AT2G02120	LCR70/PDF2.1 (Low-molecular-weight cysteine-rich 70); protease inhibitor	Defence/stress
AT3G11240	Putative arginine-tRNA-protein transferase	Other
AT3G18280	Protease inhibitor/seed storage/lipid transfer protein (LTP) family protein	Defence/stress
AT3G51240	F3H (TRANSPARENT TESTA 6); naringenin 3-dioxygenase	Defence/stress
AT4G01080	Unknown protein	Unknown
AT4G19690	IRT1 (IRON-REGULATED TRANSPORTER 1)	Transport
AT5G05270	Chalcone-flavanone isomerase family protein	Enzyme-metabolism
AT5G07690	MYB29 (myb domain protein 29); DNA binding / transcription factor	Transcription
AT5G16250	Unknown protein	Unknown
AT5G20740	Invertase/pectin methylesterase inhibitor family protein	Cell wall
AT5G42600	MRN (MARNERAL SYNTHASE)	Defence/stress
AT1G49630	ATPREP2; metalloendopeptidase	Defence/stress
AT1G54050	17.4 kDa class III heat shock protein (HSP17.4-CIII)	Defence/stress
AT1G56720	Protein kinase family protein	Signaling
AT1G60710	ATB2; oxidoreductase	Enzyme-metabolism
AT1G66540	Putative cytochrome P450	Enzyme-metabolism
AT1G66620	Putative seven in absentia (SINA) protein	Development
AT1G66970	Glycerophosphoryl diester phosphodiesterase family protein	Enzyme-metabolism
AT4G00050	UNE10 (unfertilized embryo sac 10);transcription factor	Development-embryo
AT4G01590	Unknown protein	Unknown
AT4G02130	GATL6/LGT10; polygalacturonate 4-alpha-galacturonosyltransferase	Cell wall
AT4G02410	Lectin protein kinase family protein	Defence/stress
AT4G02540	Unknown: DC1 domain-containing protein	Unknown
AT4G21760	BGLU47 (Beta-glucosidase 47)	Enzyme-metabolism
AT4G31530	Binding / catalytic/ coenzyme binding	Transport
AT5G22580	Unknown protein	Unknown
AT5G36910	THI2.2 (THIONIN 2.2); toxin receptor binding	Defence/stress
AT5G36930	Putative disease resistance protein (TIR-NBS-LRR class)	Defence/stress
AT5G39030	Protein kinase family protein	Signaling
AT5G42760	Unknown protein	Unknown
AT5G56080	Putative nicotianamine synthase	Enzyme-metabolism
AT1G17870	ATEGY3	Development
AT1G48100	Glycoside hydrolase family 28 protein / polygalacturonase family protein	Cell wall
AT1G55740	ATSIP1 (ARABIDOPSIS THALIANA SEED IMBIBITION 1)	Cell wall
AT1G62510	Protease inhibitor/seed storage/lipid transfer protein (LTP) family protein	Defence/stress
AT1G62710	BETA-VPE (vacuolar processing enzyme beta); cysteine-type endopeptidase	Defence/stress
AT1G73220	ATOCT1	Transport
AT2G25680	MOT1 (MOLYBDATE TRANSPORTER 1)	Transport
AT2G30750	CYP71A12 (CYTOCHROME P450)	Enzyme-metabolism
AT2G36630	Unknown protein	Unknown
AT2G41380	Embryo-abundant protein-related	Development-embryo
AT3G04030	Myb family transcription factor	Transcription
AT3G08730	ATPK1 (P70 RIBOSOMAL S6 KINASE); kinase/ protein binding	Signaling
AT3G12170	DNAJ heat shock N-terminal domain-containing protein	Defence/stress

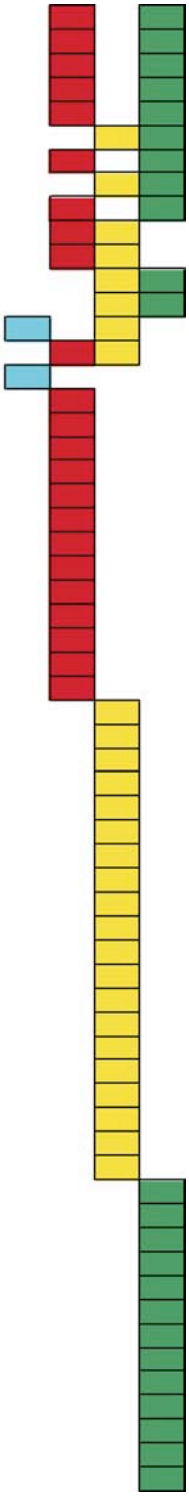

AT3G14240	Subtilase family protein	Defence/stress	
AT3G22240	Unknown protein	Unknown	
AT3G22570	Protease inhibitor/seed storage/lipid transfer protein (LTP)	Transport	
AT3G28270	Unknown protein	Unknown	
AT3G51895	SULTR3;1 (SULFATE TRANSPORTER 1)	Transport	
AT4G35090	CAT2 (CATALASE 2)	Enzyme-metabolism	
AT5G02180	Amino acid transporter family protein	Transport	
AT5G17790	VAR3 (VARIEGATED 3); binding	Development	
AT5G20360	Unknown:octicosapeptide/Phox/Bem1p (PB1) domain-containing protein	Unknown	
AT5G22890	Zinc finger (C2H2 type) family protein	Transcription	
AT5G24120	SIGE (RNA polymerase sigma subunit E); DNA binding	Other	
AT5G45070	ATPP2-A8 (Phloem protein 2-A8); transmembrane receptor	Defence/stress	
AT5G54130	Calcium-binding EF hand family protein	Transport	
AT5G67430	GCN5-related N-acetyltransferase (GNAT) family protein	Enzyme-metabolism	

TABLE S6

List of genes induced by the single mutants. Sorted according to their functional classifications. The color code denotes the gene whose expression has been induced by a particular mutation.

Gene name	Description of putative function	Function
AT3G54590	ATHRGP1; structural constituent of cell wall	Cell wall
AT1G76930	ATEXT4 (EXTENSIN 4)	Cell wall
AT3G22120	CWLP (CELL WALL-PLASMA MEMBRANE LINKER PROTEIN)	Cell wall
AT1G23720	Proline-rich extensin-like family protein	Cell wall
AT3G22800	Leucine-rich repeat family protein / extensin family protein	Cell wall
AT4G13340	Leucine-rich repeat family protein / extensin family protein	Cell wall
AT5G15780	Pollen Ole e 1 allergen and extensin family protein	Cell wall
AT5G35190	Proline-rich extensin-like family protein	Cell wall
AT3G24460	TMS membrane family protein	Cell wall
AT4G13410	ATCSLA15 (Cellulose synthase-like A15)	Cell wall
AT4G16140	Proline-rich family protein	Cell wall
AT1G09560	GLP5 (GERMIN-LIKE PROTEIN 5)	Defence/Stress
AT4G16990	Putative disease resistance protein (TIR-NBS class)	Defence/Stress
AT3G30775	ERD5 (EARLY RESPONSIVE TO DEHYDRATION 5); proline dehydrogenase	Defence/Stress
AT1G62500	protease inhibitor/seed storage/lipid transfer protein family protein	Defence/Stress
AT5G60410	ATSIZ1/SIZ1; DNA binding / SUMO ligase	Defence/Stress
AT3G05360	Disease resistance family protein / LRR family protein	Defence/Stress
AT4G26850	VTC2 (VITAMIN C DEFECTIVE 2)	Defence/Stress
AT5G12020	HSP17.6II (17.6 KDA CLASS II HEAT SHOCK PROTEIN)	Defence/Stress
AT5G51440	23.5 kDa mitochondrial small heat shock protein (HSP23.5-M)	Defence/Stress
AT5G52640	HSP81-1 (HEAT SHOCK PROTEIN 81-1)	Defence/Stress
AT4G11830	PLDGAMMA2; phospholipase D	Defence/Stress
AT5G23910	Microtubule motor	Development
AT1G11130	SUB (STRUBBELIG)	Development
AT4G38600	KAK (KAKTUS)	Development
AT2G20190	ATCLASP/CLASP	Development
AT1G50240	Armadillo/beta-catenin repeat family protein	Development
AT1G61210	Putative WD-40 repeat family protein / katanin p80 subunit,	Development
AT5G62210	Embryo-specific protein-related	Development-embryo
AT3G23530	Putative cyclopropane fatty acid synthase / CPA-FA synthase	Enzyme-Metabolism
AT1G15380	Lactoylglutathione lyase family protein / glyoxalase I family protein	Enzyme-Metabolism
AT5G42590	CYP71A16 (cytochrome P450, family 71, subfamily A, polypeptide 16)	Enzyme-Metabolism
AT3G44070	Beta-galactosidase	Enzyme-Metabolism
AT1G31710	Putative copper amine oxidase	Enzyme-Metabolism
AT3G23430	PHO1 (PHOSPHATE 1)	Enzyme-Metabolism
AT3G50400	GDSL-motif lipase/hydrolase family protein	Enzyme-Metabolism
AT5G08640	FLS (FLAVONOL SYNTHASE)	Enzyme-Metabolism
AT5G15950	Adenosylmethionine decarboxylase family protein]	Enzyme-Metabolism
AT5G02540	Short-chain dehydrogenase/reductase (SDR) family protein	Enzyme-Metabolism
ATCG00420	NADH dehydrogenase subunit J.	Enzyme-Metabolism
AT1G48130	ATPER1 (Arabidopsis thaliana 1-cysteine peroxiredoxin 1)	Enzyme-Metabololism
AT5G14760	AO (L-ASPARTATE OXIDASE); L-aspartate oxidase	Enzyme-Metabololism
ATMG01360	Cytochrome c oxidase subunit 1	Enzyme-Metabololism
AT3G47800	Aldose 1-epimerase family protein	Enzyme-Metabololism
AT5G62000	ARF2 (AUXIN RESPONSE FACTOR 2)	Hormone-related
AT5G65800	ACS5 (ACC SYNTHASE 5); 1-aminocyclopropane-1-carboxylate synthase	Hormone-related
AT5G10770	Putative chloroplast nucleoid DNA-binding protein	Light-Photosynthesis
ATCG00680	CP47, subunit of the photosystem II reaction center	Light-Photosynthesis
AT2G27510	ATFD3 (FERREDOXIN 3)	Light-Photosynthesis
ATCG00190	Chloroplast DNA-dependent RNA polymerase B subunit.	Light-Photosynthesis
ATCG00690	Encodes photosystem II 5 kD protein subunit PSII-T	Light-Photosynthesis
AT2G46340	SPA1 (SUPPRESSOR OF PHYA-105 1)	Light-Signaling
AT1G01060	LHY (LATE ELONGATED HYPOCOTYL)	Light-Signaling
AT3G22840	ELIP1 (EARLY LIGHT-INDUCABLE PROTEIN)	Light-Signaling
AT4G14690	ELIP2 (EARLY LIGHT-INDUCIBLE PROTEIN 2)	Light-Signaling
AT5G24850	CRY3 (CRYPTOCHROME 3)	Light-Signaling
AT1G33680	Nucleic acid binding protein	Other
AT4G16870	Transposable element gene	Other
AT2G28540	Nucleic acid binding / nucleotide binding binding	Other
AT1G60200	Splicing factor PWI domain-containing protein	Other
AT1G07350	Transformer serine/arginine-rich ribonucleoprotein	Other
AT5G58760	DDB2 (DAMAGED DNA-BINDING 2); nucleotide binding	Other
ATMG01270	Ribosomal protein S7 family protein	Other
AT3G50590	Transducin family protein / WD-40 repeat family protein	Signaling
AT3G08730	ATPK1 (P70 RIBOSOMAL S6 KINASE)	Signaling
AT4G11460	Protein kinase family protein	Signaling
AT2G31010	Protein kinase family protein	Signaling
AT3G07070	Protein kinase family protein	Signaling

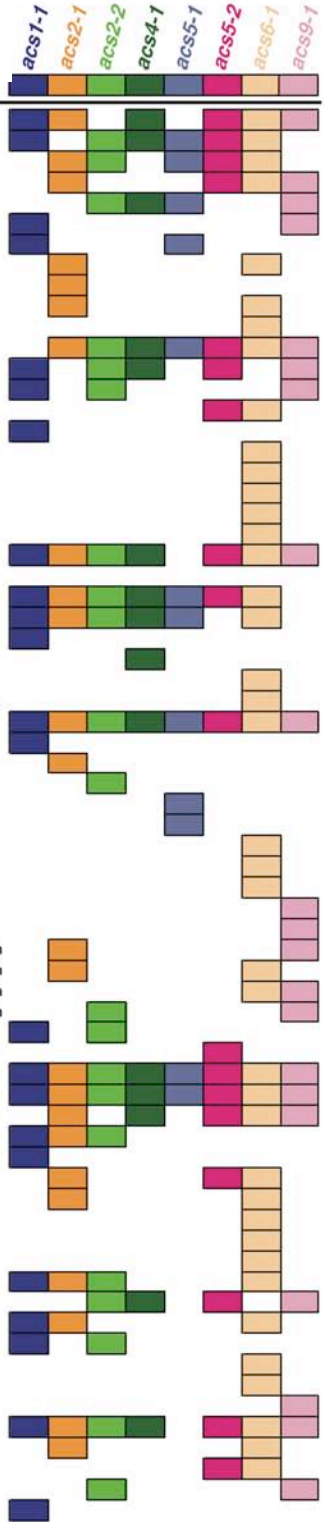

AT1G27590	Putative phosphatidylinositol 3- and 4-kinase family protein	Signaling
AT4G21410	Protein kinase family protein	Signaling
AT2G46020	ATBRM/BRM/CHR2 (ARABIDOPSIS THALIANA BRAHMA)	Transcription
AT3G28345	ABC transporter family protein	Transport
AT1G64780	ATAMT1;2 (AMMONIUM TRANSPORTER 1;2)	Transport
AT1G22570	Proton-dependent oligopeptide transport (POT) family protein	Transport
AT1G54730	Putative sugar transporter	Transport
AT3G27170	CLC-B (chloride channel protein B); voltage-gated chloride channel	Transport
AT5G13580	ABC transporter family protein	Transport
AT1G74770	Unknown Protein	Unknown
AT3G55020	Unknown:RabGAP/TBC domain-containing protein	Unknown
AT5G24710	Unknown protein	Unknown
AT2G43160	Unknown: epsin N-terminal homology (ENTH) domain-containing protein	Unknown
AT1G01320	Unknown: tetratricopeptide repeat (TPR)-containing protein	Unknown
AT2G27900	Unknown protein	Unknown
AT4G01290	Unknown Protein	Unknown
AT3G16670	Unknown protein	Unknown
AT3G23590	RFR1 (REF4-RELATED 1)	Unknown
AT3G30720	Unknown protein	Unknown
AT3G45450	Unknown protein	Unknown
AT4G19430	Unknown protein	Unknown
AT2G07360	Unknown: SH3 domain-containing protein	Unknown

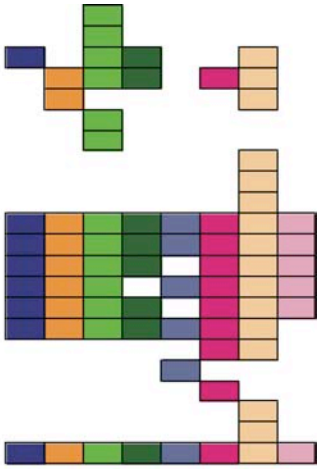

TABLE S7

List of genes repressed by the single mutants. Sorted according to their functional classifications. The color code denotes the gene whose expression has been induced by a particular mutation.

Gene name	Description of putative function	Function
AT1G02205	CER1 (ECERIFERUM 1)	Cell wall
AT1G23205	Invertase/pectin methylesterase inhibitor family protein	Cell wall
AT4G15620	Integral membrane family protein	Cell wall
AT3G47380	Invertase/pectin methylesterase inhibitor family protein	Cell wall
AT4G03510	RMA1 (Ring finger protein with Membrane Anchor 1)	Cell wall
AT5G62350	Invertase/pectin methylesterase inhibitor family protein	Cell wall
AT2G42540	COR15A (COLD-REGULATED 15A)	Defence/stress
AT2G43550	Putative trypsin inhibitor	Defence/stress
AT1G65870	Disease resistance-responsive family protein	Defence/stress
AT1G72910	Putative disease resistance protein (TIR-NBS class)	Defence/stress
AT2G35960	NHL12 (NDR1/HIN1-like 12)	Defence/stress
AT5G66400	RAB18 (RESPONSIVE TO ABA 18)	Defence/stress
AT1G02820	Late embryogenesis abundant 3 family protein / LEA3 family protein	Defence/stress
AT2G02120	LCR70/PDF2.1 (Low-molecular-weight cysteine-rich 70); protease inhibitor	Defence/stress
AT4G22212	Encodes a defensin-like (DEFL) family protein	Defence/stress
AT1G24020	MLP423 (MLP-LIKE PROTEIN 423)	Defence/stress
AT4G14060	major latex protein-related / MLP-related	Defence/stress
AT1G02300	Putative cathepsin B-like cysteine protease	Defence/stress
AT1G80920	J8; heat shock protein binding / unfolded protein binding	Defence/stress
AT2G17880	Putative DNAJ heat shock protein	Defence/stress
AT2G41430	ERD15 (EARLY RESPONSIVE TO DEHYDRATION 15)	Defence/stress
AT3G61060	ATPP2-A13 (Phloem protein 2-A13)	Defence/stress
AT3G62550	Universal stress protein (USP) family protein	Defence/stress
AT3G62950	Glutaredoxin family protein	Defence/stress
AT4G30650	Putative low temperature and salt responsive protein	Defence/stress
AT4G30660	Putativelow temperature and salt responsive protein	Defence/stress
AT5G45340	CYP707A3 (cytochrome P450, family 707, subfamily A, polypeptide 3)	Defence/stress
AT1G66100	Putative thionin	Defence/stress
AT5G03350	Legume lectin family protein	Defence/stress
AT1G16410	CYP79F1 (SUPERSHOOT 1)	Development
AT3G46600	Scarecrow transcription factor family protein	Development
AT3G53800	Armadillo/beta-catenin repeat family protein	Development
AT5G23660	MTN3 (ARABIDOPSIS HOMOLOG OF MEDICAGO TRUNCATULA MTN3)	Development
AT3G10520	AHB2 (NON-SYMBIOTIC HAEMOGLOBIN 2)	Development
AT2G36050	ATOFP15/OFP15 (Arabidopsis thaliana ovate family protein 15)	Development
AT3G26740	CCL (CCR-LIKE)	Development
AT5G56100	Glycine-rich protein / oleosin	Development
AT5G26220	ChaC-like family protein	Development
AT2G15890	MEE14 (maternal effect embryo arrest 14)	Development-embryo
AT4G00050	UNE10 (unfertilized embryo sac 10);transcription factor	Development-embryo
AT5G48850	Male sterility MS5 family protein	Development-embryo
AT1G04770	Male sterility MS5 family protein	Development-embryo
AT1G62180	APR2 (5'ADENYLYLPHOSPHOSULFATE REDUCTASE 2)	Enzyme-metabolism
AT2G15090	Putative fatty acid elongase	Enzyme-metabolism
AT4G04610	APR1 (PAPS REDUCTASE HOMOLOG 19)	Enzyme-metabolism
AT4G21990	APR3 (APS REDUCTASE 3)	Enzyme-metabolism
AT2G22190	Trehalose-phosphatase	Enzyme-metabolism
AT1G36370	SHM7 (serine hydroxymethyltransferase 7); glycine hydroxymethyltransferase	Enzyme-metabolism
AT2G23000	SCPL10 (serine carboxypeptidase-like 10)	Enzyme-metabolism
AT3G16175	Thioesterase family protein	Enzyme-metabolism
AT4G17090	CT-BMY (BETA-AMYLASE 3, BETA-AMYLASE 8)	Enzyme-metabolism
AT1G06100	Fatty acid desaturase family protein	Enzyme-metabolism
AT5G24770	VSP2 (VEGETATIVE STORAGE PROTEIN 2); acid phosphatase	Enzyme-metabolism
AT1G21130	Putative O-methyltransferase	Enzyme-metabolism
AT1G25230	Purple acid phosphatase family protein	Enzyme-metabolism
AT1G70290	ATTPS8 (Arabidopsis thaliana trehalose phosphatase/synthase 8)	Enzyme-metabolism
AT2G29300	Putative tropinone reductase	Enzyme-metabolism
AT2G39400	Hydrolase, alpha/beta fold family protein	Enzyme-metabolism
AT3G19620	Glycosyl hydrolase family 3 protein	Enzyme-metabolism
AT3G29670	Transferase family protein	Enzyme-metabolism
AT4G34250	Putative fatty acid elongase	Enzyme-metabolism
AT5G47240	ATNUDT8 (Arabidopsis thaliana Nudix hydrolase homolog 8)	Enzyme-metabolism
AT5G42180	Peroxidase 64 (PER64) (P64) (PRXR4)	Enzyme-metabolism
AT5G24150	SQP1 (Squalene monooxygenase 1)	Enzyme-metabolism
AT2G27420	Putative cysteine proteinase	Enzyme-metabolism
AT5G58770	Putative dehydrodolichyl diphosphate synthase	Enzyme-metabolism
AT5G25190	Putative ethylene-responsive element-binding protein	Hormone-related
AT3G03840	Putative auxin-responsive protein	Hormone-related

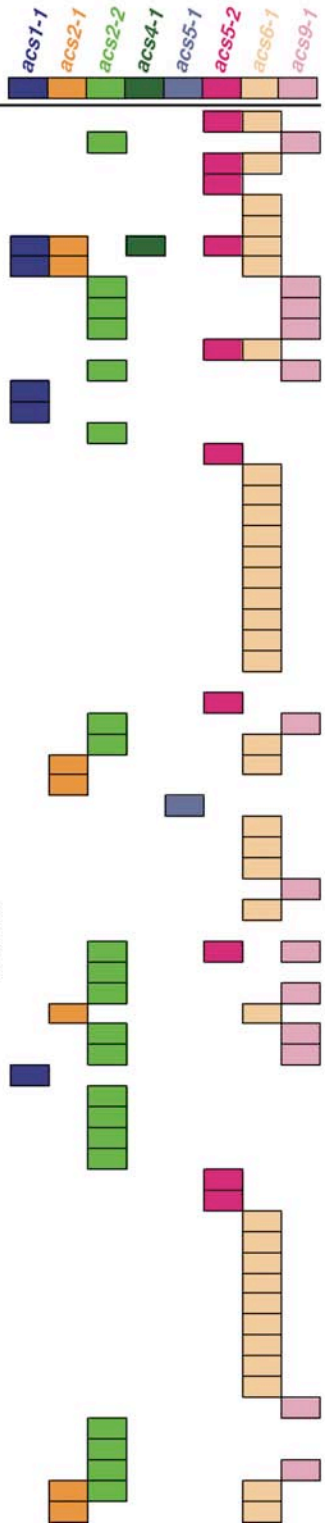

AT1G56220	Dormancy/auxin associated family protein	Hormone-related
AT1G74670	Putative gibberellin-responsive protein	Hormone-related
AT4G14550	IAA14 (SOLITARY ROOT)	Hormone-related
AT4G11280	ACS6 (1-AMINOCYCLOPROPANE-1-CARBOXYLIC ACID (ACC) SYNTHASE 6)	Hormone-related
ATCG00700	PSII low MW protein	Light-photosynthesis
AT4G27440	PORB (PROTOCHLOROPHYLLIDE OXIDOREDUCTASE B)	Light-photosynthesis
AT3G47430	PEX11B	Light-signaling
AT1G02340	HFR1 (LONG HYPOCOTYL IN FAR-RED)	Light-signaling
AT2G02950	PKS1 (PHYTOCHROME KINASE SUBSTRATE 1)	Light-signaling
ATMG00290	Mitochondrial ribosomal protein S4	Other
AT1G13650	Similar to 18S pre-ribosomal assembly protein gar2-related	Other
AT2G28720	Putative histone H2B	Other
AT5G22880	H2B/HTB2 (HISTONE H2B); DNA binding	Other
AT1G35612	Transposable element gene	Other
AT4G30690	Translation initiation factor 3 (IF-3) family protein	Other
AT3G16360	AHP4 (HPT PHOSPHOTRANSMITTER 4); kinase	Signaling
AT1G80440	Kelch repeat-containing F-box family protein	Signaling
AT2G18300	Basic helix-loop-helix (bHLH) family protein	Signaling
AT2G44130	Kelch repeat-containing F-box family protein	Signaling
AT3G11410	AHG3/ATPP2CA (ARABIDOPSIS THALIANA PROTEIN PHOSPHATASE 2CA)	Signaling
AT5G15160	bHLH family protein	Signaling
AT5G45820	CIPK20 (CBL-INTERACTING PROTEIN KINASE 20)	Signaling
AT3G49790	ATPP2-A10 (Phloem protein 2-A10)	Signaling
AT2G40435	Transcription regulator	Transcription
AT3G56400	WRKY70 (WRKY DNA-binding protein 70); transcription factor	Transcription
AT5G05090	Myb family transcription factor	Transcription
AT5G42200	Zinc finger (C3HC4-type RING finger) family protein	Transcription
AT2G23290	AtMYB70 (myb domain protein 70); DNA binding / transcription factor	Transcription
AT5G67300	ATMYB44/ATMYBR1/MYBR1 (MYB DOMAIN PROTEIN 44)	Transcription
AT5G51190	PutativeAP2 domain-containing transcription factor	Transcription
AT1G26800	Zinc finger (C3HC4-type RING finger) family protein	Transcription
AT1G68190	Zinc finger (B-box type) family protein	Transcription
AT2G18670	Zinc finger (C3HC4-type RING finger) family protein	Transcription
AT2G25900	ATCTH (Arabidopsis thaliana Cys3His zinc finger protein); transcription factor	Transcription
AT3G48360	BT2 (BTB AND TAZ DOMAIN PROTEIN 2); transcription regulator	Transcription
AT4G29190	Zinc finger (CCCH-type) family protein	Transcription
AT4G37260	AtMYB73/MYB73 (myb domain protein 73); DNA binding / transcription factor	Transcription
AT5G22920	Zinc finger (C3HC4-type RING finger) family protein	Transcription
AT5G49450	ATBZIP1 (ARABIDOPSIS THALIANA BASIC LEUCINE-ZIPPER 1)	Transcription
AT5G50450	Zinc finger (MYND type) family protein	Transcription
AT5G13170	Nodulin MtN3 family protein	Transport
AT5G46710	Zinc-binding family protein	Transport
AT2G38530	LTP2 (LIPID TRANSFER PROTEIN 2); lipid binding	Transport
AT4G14020	Rapid alkalinization factor (RALF) family protein	Transpost
AT4G33550	Lipid binding	Transpost
AT2G40460	Proton-dependent oligopeptide transport (POT) family protein	Transpost
AT4G02075	PIT1 (PITCHOUN 1); protein binding / zinc ion binding	Transpost
AT4G27280	Calcium-binding EF hand family protein	Transpost
AT5G37770	TCH2 (TOUCH 2); calcium ion binding	Transpost
AT4G13800	Permease-related	Transpost
AT1G77210	Putative sugar transporter	Transpost
AT2G17450	RHA3A (RING-H2 finger A3A); protein binding / zinc ion binding	Transpost
AT2G24240	Potassium channel tetramerisation domain-containing protein	Transpost
AT3G49580	Unknown protein	Unknown
AT5G24660	Unknown protein	Unknown
AT1G76960	Unknown protein	Unknown
AT2G07708	Unknown protein	Unknown
AT4G12970	Unknown protein	Unknown
AT1G12845	Unknown protein	Unknown
AT3G06070	Unknown protein	Unknown
AT4G14270	Unknown: PAM2 motif containing protein	Unknown
AT3G51750	Unknown protein	Unknown
AT1G47400	Unknown protein	Unknown
AT1G01240	Unknown protein	Unknown
AT2G42190	Unknown protein	Unknown
AT1G67865	Unknown protein	Unknown
AT2G40000	Unknown protein)	Unknown
AT3G10525	Unknown protein/similar to SIM (SIAMESE)	Unknown
AT4G09890	Unknown protein	Unknown
AT4G28290	Unknown protein	Unknown
AT5G62140	Unknown protein	Unknown
AT3G47295	Unknown protein	Unknown
AT1G19960	Unknown protein	Unknown

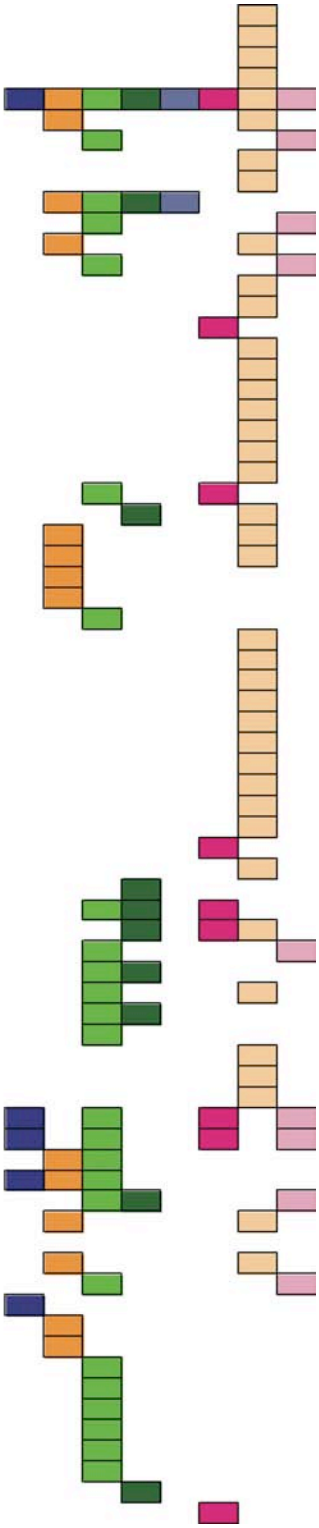

AT2G33850	Unknown protein	Unknown
AT1G25400	Unknown protein	Unknown
AT1G33055	Unknown protein	Unknown
AT1G49500	Unknown protein	Unknown
AT1G53885	Unknown protein	Unknown
AT1G54740	Unknown protein	Unknown
AT1G67050	Unknown protein	Unknown
AT1G75190	Unknown protein	Unknown
AT2G02710	Unknown; PAC motif-containing protein	Unknown
AT2G15960	Unknown protein	Unknown
AT2G24550	Unknown protein	Unknown
AT2G27830	Unknown protein	Unknown
AT2G40530	Unknown protein	Unknown
AT2G46550	Unknown protein	Unknown
AT3G10020	Unknown protein	Unknown
AT3G15630	Unknown protein	Unknown
AT3G52070	Unknown protein	Unknown
AT4G04630	Unknown protein	Unknown
AT4G05070	Unknown protein	Unknown
AT4G10910	Unknown protein	Unknown
AT4G12690	Unknown protein	Unknown
AT4G16000	Unknown protein	Unknown
AT4G23870	Unknown protein	Unknown
AT5G11070	Unknown protein	Unknown
AT5G22270	Unknown protein	Unknown
AT5G51390	Unknown protein	Unknown
AT5G57340	Unknown protein	Unknown
AT3G52740	Unknown protein	Unknown
AT1G55960	Unknown protein	Unknown
AT2G29670	Unknown protein	Unknown
AT3G47160	Unknown protein	Unknown

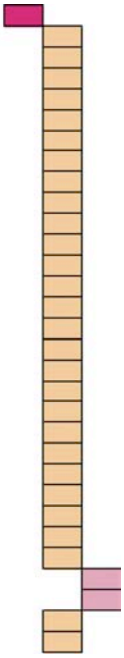

TABLE S8

List of genes induced by the high order mutants. Sorted according to their functional classifications. The color code denotes the gene whose expression has been induced by a particular mutation.

Gene name	Description of putative function	Function
AT1G76930	ATEXT4 (EXTENSIN 4)	Cell wall
AT5G19100	Extracellular dermal glycoprotein-related / EDGP-related	Cell wall
AT4G03510	RMA1 (Ring finger protein with Membrane Anchor 1)	Cell wall
AT2G26440	Pectinesterase family protein	Cell wall
AT4G02330	ATPMEPCRB; pectinesterase	Cell wall
AT5G06870	PGIP2 (POLYGALACTURONASE INHIBITING PROTEIN 2)	Cell wall
AT1G54040	ESP (EPITHIOSPECIFIER PROTEIN)	Defence/Stress
AT1G62290	aspartyl protease family protein	Defence/Stress
AT1G72060	serine-type endopeptidase inhibitor	Defence/Stress
AT2G43620	Putative chitinase	Defence/Stress
AT3G62550	Universal stress protein (USP) family protein	Defence/Stress
AT4G22470	Protease inhibitor/seed storage/lipid transfer protein (LTP) family protein	Defence/Stress
AT5G27660	Serine-type peptidase/ trypsin	Defence/Stress
AT3G26200	CYP71B22 (cytochrome P450, family 71, subfamily B, polypeptide 22)	Defence/Stress
AT4G12470	Protease inhibitor/seed storage/lipid transfer protein (LTP) family protein	Defence/Stress
AT4G23680	Major latex protein-related / MLP-related	Defence/Stress
AT5G13200	GRAM domain-containing protein / ABA-responsive protein-related	Defence/Stress
AT5G47990	CYP705A5 (cytochrome P450, family 705, subfamily A, polypeptide 5)	Defence/Stress
AT5G42600	MRN (MARNERAL SYNTHASE)	Defence/Stress
AT1G33970	Putative avirulence-responsive protein	Defence/Stress
AT1G53080	Legume lectin family protein	Defence/Stress
AT1G80920	J8; heat shock protein binding	Defence/Stress
AT3G61060	ATPP2-A13 (Phloem protein 2-A13)	Defence/Stress
AT5G20250	DIN10 (DARK INDUCIBLE 10); hydrolase	Defence/Stress
AT5G38550	Jacalin lectin family protein	Defence/Stress
AT4G12500	protease inhibitor/seed storage/lipid transfer protein (LTP) family protein	Defence/Stress
AT5G13220	JAS1/JAZ10/TIFY9 (JASMONATE-ZIM-DOMAIN PROTEIN 10)	Defence/Stress
AT3G49790	ATPP2-A10 (Phloem protein 2-A10)	Defence/Stress
AT5G23570	SGS3 (SUPPRESSOR OF GENE SILENCING 3)	Defence/Stress
AT5G23910	Microtubule motor	Development
AT1G24260	SEP3 (SEPALLATA3)	Development
AT2G44080	ARL (ARGOS-LIKE)	Development
AT3G02550	LBD41 (LOB DOMAIN-CONTAINING PROTEIN 41)	Development
AT3G26740	CCL (CCR-LIKE)	Development
AT1G04110	SDD1 (STOMATAL DENSITY AND DISTRIBUTION)	Development
AT1G16070	AtTLP8 (TUBBY LIKE PROTEIN 8)	Development
AT2G15890	MEE14 (maternal effect embryo arrest 14)	Development-embryo
AT5G48850	Male sterility MS5 family protein	Development-embryo
AT5G02540	Short-chain dehydrogenase/reductase (SDR) family protein	Enzyme-Metabolism
AT3G62950	Gllutaredoxin family protein	Enzyme-Metabolism
AT1G60810	ACLA-2 (ATP-citrate lyase A-2)	Enzyme-Metabolism
AT2G28630	beta-ketoacyl-CoA synthase family protein	Enzyme-Metabolism
AT5G23020	IMS2/MAM-L/MAM3 (METHYLTHIOALKYMALATE SYNTHASE-LIKE)	Enzyme-Metabolism
AT5G47240	ATNUDT8 (Arabidopsis thaliana Nudix hydrolase homolog 8)	Enzyme-Metabolism
AT1G15040	Glutamine amidotransferase-related protein	Enzyme-Metabolism
AT1G13700	Glucosamine/galactosamine-6-phosphate isomerase family protein	Enzyme-Metabolism
AT1G60270	Glycosyl hydrolase family 1(pseudogene)	Enzyme-Metabolism
AT1G70820	Putative phosphoglucomutase	Enzyme-Metabolism
AT2G39400	Hydrolase, alpha/beta fold family protein	Enzyme-Metabolism
AT4G34250	Putative fatty acid elongase	Enzyme-Metabolism
AT5G27200	ACP5 (ACYL CARRIER PROTEIN 5); acyl carrier	Enzyme-Metabolism
AT5G48010	Putative pentacyclic triterpene synthase	Enzyme-Metabolism
AT5G42580	CYP705A12 (cytochrome P450, family 705, subfamily A, polypeptide 12)	Enzyme-Metabolism
AT2G36690	Oxidoreductase, 2OG-Fe(II) oxygenase family protein	Enzyme-Metabolism

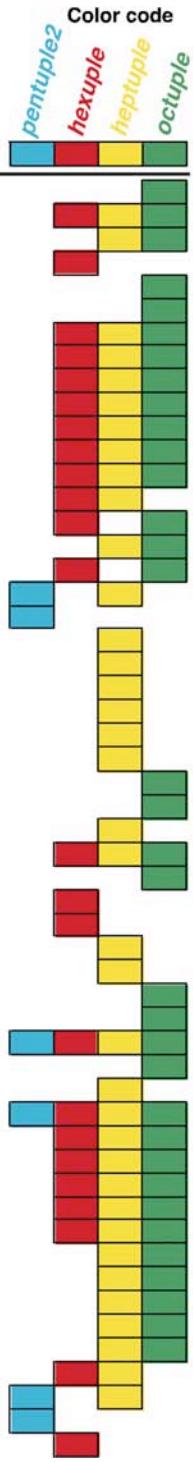

AT1G02660	Lipase class 3 family protein	Enzyme-Metabolism
AT1G66800	Cinnamyl-alcohol dehydrogenase familyprotein	Enzyme-Metabolism
AT1G67810	Fe-S metabolism associated domain-containing protein	Enzyme-Metabolism
AT5G23220	NIC3 (NICOTINAMIDASE 3)	Enzyme-Metabolism
AT5G37980	Putative NADP-dependent oxidoreductase	Enzyme-Metabolism
AT5G38010	UDP-glucoronosyl/UDP-glucosyl transferase family protein	Enzyme-Metabolism
AT5G38020	S-adenosyl-L-methionine:carboxyl methyltransferase family protein	Enzyme-Metabolism
AT5G38710	Putative proline oxidase	Enzyme-Metabolism
AT5G43440	Putative 2-oxoglutarate-dependent dioxygenase	Enzyme-Metabolism
AT1G61810	BGLU45; hydrolase, hydrolyzing O-glycosyl compounds	Enzyme-Metabolism
AT3G07800	Putative thymidine kinase	Enzyme-Metabolism
AT3G25760	AOC1 (ALLENE OXIDE CYCLASE 1)	Enzyme-Metabolism
AT3G27060	TSO2 ; ribonucleoside-diphosphate reductase	Enzyme-Metabolism
AT4G02390	APP ; NAD+ ADP-ribosyltransferase	Enzyme-Metabolism
AT4G22753	SMO1-3 (STEROL 4-ALPHA METHYL OXIDASE)	Enzyme-Metabolism
AT5G16990	Putative NADP-dependent oxidoreductase	Enzyme-Metabolism
AT3G47800	Aldose 1-epimerase family protein	Enzyme-Metabololism
AT1G13260	RAV1 (Related to ABI3/VP1 1)	Hormone-related
AT1G56220	Dormancy/auxin associated family protein	Hormone-related
AT4G34770	Auxin-responsive family protein	Hormone-related
AT4G12550	AIR1 (Auxin-Induced in Root cultures 1)	Hormone-related
AT4G26200	ACS7	Hormone-related
AT1G06160	Ethylene-responsive factor	Hormone-related
AT2G23170	GH3.3; indole-3-acetic acid amido synthetase	Hormone-related
AT5G54190	PORA (Protochlorophyllide reductase A)	Light-Photosynthesis
AT4G27440	PORB (PROTOCHLOROPHYLLIDE OXIDOREDUCTASE B)	Light-Photosynthesis
AT3G19850	Phototropic-responsive NPH3 family protein	Light-Signaling
AT1G50280	Phototropic-responsive NPH3 family protein	Light-Signaling
AT2G42870	HLH1/PAR1 (PHY RAPIDLY REGULATED 1); transcription regulator	Light-Signaling
AT4G16870	Transposable element gene	Other
AT3G21020	Transposable element gene	Other
AT1G60020	Transposable element gene	Other
AT3G22880	ATDMC1 (RECA-LIKE GENE); ATP binding / DNA-dependent ATPase	Other
AT4G22280	F-box family protein	Signaling
AT5G24240	Phosphatidylinositol 3- and 4-kinase family protein	Signaling
AT1G64460	Phosphatidylinositol 3- and 4-kinase family protein	Signaling
AT1G64470	Ubiquitin family protein	Signaling
AT3G46280	Protein kinase-related	Signaling
AT4G21510	F-box family protein	Signaling
AT1G65390	ATPP2-A5; carbohydrate binding protein	Signaling
AT2G25470	Leucine-rich repeat family protein	Signaling
AT5G46330	FLS2 (FLAGELLIN-SENSITIVE 2)	Signaling
AT1G76410	ATL8; protein binding / zinc ion binding	Signaling
AT1G15670	Kelch repeat-containing F-box family protein	Signaling
AT1G20590	CYCB2;3 cyclin-dependent protein kinase regulator	Signaling
AT1G76540	CDKB2;1 (CYCLIN-DEPENDENT KINASE B2;1)	Signaling
AT2G18600	Putative RUB1-conjugating enzyme	Signaling
AT2G27970	CKS2 (CDK-SUBUNIT 2); cyclin-dependent protein kinase	Signaling
AT4G21070	ATBRCA1 (BREAST CANCER SUSCEPTIBILITY1); ubiquitin-protein ligase	Signaling
AT4G28950	ARAC7/ATRAC7/ATROP9/RAC7/ROP9 ;RHO-RELATED PROTEIN	Signaling
AT4G37490	CYC1 (CYCLIN 1); cyclin-dependent protein kinase regulator	Signaling
AT5G56580	ATMKK6 (ARABIDOPSIS NQK1); kinase	Signaling
AT5G32460	Transcriptional factor B3 family(pseudogene)	Transcription
AT1G25560	Putative AP2 domain-containing transcription factor	Transcription
AT5G22920	Zinc finger (C3HC4-type RING finger) family protein	Transcription
AT5G27280	Zinc finger (DNL type) family protein	Transcription
AT5G49450	ATBZIP1 (ARABIDOPSIS THALIANA BASIC LEUCINE-ZIPPER 1)	Transcription
AT4G14365	Zinc finger (C3HC4-type RING finger) family protein	Transcription
AT1G68190	Zinc finger (B-box type) family protein	Transcription
AT1G71030	ATMYBL2 (Arabidopsis myb-like 2)	Transcription
AT4G37260	AtMYB73/MYB73 (myb domain protein 73)	Transcription
AT5G44260	Zinc finger (CCCH-type) family protein	Transcription

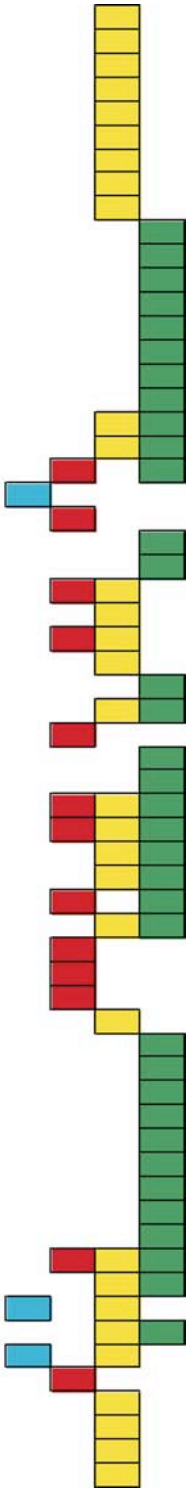

AT5G07100	WRKY26 (WRKY DNA-binding protein 26)	Transcription
AT5G60250	Zinc finger (C3HC4-type RING finger) family protein	Transcription
AT5G61590	AP2 domain-containing transcription factor family protein	Transcription
AT5G64060	ANAC103 (Arabidopsis NAC domain containing protein 103)	Transcription
AT5G67480	BT4 (BTB AND TAZ DOMAIN PROTEIN 4)	Transcription
AT5G18840	Putative sugar transporter	Transport
AT1G64170	ATCHX16 (CATION/H+ EXCHANGER 16); monovalent cation:proton antiporter	Transport
AT3G21080	ABC transporter-related	Transport
AT5G46050	ATPTR3/PTR3 (PEPTIDE TRANSPORTER PROTEIN 3)	Transport
AT1G77210	Putative sugar transporter	Transport
AT4G28040	Nodulin MtN21 family protein	Transport
AT1G78460	SOUL heme-binding family protein	Transport
AT3G12520	SULTR4;2 (sulfate transporter 4;2); sulfate transmembrane transporter	Transport
AT3G18830	ATPLT5 (POLYOL TRANSPORTER 5);sugar transporter	Transport
AT3G23550	MATE efflux family protein	Transport
AT4G12480	pEARLI 1; lipid binding	Transport
AT4G36670	Putative mannitol transporter	Transport
AT5G52750	Heavy-metal-associated domain-containing protein	Transport
AT5G48720	Unknown protein	Unknown
AT3G47160	Unknown Protein	Unknown
AT3G15630	Unknown protein	Unknown
AT1G50290	Unknown protein	Unknown
AT3G10020	Unknown protein	Unknown
AT5G15360	Unknown protein	Unknown
AT5G19250	Unknown protein	Unknown
AT5G15420	Unknown protein	Unknown
AT2G15960	Unknown protein	Unknown
AT4G14270	Unknown; contains PAM2 motif	Unknown
AT5G22270	Unknown protein	Unknown
AT5G26270	Unknown protein	Unknown
AT2G14560	Unknown protein	Unknown
AT4G31570	Unknown protein	Unknown
AT5G16380	Unknown protein	Unknown
AT5G20150	Unknown; SPX (SYG1/Pho81/XPR1) domain-containing protein	Unknown
AT2G02710	Unknown protein	Unknown
AT2G29670	Unknown protein	Unknown
AT3G15450	Unknown protein	Unknown
AT4G05070	Unknown protein	Unknown
AT4G27450	Unknown protein	Unknown
AT5G18130	Unknown protein	Unknown
AT1G05575	Unknown protein	Unknown
AT1G19380	Unknown protein	Unknown
AT1G22890	Unknown protein	Unknown
AT2G25735	Unknown protein	Unknown
AT3G17680	Unknown protein	Unknown
AT3G49580	Unknown protein	Unknown
AT4G22960	Unknown protein	Unknown
AT5G03230	Unknown protein	Unknown
AT5G05180	Unknown protein	Unknown
AT5G17160	Unknown protein	Unknown
AT5G24280	Unknown protein	Unknown
AT5G62550	Unknown protein	Unknown

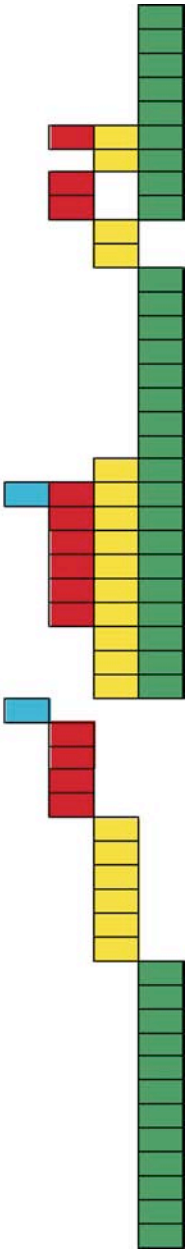

TABLE S9

List of genes repressed by the high order mutants. Sorted according to their functional classifications. The color code denotes the gene whose expression has been induced by a particular mutation.

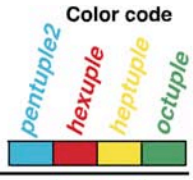

Gene name	Description of putative function	Function
AT1G23205	Invertase/pectin methylesterase inhibitor family protein	Cell wall
AT3G12110	ACT11 (ACTIN-11); structural constituent of cytoskeleton	Cell wall
AT3G24460	TMS membrane family protein	Cell wall
AT4G25810	XTR6 (XYLOGLUCAN ENDOTRANSGLYCOSYLASE 6)	Cell wall
AT5G20740	Invertase/pectin methylesterase inhibitor family protein	Cell wall
AT4G02130	GATL6/LGT10; polygalacturonate 4-alpha-galacturonosyltransferase	Cell wall
AT1G48100	Glycoside hydrolase family 28 protein / polygalacturonase family protein	Cell wall
AT1G55740	ATSIP1 (ARABIDOPSIS THALIANA SEED IMBIBITION 1)	Cell wall
AT1G02820	Late embryogenesis abundant 3 family protein / LEA3 family protein	Defence/stress
AT2G02120	LCR70/PDF2.1 (Low-molecular-weight cysteine-rich 70); protease inhibitor	Defence/stress
AT1G66100	Putative thionin	Defence/stress
AT5G03350	Legume lectin family protein	Defence/stress
AT5G05040	Cysteine protease inhibitor]	Defence/stress
AT5G22860	Serine carboxypeptidase S28 family protein	Defence/stress
AT5G35450	Putative disease resistance protein (CC-NBS-LRR class)	Defence/stress
AT1G56510	Putative disease resistance protein (TIR-NBS-LRR class)	Defence/stress
AT1G58807	Putative disease resistance protein (CC-NBS-LRR class)	Defence/stress
AT1G59218	Putative disease resistance protein (CC-NBS-LRR class)	Defence/stress
AT1G63880	Putative disease resistance protein (TIR-NBS-LRR class)	Defence/stress
AT3G14210	ESM1 (EPITHIOSPECIFIER MODIFIER 1); carboxylesterase	Defence/stress
AT3G16450	Jacalin lectin family protein	Defence/stress
AT5G11580	UVB-resistance protein-related / (RCC1) family protein	Defence/stress
AT5G15960	KIN (COLD-RESPONSIVE 6.6)	Defence/stress
AT5G17890	LIM domain-containing protein / disease resistance protein-related	Defence/stress
AT5G38910	Putative germin-like protein	Defence/stress
AT3G18280	Protease inhibitor/seed storage/lipid transfer protein (LTP) family protein	Defence/stress
AT3G51240	F3H (TRANSPARENT TESTA 6); naringenin 3-dioxygenase	Defence/stress
AT5G42600	MRN (MARNERAL SYNTHASE)	Defence/stress
AT1G49630	ATPREP2; metalloendopeptidase	Defence/stress
AT1G54050	17.4 kDa class III heat shock protein (HSP17.4-CIII)	Defence/stress
AT4G02410	Lectin protein kinase family protein	Defence/stress
AT5G36910	THI2.2 (THIONIN 2.2); toxin receptor binding	Defence/stress
AT5G36930	Putative disease resistance protein (TIR-NBS-LRR class)	Defence/stress
AT1G62510	Protease inhibitor/seed storage/lipid transfer protein (LTP) family protein	Defence/stress
AT1G62710	BETA-VPE (vacuolar processing enzyme beta); cysteine-type endopeptidase	Defence/stress
AT3G12170	DNAJ heat shock N-terminal domain-containing protein	Defence/stress
AT3G14240	Subtilase family protein	Defence/stress
AT1G63090	ATPP2-A11 (Phloem protein 2-A11); carbohydrate binding	Defence/stress
AT1G58270	ZW9	Development
AT5G03340	(Cell division control protein 48 homolog E); ATPase	Development
AT5G10140	FLC (FLOWERING LOCUS C)	Development
AT1G66620	Putative seven in absentia (SINA) protein	Development
AT1G17870	ATEGY3	Development
AT5G17790	VAR3 (VARIEGATED 3); binding	Development
AT4G00050	UNE10 (unfertilized embryo sac 10);transcription factor	Development-embryo
AT5G27270	EMB976 (EMBRYO DEFECTIVE 976)	Development-embryo
AT2G41380	Embryo-abundant protein-related	Development-embryo
AT5G22510	Putative beta-fructofuranosidase	Enzyme-metabolism
AT5G24150	SQP1 (Squalene monooxygenase 1)	Enzyme-metabolism
AT2G27420	Putative cysteine proteinase	Enzyme-metabolism
AT1G59900	AT-E1 ALPHA (pyruvate dehydrogenase complex E1 alpha subunit)	Enzyme-metabolism
AT1G62430	ATCDS1 (CDP-diacylglycerol synthase 1)	Enzyme-metabolism
AT3G14650	CYP72A11 (cytochrome P450, family 72, subfamily A, polypeptide 11)	Enzyme-metabolism
AT3G21950	S-adenosyl-L-methionine:carboxyl methyltransferase family protein	Enzyme-metabolism

AT5G16980	Putative NADP-dependent oxidoreductase	Enzyme-metabolism
AT5G23070	Putative thymidine kinase	Enzyme-metabolism
AT5G58770	Putative dehydrodolichyl diphosphate synthase	Enzyme-metabolism
AT2G18150	Putative peroxidase	Enzyme-metabolism
AT5G05270	Chalcone-flavanone isomerase family protein	Enzyme-metabolism
AT1G60710	ATB2; oxidoreductase	Enzyme-metabolism
AT1G66540	Putative cytochrome P450	Enzyme-metabolism
AT1G66970	Glycerophosphoryl diester phosphodiesterase family protein	Enzyme-metabolism
AT4G21760	BGLU47 (Beta-glucosidase 47)	Enzyme-metabolism
AT5G56080	Putative nicotianamine synthase	Enzyme-metabolism
AT2G30750	CYP71A12 (CYTOCHROME P450)	Enzyme-metabolism
AT4G35090	CAT2 (CATALASE 2)	Enzyme-metabolism
AT5G67430	GCN5-related N-acetyltransferase (GNAT) family protein	Enzyme-metabolism
AT4G11280	ACS6 (1-AMINOCYCLOPROPANE-1-CARBOXYLIC ACID (ACC) SYNTHASE 6)	Hormone-related
AT4G26150	CGA1 (CYTOKININ-RESPONSIVE GATA FACTOR 1); transcription factor	Hormone-related
AT5G17880	CSA1 (CONSTITUTIVE SHADE-AVOIDANCE1)	Light-signaling
AT1G01060	LHY (LATE ELONGATED HYPOCOTYL)	Light-signaling
AT3G22840	ELIP1 (EARLY LIGHT-INDUCABLE PROTEIN); chlorophyll binding	Light-signaling
AT5G24850	CRY3 (CRYPTOCHROME 3)	Light-signaling
AT1G53900	GTP binding / translation initiation factor	Other
AT1G54260	Histone H1/H5 family protein	Other
AT1G58380	XW6; structural constituent of ribosome	Other
AT3G15310	Transposable element gene	Other
AT3G15590	Putative DNA-binding protein	Other
AT5G08600	U3 ribonucleoprotein (Utp) family protein	Other
AT5G10400	Histone H3	Other
AT1G62150	Mitochondrial transcription termination factor-related / mTERF-related	Other
AT1G20390	Transposable element gene	Other
AT3G11240	Putative arginine-tRNA-protein transferase	Other
AT5G24120	SIGE (RNA polymerase sigma subunit E); DNA binding	Other
AT1G65190	Protein kinase family protein	Signaling
AT4G25710	Kelch repeat-containing F-box family protein	Signaling
AT5G23410	Similar to FKF1 (FLAVIN-BINDING KELCH DOMAIN F BOX PROTEIN)	Signaling
AT4G23300	Protein kinase family protein	Signaling
AT1G56720	Protein kinase family protein	Signaling
AT5G39030	Protein kinase family protein	Signaling
AT3G08730	ATPK1 (P70 RIBOSOMAL S6 KINASE); kinase/ protein binding	Signaling
AT5G45070	ATPP2-A8 (Phloem protein 2-A8); transmembrane receptor	Signaling
AT4G31805	WRKY family transcription factor	Transcription
AT5G07690	MYB29 (myb domain protein 29); DNA binding / transcription factor	Transcription
AT3G04030	Myb family transcription factor	Transcription
AT5G22890	Zinc finger (C2H2 type) family protein	Transcription
AT5G20380	Transporter-related	Transport
AT5G02270	ATNAP9 (Non-intrinsic ABC protein 9)	Transport
AT2G38530	LTP2 (LIPID TRANSFER PROTEIN 2); lipid binding	Transport
AT4G19690	IRT1 (IRON-REGULATED TRANSPORTER 1)	Transport
AT4G31530	Binding / catalytic/ coenzyme binding	Transport
AT1G73220	ATOCT1	Transport
AT2G25680	MOT1 (MOLYBDATE TRANSPORTER 1)	Transport
AT3G22570	Protease inhibitor/seed storage/lipid transfer protein (LTP)	Transport
AT3G51895	SULTR3;1 (SULFATE TRANSPORTER 1)	Transport
AT5G02180	Amino acid transporter family protein	Transport
AT5G54130	Calcium-binding EF hand family protein	Transport
AT1G65370	Unknown: meprin and TRAF homology domain-containing protein	Unknown
AT5G26260	Unknown: meprin and TRAF domain-containing protein	Unknown
AT5G26270	Unknown protein	Unknown
AT5G35490	Unknown protein	Unknown
AT1G55960	Unknown protein	Unknown
AT4G24130	Unknown protein	Unknown
AT5G06790	Unknown protein	Unknown
AT5G15020	Unknown protein	Unknown
AT5G15980	Unknown:pentatricopeptide (PPR) repeat-containing protein	Unknown

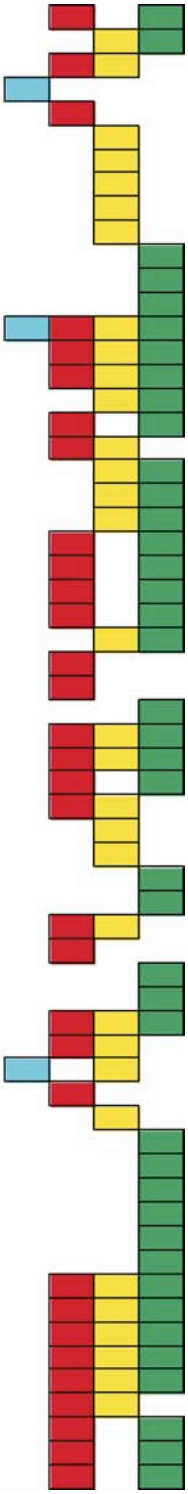

AT5G16220	Unknown: octicosapeptide/Phox/Bem1p (PB1) domain-containing protein	Unknown
AT5G28350	Unknown protein	Unknown
AT1G58150	Unknown protein	Unknown
AT4G01080	Unknown protein	Unknown
AT5G16250	Unknown protein	Unknown
AT4G01590	Unknown protein	Unknown
AT4G02540	Unknown: DC1 domain-containing protein	Unknown
AT5G22580	Unknown protein	Unknown
AT5G42760	Unknown protein	Unknown
AT2G36630	Unknown protein	Unknown
AT3G22240	Unknown protein	Unknown
AT3G28270	Unknown protein	Unknown
AT5G20360	Unknown:octicosapeptide/Phox/Bem1p (PB1) domain-containing protein	Unknown
AT1G74770	Unknown protein	Unknown

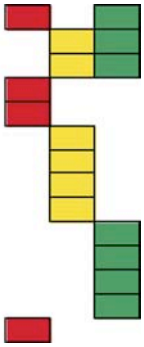

TABLE S10

(A) A list of genes with the highest fold change in gene expression in the high order mutants.

(B) List of light-related genes whose expression in more than 2 fold (M>1, M<-1).

Table S10, part A. A list of gene with the highest fold change in gene expression in the high order mutants.

Gene name	Description of putative function	Function	pentuple2	hexuple	heptuple	octuple
Induced-high M value						
AT1G54040	ESP (EPITHIOSPECIFIER PROTEIN)	Defence/Stress		5.1	5.8	5.9
AT3G62550	Universal stress protein (USP) family protein	Defence/Stress		1.5	2.8	2.1
AT2G15890	MEE14 (maternal effect embryo arrest 14)	Development-embryo	1.5	1.1	2.3	2.3
AT5G15360	Unknown protein	Unknown		3.3	2.5	3.2
AT1G50290	Unknown protein	Unknown		3.3	2.6	3
AT5G23020	IMS2/MAM-L/MAM3 (METHYLTHIOALKYMALATE SYNTHASE-LIKE)	Enzyme-Metabolism		1.6	1.5	1.4
AT1G04110	SDD1 (STOMATAL DENSITY AND DISTRIBUTION)	Development				1.2
Repressed-high M value						
AT1G66100	Putative thionine	Defence/stress		-1.4	-6.7	-6.6
AT3G16450	Jacalin lectin family protein	Defence/stress		-4.8		-4.5
AT5G03350	Legume lectin family protein	Defence/stress		-3.7	-1.4	-4.6
AT3G14210	ESM1 (EPITHIOSPECIFIER MODIFIER 1); carboxylesterase	Defence/stress		-3.4		-4.3
AT1G59218	Putative disease resistance protein (CC-NBS-LRR class)	Defence/stress			-3.5	-3.7
AT5G05040	Cysteine protease inhibitor	Defence/stress		-3.6	-1.3	-3.4
AT1G56510	Putative disease resistance protein (TIR-NBS-LRR class)	Defence/stress			-2.8	-2.8
AT1G63880	Putative disease resistance protein (TIR-NBS-LRR class)	Defence/stress			-2.8	-2.6
AT1G58270	ZW9	Development		-1.1	-3.9	-4.2
AT1G59900	AT-E1 ALPHA (pyruvate dehydrogenase complex E1 alpha subunit)	Enzyme-metabolism			-3.2	-3.1
AT5G24150	SQP1 (Squalene monooxygenase 1)	Enzyme-metabolism		-2.8	-2.9	-2.7
AT5G17880	CSA1 (CONSTITUTIVE SHADE-AVOIDANCE1)	Light-signaling		-2.5	-1	-2.9
AT5G10400	Histone H3	Other		-3.4		-3.5
AT5G26260	Unknown: meprin and TRAF domain-containing protein	Unknown		-3.5	-3.3	-3.1

Table S10, part B. List of light-related gene whose gene expression in more than 2 fold (M >1, M < -1)

Gene name	Description of putative function	Function	pentuple2	hexuple	heptuple	octuple
Induced-light						
AT5G54190	PORA (Protochlorophyllide reductase A)	Light-Photosynthesis		1.3	1.3	
AT4G27440	PORB (PROTOCHLOROPHYLLIDE OXIDOREDUCTASE B)	Light-Photosynthesis			1.1	
AT3G19850	Phototropic-responsive NPH3 family protein	Light-Signaling		1	1.3	
AT1G50280	Phototropic-responsive NPH3 family protein	Light-Signaling			1.5	
AT2G42870	HLH1/PAR1 (PHY RAPIDLY REGULATED 1); transcription regulator	Light-Signaling				1
Repressed-light						
AT5G17880	CSA1 (CONSTITUTIVE SHADE-AVOIDANCE1)	Light-signaling		-2.5	-1	-2.9
AT1G01060	LHY (LATE ELONGATED HYPOCOTYL)	Light-signaling			-1	-1
AT3G22840	ELIP1 (EARLY LIGHT-INDUCABLE PROTEIN); chlorophyll binding	Light-signaling		-1.2		-1.3
AT5G24850	CRY3 (CRYPTOCHROME 3)	Light-signaling		-1.2	-1.1	
AT5G67430	GCN5-related N-acetyltransferase (GNAT) family protein	Light-signaling				-1.2
AT5G23410	Similar to FKF1 (FLAVIN-BINDING KELCH DOMAIN F BOX PROTEIN)	Light-signaling		-1.4		-1.1

The M = log2(X); where X is the fold increase / decrease of gene expression compared to the control. M > 1 for induced genes. M < -1 for repressed genes.